

HEPATITIS C VIRUS ENTRY INTO HEPATOCYTES AND ENGAGEMENT OF
INNATE IMMUNE DEFENSES

APPROVED BY SUPERVISORY COMMITTEE

Michael Gale, Jr., Ph.D.
Supervising Professor

Julie Pfeiffer, Ph.D.
Chair, Examining Committee

Vanessa Sperandio, Ph.D.
Committee Member

Jin Ye, Ph.D.
Committee Member

DEDICATION

This work is dedicated to my family whose constant love, support, and encouragement have provided the foundation for allowing me to pursue a career in biomedical science. It is also dedicated to my future patients. I hope that the training I have received will be useful to you and I will continue to judge the success of this and future endeavors by their potential benefit to you.

ACKNOWLEDGEMENTS

There are several people I would like to thank for making the work described in this thesis possible. First I would like to thank my mentor Dr. Michael Gale, Jr. It was a privilege to train under a world-class scientist who, while highly sought out for collaborations and speaking engagements, was also down-to-earth, approachable, supportive and encouraging as a mentor. I also want to thank all the current and former members of the Gale lab for being fun to work and hang out with on a day to day basis as well as for the great science conversations, helpful troubleshooting advice and being role models for scientific excellence. I'd like to thank Chunfu Wang for initial training and introduction to the lab during my rotation, Brenda Fredricksen for BSL2+/BL3 training, Ming Loo, Cindy Johnson and Takeshi Saito for opportunities to collaborate and contribute to their projects. Andrea Erickson for sharing slides for talks and protocols in setting up the JFH1 system. Fellow MSTP students Rhea Sumpter, Eileen Foy, Brian Keller and Cindy Johnson for establishing the reputation of the Gale lab as a great place for an MD/PhD to train. Spencer Carney for providing a clinical perspective on HCV. Postdocs Ming Loo, Takeshi Saito, Brian Doehle, Mehul Suthar, Stacy Horner, Courtney Wilkins, and Helen Liu for sharing their scientific expertise, advice, and applied biology (home brewing, gardening, and medical) knowledge. Fellow grad students John Errett and Olivia Perwitasari, lab managers Penny Fish and Nanette Crochete for keeping the lab running smoothly and taking care of all the details we don't even know about so we can focus on doing the science. Technicians Jessica Briley and Kristina Chang for assistance and taking over the lab jobs. I'd like to thank Amgen scholar Janelle Ruiz and

rotation student Amina Negash for putting up with my first attempts at training students and for their contributions to my research.

I'd like to thank my committee members Drs. Julie Pfeiffer, Vanessa Sperandio, and Jin Ye for their helpful suggestions on the thesis work and for being flexible in arranging their schedules to coordinate with me coming in from out of town. Thanks to all of the administrative personnel, Peggy McCune and Barbara Lovseth in the UW immunology office, Stephanie Mode at the UTSW microbiology department, Robin Downing and Stephanie Robertson at the UTSW MSTP office. Also thanks to all the support personnel who keep the buildings clean and running, glassware washed, and everything else I don't even think about. I also want to thank a patient who cannot be named for generously sharing their serum, without which few of these experiments would have been possible. I want to thank family and friends from med school and church in Dallas and Seattle for enriching my life outside the lab and supporting me in innumerable ways. I also want to thank Lucy and Henry Billingsley for generously providing a place for me to live during the first half of grad school and for making the move back to Dallas easy in letting me return there. To all of you I want to say the past four years have been very educational, fun, and rewarding, but also challenging and I couldn't have done it without you.

HEPATITIS C VIRUS ENTRY INTO HEPATOCYTES AND ENGAGEMENT OF
INNATE IMMUNE DEFENSES

by

DAVID MATTHEW OWEN

DISSERTATION

Presented to the Faculty of the Graduate School of Biomedical Sciences

The University of Texas Southwestern Medical Center at Dallas

In Partial Fulfillment of the Requirements

For the Degree of

DOCTOR OF PHILOSOPHY

The University of Texas Southwestern Medical Center at Dallas

Dallas, Texas

June, 2009

Copyright

by

David Matthew Owen, 2009

All Rights Reserved

HEPATITIS C VIRUS ENTRY INTO HEPATOCYTES AND ENGAGEMENT OF
INNATE IMMUNE DEFENSES

Publication No. _____

David Matthew Owen, Ph.D.

The University of Texas Southwestern Medical Center at Dallas, 2009

Supervising Professor: Michael Gale, Jr., Ph.D.

Hepatitis C virus (HCV) infection is a major cause of liver disease and a global health problem with inadequate treatment options. An improved understanding of how HCV exploits and subverts host factors to establish infection should yield potential targets for therapy. This study uses a recently developed cell culture model of HCV infection to examine HCV entry and engagement of innate immune defenses. HCV associates with host apolipoproteins and enters hepatocytes through complex processes involving some combination of CD81, claudin-I, occludin, and scavenger receptor BI.

Here I show that HCV forms a complex with very low density lipoprotein (VLDL) within infected hepatocytes and uses this association to support infection through the low density lipoprotein receptor (LDL-R). Blocking experiments demonstrate that β -VLDL and apolipoprotein E (apoE) can compete with HCV for entry. Knockdown of the LDL-R by treatment with 25-hydroxycholesterol or siRNA ablated ligand uptake and reduced HCV infection of cells, whereas infection was rescued upon cell ectopic LDL-R expression. Analyses of gradient-fractionated HCV demonstrate that apoE is associated with HCV virions exhibiting peak infectivity and dependence upon the LDL-R for cell entry. These results define the LDL-R as a cooperative HCV co-receptor that supports viral entry and infectivity through interaction with apoE ligand present in an infectious HCV/lipoprotein complex comprising the virion. Furthermore, upon entry HCV induces an initial transient activation of interferon regulatory factor-3 (IRF3) which is dependent on retinoic acid inducible gene I (RIG-I) and interferon-beta promoter stimulator-1 (IPS-1). This activation produces an antiviral activity which inhibits HCV entry and replication. HCV NS3/4A protease activity blocks this activation within 48 hours. At later time points post infection HCV activates NF κ B in a RIG-I independent manner leading to inflammatory cytokine production. These studies identify 3 potential targets for future HCV therapy: 1) alteration of HCV-lipoprotein interaction to disrupt entry, 2) blockade of NS3/4A protease activity to restore innate antiviral response, and 3) modulation of HCV induced NF κ B signaling to downregulate chronic inflammation.

TABLE OF CONTENTS

DEDICATION	ii
ACKNOWLEDGEMENTS	ii
ABSTRACT	vii
PUBLICATIONS	xiv
LIST OF FIGURES	xv
LIST OF TABLES	xvii
ABBREVIATIONS	xviii
CHAPTER 1: INTRODUCTION	1
History	1
Genome organization	2
Epidemiology	3
Clinical course	5
Therapy	6
Model systems	8
Animal models	8
Replicon	8
Pseudoparticles	9
Cell culture infection	9
Entry receptors	10
CD81	11
SR-BI	12

Claudin-1	13
Occludin	13
LDL-R	14
HCV & Lipoprotein metabolism	14
Lipids & The liver	14
Lipids & HCV	17
LDL-R as an HCV receptor	18
Innate immune defenses	19
RIG-I like receptors	21
Toll-like receptors	22
NOD-like receptors	22
Interferon signaling	23
CHAPTER 2: MATERIALS & METHODS	25
Cell culture	25
Media & culture conditions	25
Construction of SGR-JFH1 cell lines	25
Construction of HepG2-CD81 cell line	26
IFNs, cytokines, and bioactive chemicals	27
DNA protocols	27
Molecular cloning techniques	27
Sequencing and sequence data analysis	28
Cloning JFH1 expression constructs	28
Cloning interferon- λ promoter luciferase constructs	30

RNA protocols	31
In vitro transcription of HCV RNA	31
RNA extraction	32
SYBR green relative RT-PCR	32
Taqman quantitative RT-PCR	34
siRNA knockdown	34
Microarray analysis	35
Protein protocols	36
Western blot	36
Immunoprecipitation	37
Virology assays	38
Infection	38
Virus production	38
Focus forming unit assay	39
Gradient fractionation	39
Interferon bioassay	40
Cellular Assays	40
Luciferase	40
LDL-R function assay	41
25-hydroxycholesterol treatment	41
Microscopy	42
Immunofluorescence staining	42
Flow cytometry	43

Intracellular staining of HCV	43
Surface CD81 expression	43
Statistics	43
CHAPTER 3: THE JFH1 CULTURE MODEL	44
Introduction	44
Results & Discussion	46
Virus infection parameters	48
Virus stability	50
Interferon sensitivity	52
Susceptible cell lines	53
CHAPTER 4: HCV ENTRY VIA LIPOPROTEIN INTERACTIONS	57
Introduction	57
Results	60
HCV interacts with lipoprotein metabolism	60
β -VLDL blocks HCV infection via apoE	64
Infectious HCV particles contain apoE	66
LDL-R is a co-receptor for HCV	69
Characteristics of HCV infectious particles	76
Discussion	80
CHAPTER 5: HCV ENGAGEMENT OF HOST INNATE IMMUNE DEFENSES	86
Introduction	86
Results	89
HCV infection induces an antiviral response	89

RIG-I is a key mediator of HCV control	92
HCV cleaves IPS-1 to disrupt innate immunity	95
HCV induces RIG-I independent innate immunity	99
Discussion	106
CHAPTER 6: TOWARDS THERAPY	110
APPENDIX A: 269 Genes regulated by HCV infection	112
REFERENCES	124

PUBLICATIONS

Owen DM, Huang H, Ye J, Gale M Jr. (2009) Hepatitis C virus infection via host interaction between apolipoprotein E and low density lipoprotein receptor. *Virology*. Nov 10;394(1):99-108.

Owen DM, Gale M Jr. (2009) Fighting the flu with inflammasome signaling. *Immunity*. Apr 17;30(4):476-478.

Suthar MS, Gale M Jr, **Owen DM**. (2009) Evasion and disruption of innate immune signaling by hepatitis C and West Nile viruses. *Cellular Microbiology*. Jun;11(6):880-888.

Saito T, **Owen DM**, Jiang F, Marcotrigiano J, Gale M Jr. (2008) Innate immunity induced by composition-dependent RIG-I recognition of hepatitis C virus RNA *Nature*. Jul 24;454(7203):523-7.

Lau DT, Fish PM, Sinha M, **Owen DM**, Lemon SM, Gale M Jr. (2008) Interferon regulatory factor-3 activation, hepatic interferon-stimulated gene expression, and immune cell infiltration in hepatitis C virus patients. *Hepatology* Mar;47(3):799-809.

Johnson CL, **Owen DM**, Gale M Jr. (2007) Functional and therapeutic analysis of hepatitis C virus NS3.4A protease control of antiviral immune defense. *J Biol Chem*. Apr 6;282(14):10792-803.

Huang H, Sun F, **Owen DM**, Li W, Chen Y, Gale M Jr, Ye J. (2007) Hepatitis C virus production by human hepatocytes dependent on assembly and secretion of very low-density lipoproteins *Proc Natl Acad Sci U S A*. Apr 3;104(14):5848-53.

Saito T, Hirai R, Loo YM, **Owen D**, Johnson CL, Sinha SC, Akira S, Fujita T, Gale M Jr. (2007) Regulation of innate antiviral defenses through a shared repressor domain in RIG-I and LGP2. *Proc Natl Acad Sci U S A*. Jan 9;104(2):582-7.

Loo YM, **Owen DM**, Li K, Erickson AK, Johnson CL, Fish PM, Carney DS, Wang T, Ishida H, Yoneyama M, Fujita T, Saito T, Lee WM, Hagedorn CH, Lau DT, Weinman SA, Lemon SM, Gale M Jr. (2006) Viral and therapeutic control of IFN-beta promoter stimulator 1 during hepatitis C virus infection. *Proc Natl Acad Sci U S A*. Apr 11;103(15):6001-6.

LIST OF FIGURES

Figure 1-1. HCV genome organization	3
Figure 1-2. Global prevalence of HCV infection	4
Figure 1-3. Stages of liver fibrosis	6
Figure 1-4. Lipoprotein metabolism	16
Figure 1-5. Pathways of intracellular innate immune response	20
Figure 3-1. Identification of HCV JFH1 immunoreactive human sera	47
Figure 3-2. HCV JFH1 entry kinetics	49
Figure 3-3. HCV JFH1 one step growth curve	50
Figure 3-4. Temperature stability of HCV JFH1	51
Figure 3-5. HCV JFH1 sensitivity to UV light	52
Figure 3-6. HCV JFH1 sensitivity to IFN- α	53
Figure 3-7. Cell line susceptibility to HCV JFH1 virus	55
Figure 3-8. CD81 expression in HepG2 cells	56
Figure 4-1. Microsomal triglyceride transferase activity required for efficient HCV release	62
Figure 4-2. Lipid modulation affects HCV lifecycle	64
Figure 4-3. β -VLDL competes with apoE for HCV binding and entry	65
Figure 4-4. ApoE is an HCV entry factor	66
Figure 4-5. ApoE associates with HCV RNA and infectious HCV particles	68
Figure 4-6. 25-hydroxycholesterol specifically inhibits LDL-R expression and function	70

Figure 4-7. Inhibition of HCV infection through suppression of LDL-R expression and function	72
Figure 4-8. 25-hydroxycholesterol inhibits LDL-R function but not HCV replication . .	73
Figure 4-9. Knockdown of LDL-R expression decreases HCV infection	75
Figure 4-10. ApoE is a component of low density infectious HCV particles	77
Figure 4-11. HCV peak infectivity occurs at low density	78
Figure 4-12. LDL-R modulation blocks entry of low density infectious HCV particles .	79
Figure 4-13. Model of HCV entry	85
Figure 5-1. HCV infection activates IRF3	90
Figure 5-2. Antiviral activity in supernatant of HCV RNA treated cells	92
Figure 5-3. RIG-I controls early HCV infection	94
Figure 5-4. HCV cleaves IPS-1 to block innate immune signaling	97
Figure 5-5. NS3/4A protease inhibitor restores innate immune response	99
Figure 5-6. HCV stimulates a RIG-I independent host response	102
Figure 5-7. HCV activates NFκB	104
Figure 5-8. Model of HCV interaction with innate immune system	109

LIST OF TABLES

Table 2-1. Cell lines used in this study	26
Table 2-2. Primers for cloning JFH1 protein expression vectors	29
Table 2-3. Primers for RT-PCR assays	33
Table 2-4. Antibodies used in this study	37

LIST OF ABBREVIATIONS

25-HC	25-hydroxycholesterol
ALT	alanine aminotransferase (serum marker of hepatic inflammation)
apo	apolipoprotein
AST	aspartate aminotransferase (serum marker of hepatic inflammation)
CARD	caspase recruitment domain
DAPI	diamidino-2-phenylindole
EMCV	encephalomyocarditis virus
ER	endoplasmic reticulum
FFU	focus forming unit
FH	familial hypercholesterolemia
HCV	hepatitis c virus
HDL	high density lipoprotein
HVR	hypervariable region
IDL	intermediate density lipoprotein
IFA	immunofluorescence analysis
IFN	interferon
IHH	immortalized human hepatocytes
IRES	internal ribosome entry site
ISG	interferon stimulated gene
IV	intravenous
JFH	Japan fulminant hepatitis

LIST OF ABBREVIATIONS

LDL	low density lipoprotein
MOI	multiplicity of infection
MTP	microsomal triglyceride transfer protein
NANB	non-A, non-B (hepatitis)
PAMP	pathogen associated molecular pattern
PBS(T)	phosphate buffered saline (0.1%Tween-20)
PFA	paraformaldehyde
RT-PCR	real time polymerase chain reaction
SCID	severe combined immunodeficiency
SREBP	sterol response element binding protein
SVR	sustained virologic response
TBS	tris buffered saline
UV	ultraviolet
VLDL	very low density lipoprotein

CHAPTER 1: INTRODUCTION

History

The exact time and place when hepatitis C virus (HCV) entered the human population is unknown. There are no known natural reservoirs of the virus other than humans so it is possible that HCV has been maintained in human populations for quite some time at low levels. The most closely related virus, GB virus B has been found in tamarins, so a remote monkey to human transmission may be the original source (123). The virus is relatively difficult to transmit person-to-person and as such it is likely that the modern pandemic has its origins in new patterns of human behavior made possible by medical technologies such as blood transfusions and hypodermic syringes. The first successful blood transfusion was performed by George Crile in 1906 (104). However, blood transfusions did not become common until the 1940s (8). Shortly thereafter, cases of post-transfusion hepatitis were recognized as a clinical entity. As antibodies for hepatitis A and B became available, these viruses were found to explain only a minority of post transfusion hepatitis cases. The remaining cases were then termed non-A, non-B (NANB) hepatitis (29). In 1989 scientists at the Chiron corporation cloned a gene sequence that, when expressed, reacted with sera from chimpanzees infected with NANB hepatitis (23). This new virus was termed hepatitis C virus and was found to explain the majority (90%) of NANB hepatitis cases.

Genome organization

HCV is an enveloped virus containing a 9600 nt single strand positive-sense RNA genome encoding a polyprotein that is processed by host and viral proteases into a set of structural and nonstructural proteins. The structural proteins include the core nucleocapsid protein and the envelope glycoproteins E1 and E2. E1 and E2 are components of the virus lipid envelope and function to mediate binding to co-receptors on hepatocytes, the target cell of HCV infection (30;108;118). The core protein consists of 2 domains, D1 which is highly basic and interacts with RNA and D2 which contains a hydrophobic motif mediating association with lipid droplets (47). P7 is pore forming protein of unknown function in the HCV lifecycle. The nonstructural proteins NS2, NS3/4A, NS4B, NS5A, and NS5B form the virus replicase and also function in virus-host interactions that modulate host defenses and cellular permissiveness for infection (32;35;79). NS3 contains helicase and protease domains and, when complexed with NS4A, efficiently cleaves the HCV polyprotein to liberate the separate NS proteins. It also targets host proteins for cleavage to disrupt innate immune signalling pathways discussed in more detail in Chapter 5. NS4B induces the formation of membranous webs associated with HCV replication (27). NS5A is a phosphoprotein that interacts with other HCV proteins and interferes with the host RNA-sensing molecule protein kinase R (PKR). NS5B is the error-prone RNA-dependent RNA polymerase with a mutation frequency of about 10^{-3} . As a result of this high mutation rate, HCV is present as a genetically heterogeneous population termed quasispecies within an infected individual. Sequence analysis divides HCV into 6 genotypes varying in geographic distribution

(122). Genotype 1, 2 and 3 viruses are the most prevalent in North America, while genotype 4 is found in Egypt, genotype 5 in South Africa, and genotype 6 in Southeast Asia. Sequence identity varies by about 30-35% between genotypes.

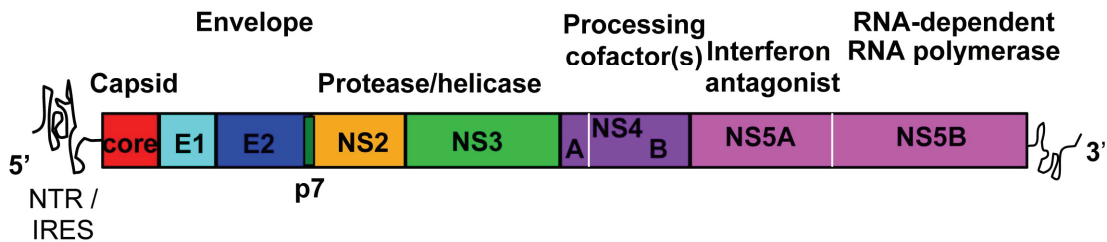


Figure 1-1. HCV genome organization.

Epidemiology

HCV is a hepatotropic virus, infecting greater than 170 million people worldwide. Within the United States, it is estimated that approximately 2% of adults are infected with HCV, while infection rates in countries worldwide range from less than 1% to as high as 20% (71). HCV is a blood-borne pathogen so, as mentioned above, patients receiving blood transfusion or other blood products as therapy were the first risk group identified. Implementing HCV screening protocols for donated blood has virtually eliminated this risk in the US. Differences in medical practices among healthcare systems such as blood supply screening and practices surrounding the use of injectable therapies likely explain the large variation in infection rates between different countries (Fig. 1-2).

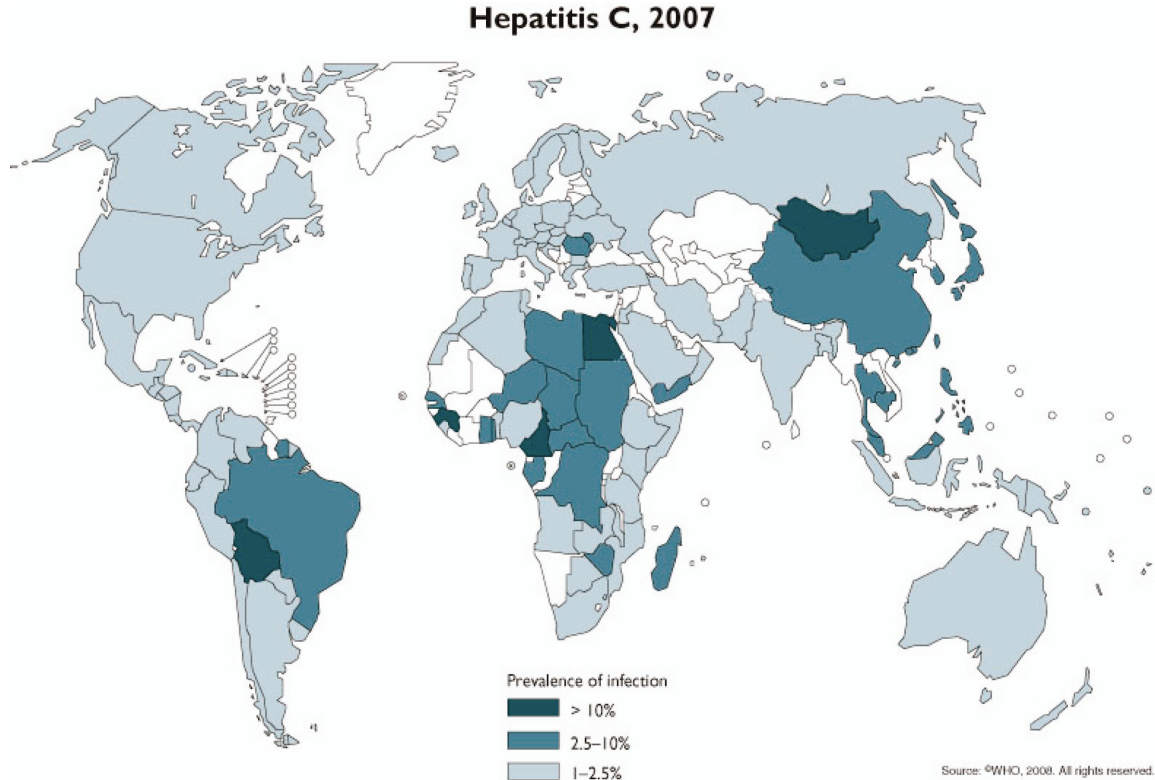


Figure 1-2. Global prevalence of HCV infection. Image ©WHO, 2008. Used with permission.

In the US and Western Europe most new infections now occur in IV drug users as a result of sharing needles or common preparation equipment (121). Other less common modes of transmission are occupational exposure (needle stick injury) in health care workers or sexual transmission, although the long term risk of transmission between discordant monogamous partners is less than 1% (131). There is also an approximate 5% risk of mother to child transmission. The incidence of new HCV infections in the US peaked in the 1980s and has since been on the decline (80). However, persistent HCV infections from this period are contributing to an increasing incidence of HCV-related

liver failure. HCV infection is the primary indication for liver transplant in the US and the leading cause of death among HIV HCV co-infected patients.

Clinical course

Acute HCV infection is often asymptomatic, and most HCV positive patients are unaware of their status until it comes to clinical attention years after infection. However studies of acute infection from a known exposure show that about 15% of patients are able to clear acute infection. The other 85% go on to develop chronic infection. Of these most will maintain a stable chronic hepatitis marked by mildly elevated liver enzymes (AST and ALT). However, 20% will develop liver fibrosis which progresses from mild fibrosis to moderate fibrosis, bridging the portal triad to the central vein, and finally to cirrhosis, the complete destruction of hepatic architecture (40) (Fig. 1-3). The mechanism of fibrosis is not entirely understood but involves activation of hepatic stellate cells which produce collagen in response to chronic inflammatory stimuli (88). Progression to cirrhosis results in a 5% annual risk for developing hepatocellular carcinoma, and may result in liver failure requiring transplant (71). Thus in addition to sustained virologic response, an important secondary target for therapy could be modulation of the pathologic chronic inflammation associated with fibrosis progression.

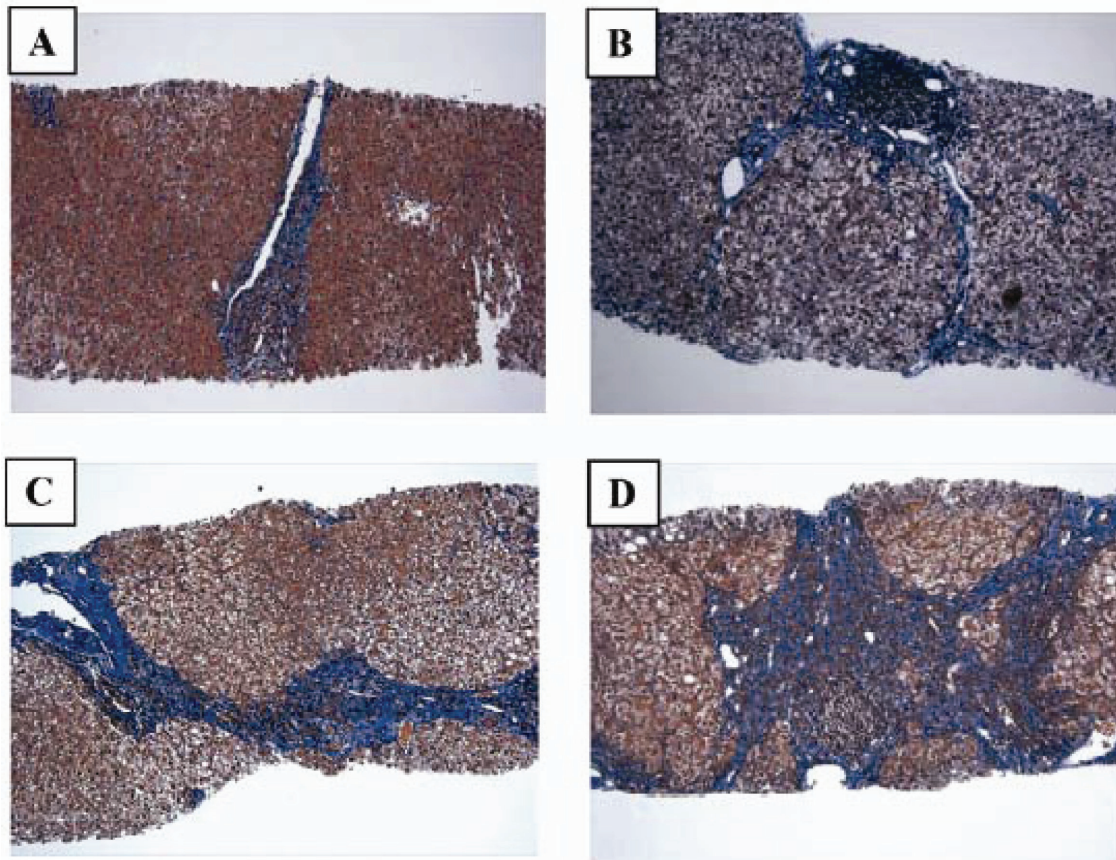


Figure 1-3. Stages of liver fibrosis. Staging of chronic hepatitis C virus (HCV) liver disease: absence of fibrosis (A), followed by low stage fibrosis (B), bridging fibrosis (C), and cirrhosis (D) (trichrome, 20x). Figure from Guzman, G. Overview of Liver Pathology (2008) *Disease-a-Month* **54**, 419-431. ©Elsivier Limited, 2008. Used with permission.

Therapy

Beginning in the 1970s and 1980s, advances in recombinant DNA technology facilitated the development and mass production of proteins as drugs, a general area of therapy referred to as “biologics” to distinguish it from “small molecules”. Recombinant interferon alpha was among these drugs and clinical trials were conducted using interferon for a range of infections and cancers. It was approved as a therapy for HCV in

1991 with studies showing an approximate 20% sustained virologic response (SVR), meaning no detectable HCV RNA 6 months after stopping therapy (46). Combination therapy with interferon alpha and the small molecule nucleoside analog ribavirin increased SVR to 40%. A further improvement was achieved by modifying interferon with polyethelene glycol (PEG-interferon) to increase its half life and bioavailability. Pegylated interferon resulted in 55% SVR against genotype 1 strains and 80% efficacy against genotypes 2 and 3.

Interferon and ribavirin are relatively non-specific antiviral therapies with varying efficacies against a range of viruses. Interferon works by binding to and signaling through the type 1 interferon receptor leading to the expression of interferon stimulated genes (ISGs) with antiviral activity. Various mechanisms for the efficacy of ribavirin have been proposed including inhibition of RNA replication, error catastrophe, and stimulation of innate immunity(70). Treatment with this regimen results in not only suboptimal SVR rates, but is also expensive (\$30,000-\$40,000) and associated with a range of side effects commonly including fatigue and depression. Therefore there is a need for improved and HCV-specific therapy such as protease and polymerase inhibitors targeting the virus enzymes. The high error rate of the NS5B polymerase leads to escape mutations for HCV-specific monotherapy so a combination therapy approach analogous to the highly active antiretroviral therapy (HAART) employed for the treatment of HIV will likely be required to improve therapy. Indeed two recent studies using the NS3/4A protease inhibitor telaprevir in combination with interferon and ribavirin resulted in a 67-69% SVR against genotype 1 infection, demonstrating the potential of this approach (43;87).

Model systems

Animal models

Prior to the identification of HCV it was demonstrated that injecting sera from NANB hepatitis infected patients into chimpanzees led to the development of hepatitis in these animals (7;45). After HCV was identified it was confirmed as the infectious agent by showing that HCV RNA alone injected into the liver of chimpanzees was infectious (67). Thus chimpanzees are able to serve as an animal model system for studying HCV pathogenesis. Another animal model system has been developed in which human hepatocytes are transplanted into severe combined immunodeficiency (SCID) mice where they repopulate the endogenous liver which has been destroyed by expression of plasminogen activator from a liver specific (albumin) promoter (89). However, given the expense associated with these systems, attempts have been made to develop tissue culture based assays of the HCV lifecycle.

Replicon

An important advancement was made with the HCV replicon system in which a hybrid HCV RNA expressing a neomycin resistance selectable marker under the control of the HCV internal ribosome entry site (IRES) is combined with the HCV nonstructural proteins under the control of an encephalomyocarditis virus (EMCV) IRES (78). When this RNA is transfected into cells and then selected with the antibiotic G418, colonies containing the stably replicating RNA can be found. The replicon system can be extended to include full genome length replicons as well as reporter tagged replicons expressing

green fluorescence protein (GFP) or luciferase to read out HCV replication (69;98).

These systems have been useful in developing high throughput screening assays for drug compounds that affect HCV replication. While the replicon model has been very useful in understanding the factors involved in HCV RNA replication, it does not support the production of infectious particles thus limiting its use in understanding HCV binding/entry.

Pseudoparticles

In order to address this limitation another model system, the HCV pseudotyped particle system, was developed to study virus entry. In this system HCV envelope proteins are expressed on the surface of a retrovirus particle (12;26;51). This system is useful for studying interactions between the HCV envelope proteins and putative cellular receptors and has validated receptors identified from soluble binding assays. However, it does not recapitulate important features of authentic HCV virions, namely the association with host lipoproteins which will be discussed in more detail below.

Cell culture infection

Early attempts to infect cell lines with clinical isolates of HCV were largely unsuccessful and did not result in robust replication. Some groups were able to detect cell associated HCV RNA, but limitations of these assays such as the difficulty in distinguishing between binding and entry, as well as the potential for false positive results in PCR assays to detect negative strand synthesis, limited their use (82). Finally in 2005 Wakita and colleagues reported the development of a genotype 2a virus termed JFH1. In

vitro transcribed RNA from this genome is able to robustly infect human hepatoma cell culture leading to the production of infectious particles (77;134). This system has allowed me to study HCV entry with an authentic HCV virion as well the early events in HCV engagement of the innate immune response. This model system is more fully described in Chapter 3.

Entry receptors

Initial attempts to understand HCV entry used binding assays with a soluble form of the HCV glycoprotein E2 in which the transmembrane region was deleted. Rosa et al. showed that recombinant soluble E2 produced in mammalian, but not yeast or insect cells, bound a human cell line but not mouse cell lines, and that antibodies which disrupted binding also protected chimpanzees from infection (113). This established a role for E2 in the infection process and also suggested that protein modifications such as correct glycosylation in mammalian cells may be important for proper interaction with the target cell. To identify receptors mediating this E2 dependent infection, Pileri et al. screened a cDNA library to identify factors that would facilitate E2 binding to mouse cells. This search identified the 25kDa membrane tetraspanin protein CD81 as a factor that could bind E2 (108). Similar iterative approaches were carried out to identify a number of molecules involved in HCV entry.

CD81

As mentioned above CD81 was the first HCV specific entry factor identified. CD81 is widely expressed in many cell types with the exception of red blood cells and platelets and is involved in a range of functions including integrin signaling and B-cell and T-cell activation (reviewed in (74)). The interaction between CD81 and E2 was mapped to the large extracellular loop of CD81 (30;107). Interestingly this region is identical in humans and chimps which are susceptible to HCV but differs by 4 amino acids in African green monkeys which do not bind E2 or become infected with HCV. One of these amino acids F186 was found to be critical for E2 binding (44). On E2 the conserved region at AA613-618 was important for binding, but differences in two hypervariable regions(HVR) HVR1 at 384-410 and HVR2 at 476-481 led to strain specific differences in E2 binding ability (112). The importance of this E2-CD81 interaction for entry was confirmed using the pseudoparticle system in which soluble CD81 or anti CD81 antibodies blocked entry by 30-100% (12;24;90;90;144). Expressing CD81 on HepG2 cells which do not otherwise express this receptor renders them permissive for pseudoparticle infection (24;144) Anti CD81 antibodies, soluble CD81, or siRNA knockdown of CD81 can also block infection with HCV JFH1 (77;134;145). While CD81 sequence variation helps explain the species tropism of HCV it does not explain the tissue tropism of the virus. Additionally CD81 does not efficiently internalize ligands and its activity in HCV infection can be blocked with antibodies at a post binding step, so it is likely that other molecules are also involved in HCV infection (28;107).

SR-BI

Scarselli and colleagues identified an additional E2 binding protein by incubating HepG2 cells which do not express CD81 with E2 and then crosslinking and immunoprecipitating cell surface proteins that bound E2. This search resulted in the identification of scavenger receptor class B type I (SR-BI). They also showed that SR-BI expressed on CHO cells could mediate E2 binding and that binding was dependent on HVR1 of E2 (118). The natural function of SR-BI is in binding high density lipoprotein (HDL) to mediate transfer of cholesterol from HDL particles to the membrane.

Reports on the role of SR-BI in infection have been conflicting. One study found that anti-SR-BI antibodies blocked uptake of HCV pseudoparticles by 70% while another observed no effect (13;51). Both studies used genotype 1a pseudoparticles on Huh7 derived cell lines, so the reasons for this discrepancy are unclear. In another study, knockdown of SR-BI by siRNA, or infection in the presence of anti-SR-BI antibodies, was shown to reduce pseudoparticle infection by about 50% (72). Voisset and colleagues found that HDL could enhance pseudoparticle entry through activity at a post binding step (133). This enhancement could be blocked by siRNA knockdown of SR-BI, although such treatment did not decrease pseudoparticle entry below baseline. Thus SR-BI may support infection indirectly via altering membrane cholesterol concentration. Alternatively these differences may be due to mutations which alter the binding affinity of E2 for SR-BI between different strains (39).

Using the JFH1 cell culture model, two studies showed that anti-SR-BI antibodies could block HCV infection. However it is still unclear if this blockade represents a specific disruption of E2-SR-BI binding or if the blockade is due to a disruption of an

SR-BI activity on membrane cholesterol concentration required for optimal HCV infection. The variable effect of antibodies, HDL-mediated enhancement, and the fact that depletion of membrane cholesterol with methyl- β -cyclodextrin inhibits HCV infection all argue for the latter possibility (62).

Claudin-1

CD81 and SR-BI were not yet sufficient to explain HCV entry as cell lines were identified which expressed both factors but were yet not permissive for pseudoparticle entry. Evans and colleagues screened a cDNA library to find factors that would make initially nonpermissive CD81⁺ SR-BI⁺ 293T cells permissive for pseudoparticle infection. These efforts identified the tight junction protein claudin-1 (28). Expressing claudin-1 on 293T cells also made them susceptible to infection with HCV JFH1, albeit at much lower levels than Huh7. By examining the effect on infection of antibody added at different times post binding, they found that claudin-1 acts at a later stage in the entry process than CD81. Interestingly murine claudin-1 was also able to support infection suggesting that claudin-1 is not a factor restricting species tropism.

Occludin

Most recently another tight junction protein occludin was identified. In a similar approach as that described above, a mouse embryonic fibroblast line, NIH3T3, overexpressing human CD-81, SR-BI, and claudin-1 was transfected with a cDNA library prepared from Huh7.5 cells and screened for pseudoparticle entry. This screen identified occludin, a transmembrane protein found as a component of tight junctions in polarized

epithelial cells, as a factor conferring infection (109). By expressing different combinations of human and murine CD81, SR-BI, claudin-1, and occludin, it was determined that human CD81 and human occludin are required for pseudoparticle infection and are thus important factors restricting species tropism of HCV infection.

LDL-R

There is also evidence for the role of the low density lipoprotein receptor in HCV infection which will be discussed below after a short review of lipoprotein metabolism.

HCV & Lipoprotein metabolism

Lipids & The liver

The liver is a key organ in the regulation of lipid metabolism. Following a meal lipids are taken up into the intestines where they are packaged into large particles called chylomicrons. These chylomicrons are targeted to the liver via the interaction between ApoB₄₈ and the low density lipoprotein receptor (LDL-R) on hepatocytes. The liver is a site of lipid repackaging as well as synthesis for subsequent distribution to the rest of the body through the production of very low density lipoprotein (VLDL) particles. VLDL synthesis begins on the endoplasmic reticulum (ER) membrane with an interaction between apolipoprotein B and microsomal triglyceride transfer protein (MTP) (53). MTP transfers lipid and cholesterol to a growing apoB-lipid complex. As this complex acquires more lipid it buds into the lumen of the ER where it then acquires additional lipid and apoE by fusion with intraluminal lipid droplets. VLDL is then processed through the

golgi apparatus and released into the bloodstream. Nascent VLDL delivers cholesterol and lipid to surrounding tissues through the action of lipoprotein lipase. Upon processing by lipoprotein lipase, VLDL loses lipid and apoC to become intermediate density lipoprotein (IDL). 50-70% of IDL is recycled back to the liver via an interaction between apoE and the LDL-R (130). The remaining IDL is further processed by hepatic lipase to become LDL which is taken up into hepatocytes and other tissues via the apoB-LDL-R interaction (Fig. 1-4).

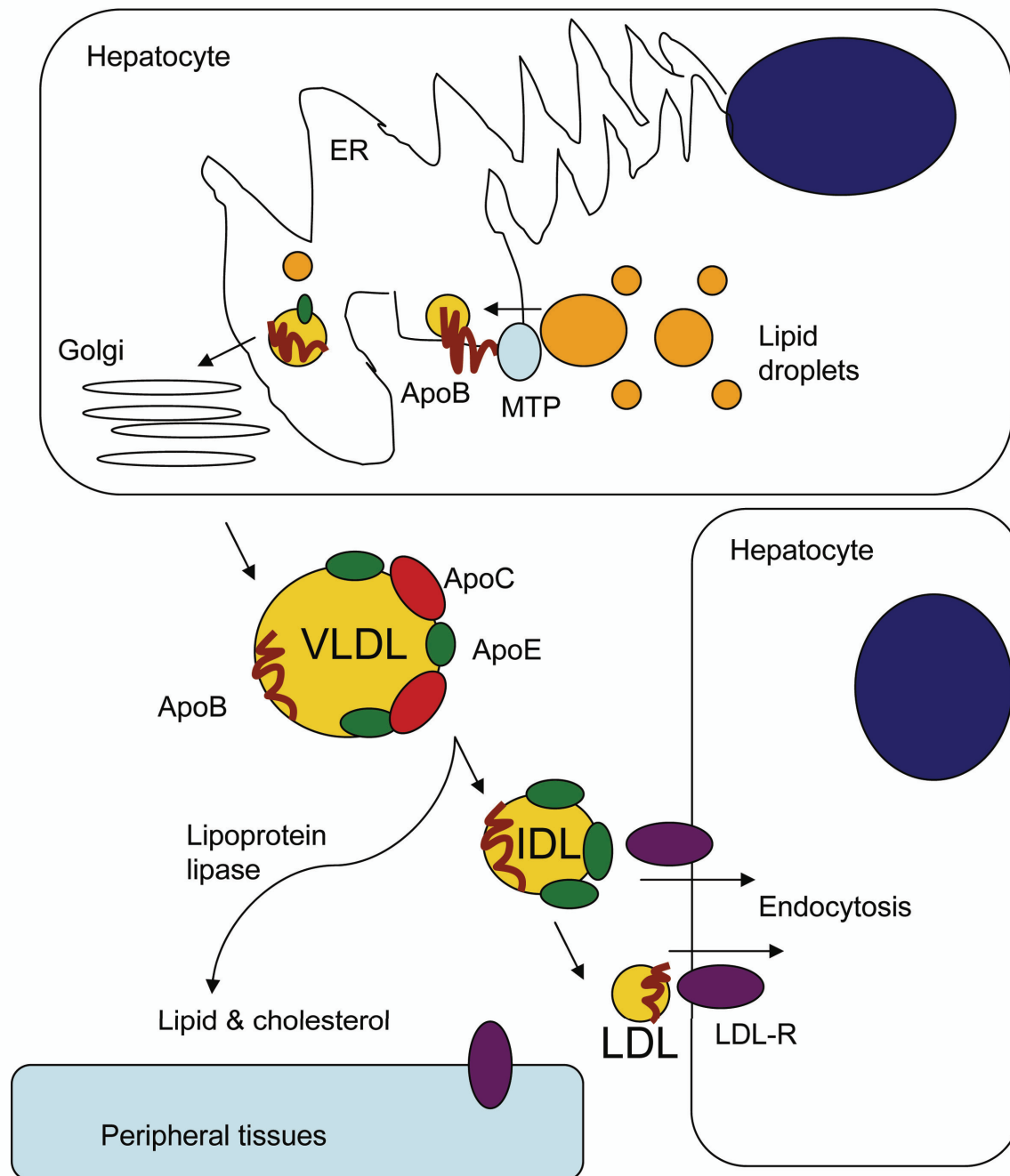


Figure 1-4. Lipoprotein metabolism.

Lipids & HCV

Early evidence for a link between HCV infection and lipid metabolism came from the observation that hepatic steatosis, the accumulation of fat within the liver, is a common complication of HCV infection (38). It is particularly associated with genotype 3 infections and has been linked to a mutation in the HCV core protein (50;92). In an attempt to understand the pathophysiology of this condition, transgenic mice expressing HCV proteins have been created and show that animals expressing a full length genome or just the HCV core protein develop hepatic steatosis (73;100). An explanation for this is provided by the observation that HCV core can block microsomal triglyceride transfer protein activity, a key enzyme required for the production and secretion of VLDL particles (106). In the absence of a functional secretory pathway lipid then accumulates in the liver. Immunofluorescence and electron microscopy studies show HCV core localized to the surface of lipid droplets (11). Thus HCV core protein present in lipid droplets seems to alter the ability of the liver to release VLDL.

Other observations suggesting a link between HCV and lipoprotein metabolism come from studies of HCV in infected patient sera. HCV RNA is present across a broad range of densities from 1.03 to 1.20 g/mL suggesting heterogeneity in the structure of HCV virions (128). However by infecting chimpanzees with HCV from fractionated serum it was determined that lower density fractions were more infectious (17). Anti-lipoprotein antibodies (apoB or apoE) could also precipitate HCV RNA from serum, suggesting that association of HCV virions with lipoprotein particles could explain the lower density particles (9;105;111;128).

LDL-R as an HCV receptor

Given that HCV was present in the serum of infected patients as a complex with lipoproteins, many groups speculated that LDL-R could play a role in the binding or internalization of HCV. At the time I began my studies, 3 papers had reported a role for LDL-R in the binding or internalization of patient derived HCV, although at the time it was impossible to determine if this represented non-specific uptake of HCV virions that happened to stick to lipoproteins in serum, or if this represented a coordinated event important for the lifecycle of productive HCV infection.

Monazahian et al. conducted binding studies using RT-PCR to detect cell associated HCV RNA upon incubation of cell lines with patient-derived virus (96). HCV from 10/13 patients was able to bind to human fibroblasts, although it generally represented less than 1% of the input RNA. Binding could be disrupted by 200ug/mL LDL and no binding was observed to LDL-R deficient familial hypercholesterolemia (FH) fibroblasts. Expressing LDL-R in African green monkey cells increased HCV binding from 3/12 serum samples to 10/12 samples.

Agnello et al. used an in situ hybridization assay to detect intracellular HCV RNA following incubation of HepG2 cells with patient-derived HCV (3). Although the sensitivity of this method is not very high, they were able to show qualitative differences in the staining patterns between infected and uninfected cells as well as show that the HCV staining pattern was dependent on LDL-R by demonstrating its absence when cells were infected in the presence of anti-LDL-R antibodies. Additionally, cells incubated with equal numbers of genome copies of HCV from VLDL and LDL fractions showed

positive staining while cells incubated with virus from HDL fractions did not, despite the fact that most of the HCV RNA was present in HDL fractions.

The most comprehensive data for HCV entry via a lipoprotein-LDL-R interaction came from Andre et al. who identified low density 100nm HCV RNA-containing particles which they termed lipoviral particles (LVP) (9). Binding of these LVP to cells (cell associated HCV RNA by RT-PCR) was much more efficient on a per genome copy basis than HCV RNA-containing material from whole serum. LVP binding could be blocked by VLDL, LDL, and a combination of apoB and apoE antibodies. LVPs did not bind to FH fibroblasts which lack the LDL-R. These observations all point to efficient HCV binding/entry mediated by lipoprotein associated HCV through the LDL-R, however the mechanism of HCV association with lipoproteins and the significance of this binding/entry pathway for productive infection remained unclear.

Innate immune defenses

After a virus has entered a cell it may be encounter the intracellular pathogen sensing components of the innate immune defenses. Type I IFN and the actions of innate immune genes form the first line of defense employed by the host to combat virus infection and are responsible for deterring virus replication and spread. Triggering type I IFN induction during infection begins with host recognition of an invading pathogen through unique biological structures called pathogen-associated molecular patterns (PAMP). In mammals, the major pattern recognition receptor (PRR) pathways include the RIG-I like receptor (RLR) and Toll-like receptor (TLR) signaling pathways. In the

case of RNA virus infections, viral nucleic acid structures and motifs, recognized by RLRs or TLRs, are the major stimulators of type I IFN induction (Fig.1-5). NOD-like receptors can serve as PRRs for bacterial products and generally lead to an inflammatory cytokine program as opposed to a type 1 interferon program, however evidence is accumulating that they may also play a role in innate immune response to viruses.

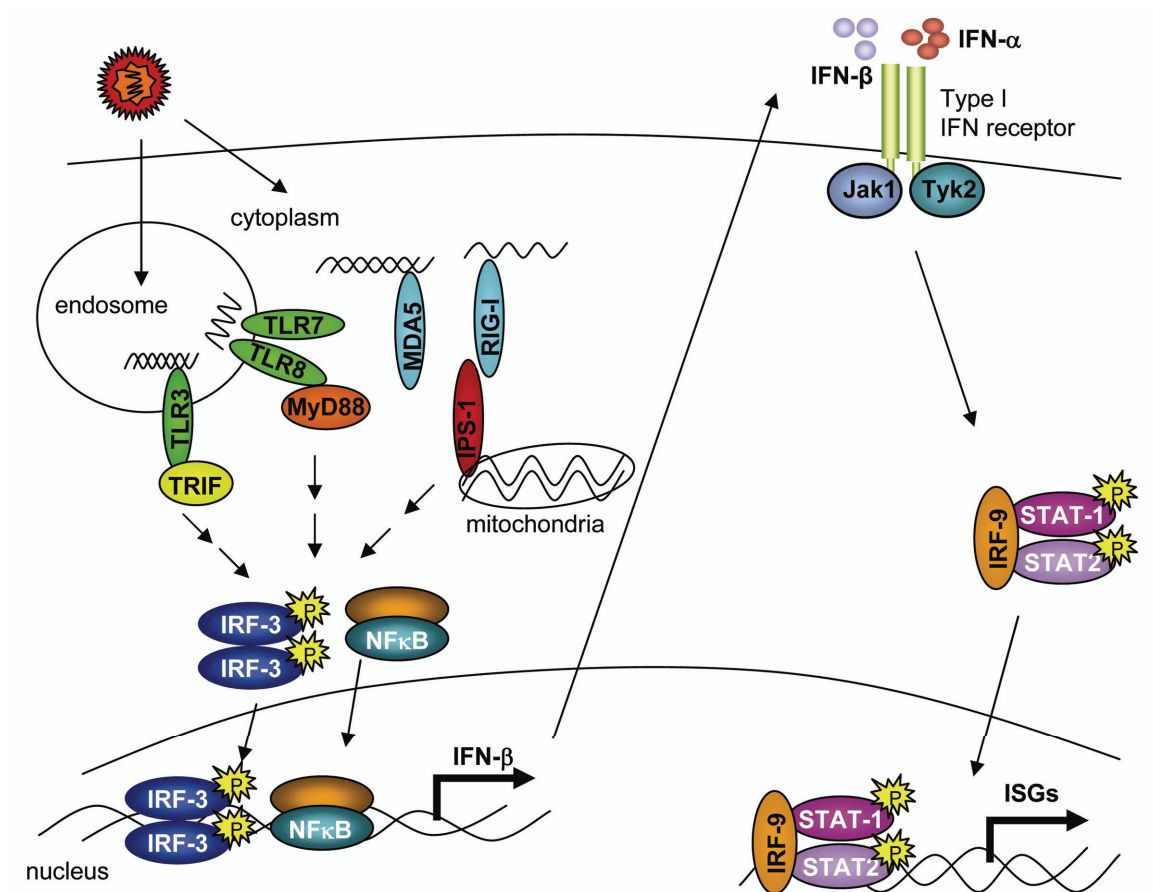


Figure 1-5. Pathways of intracellular innate immune response.

RIG-I like receptors

The RIG-I like receptors are cytoplasmic sensors of viral RNA, consisting of three members: retinoic acid inducible gene-I (RIG-I), melanoma differentiation antigen 5 (MDA5), and laboratory of genetics and physiology-2 (LGP2) (60;115;124;142;143). The molecular structures of RIG-I and MDA5 are similar, consisting of two tandem caspase association and recruitment domains (CARD) in the N-terminus and an RNA helicase domain in the C-terminus (142). In addition, RIG-I has a repressor domain that interacts with the CARD domains to maintain the receptor in a closed and non-active conformation in the absence of infection (116). LGP-2 contains an RNA helicase domain but lacks the CARD domains and may function as a regulator of RLR signaling (101;116;132). RIG-I and MDA-5 recognize unique structures and sequence motifs of viral RNA (64;65;117). Single-stranded (ss) RNA containing a 5' triphosphate, short double-stranded (ds) RNA, and uridine- or adenosine-rich viral RNA motifs have been identified as RIG-I ligands (48;117;125). The minimum length RNA for RIG-I recognition is 21 nucleotides, while MDA-5 is believed to recognize long dsRNA (>5kb) (63;83). When activated after binding to RNA ligand, RIG-I and MDA5 bind to the interferon-beta promoter stimulator-1 (IPS-1; also known as Cardif, MAVS, and VISA) (66;91;120;139), IPS-1 is a CARD protein and essential adaptor of RLR signaling, wherein it functions to bind RIG-I or MDA5 through CARD-CARD interaction that promotes the activity of a poorly defined macromolecular complex consisting of signaling components that result in the activation of the transcription factors interferon regulatory factor-3 (IRF3) and nuclear factor- κ B, (NF κ B). RLR signaling through IPS-1

leads to assembly of the IFN- β enhancer complex within the nucleus, consisting of IRF3, NF κ B, CBP/p300, and ATF-2/c-Jun, and triggering induction of IFN- β (57).

Toll-like receptors

The TLR family of innate immune signaling proteins consist of more than 10 different members, of which three recognize unique nucleic acid structures and motifs (4). TLR3, TLR7 and TLR8 are important for host defense against RNA viruses. Whereas TLR3 recognizes dsRNA ligands, TLR7 and TLR8 recognize uridine and guanosine-rich ssRNA ligands (5;25;42). TLR3 is expressed either on the cell surface or within the endosomal compartment (56;85;86). Upon binding dsRNA TLR3 recruits the adaptor molecule TIR domain containing adaptor inducing IFN- α (TRIF) and activates the transcription factors IRF3 and NF κ B to trigger IFN- α transcription (4). TLR7 and TLR8 are expressed within the endosomal compartment (41). Upon binding ssRNA ligands, the adaptor molecule myeloid differentiation factor 88 (MyD88) is recruited to the TLR and the transcription factors IRF7 and NF κ B are activated to trigger proinflammatory cytokines and type I IFN induction (4).

NOD-like receptors

The NLR family contains 23 members, of which a handful have begun to be characterized (33). The first NLRs identified, NOD1 and NOD2, detect bacterial peptidoglycan leading to NF κ B and MAP kinase signaling. Three other family members NLRC4/IPAF, NLRP1, and NLRP3/Cryopyrin/NALP3 form distinct caspase-1 activating complexes termed inflammasomes. NLRC4 responds to bacterial flagellin and

oligomerizes to recruit caspase 1 via interactions between the caspase activation and recruitment (CARD) domains present on each molecule. Caspase 1 is autocatalytically cleaved to its active form and is able to process proIL-1 β and proIL-18 into their mature secreted forms. This processing is the hallmark of inflammasome activity. NLRP1 responds to muramyl dipeptide, but does not contain a CARD domain so it relies on the adaptor protein apoptotic speck-like protein containing a CARD (ASC). NLRP3 also acts through ASC and is reported to respond to numerous stimuli including bacterial DNA and RNA, pore forming toxins, silica, asbestos, uric acid, and ion flux. A role for NLRP3 inflammasomes in response to virus infection is also emerging. Adenovirus DNA can stimulate inflammasome signaling in a NLRP3 dependent manner (102). Myxomavirus encodes a protein which interferes with ASC-mediated inflammasome signaling highlighting the importance of inflammasomes as a target for antiviral activity (59). Kanneganti et al. first demonstrated a role for NLRP3 during virus infection using in vitro infection of influenza or Sendai virus in macrophages (61). More recently, three groups have shown that NLRP3 inflammasome signaling plays a critical role in vivo in the immune response to influenza infection (6;55;55;127).

Interferon signaling

Induction of an antiviral state within a cell results from activation of JAK/STAT signaling leading to expression of interferon stimulated gene (ISG) products. Secreted type I IFN (IFN- α and IFN- β) bind in an autocrine or paracrine manner to cells through the IFN- α receptors (IFNAR)-1 and -2 to initiate the JAK/STAT signaling pathway. Once IFN is bound to its cognate receptors, receptor-associated Janus kinase 1 (Jak1) and

tyrosine kinase 2 (Tyk2) are activated and subsequently phosphorylate key tyrosine residues on the cytoplasmic subunit of the receptor and allow for the recruitment and phosphorylation of the signal transducer and activator of transcription 1 and 2 (STAT1 and STAT2). STAT1 and STAT2 heterodimerize and associate with interferon regulatory factor 9 (IRF9) to form the ISGF3 transcription factor complex. This complex translocates to the nucleus and binds to specific regions of DNA known as interferon stimulated response elements (ISRE), and turns on transcription of ISGs. Amplification of the type I IFN response occurs through a positive feedback loop involving IFN-induced expression of IRF7 followed by IRF7 dependent transcription of various IFN- α species (49;76;119).

CHAPTER 2: MATERIALS & METHODS

Cell culture

Media & culture conditions

Unless otherwise noted cell lines were maintained in Dulbecco's modified eagle medium (DMEM) (Cellgro) containing 10% fetal bovine serum (FBS) (Hyclone) supplemented with 1x non-essential amino acids (Cellgro), 1mM sodium pyruvate (Cellgro), 10mM HEPES buffer (Cellgro) and antibiotic/antimycotic solution (Cellgro, 100 IU/mL penicillin, 100 ug/mL streptomycin, 0.25 ug/mL amphotericin B final concentration) (normal media) and grown in an incubator at 37°C and 5% CO₂. A list of the cell lines used in this study and their selective media (if any) is listed in Table 2-1. Stocks of cell lines for long term storage were prepared by suspending cells in normal media containing 10% dimethyl sulfoxide (DMSO) and freezing in liquid nitrogen.

Construction of SGR-JFH1 cell lines

JFH1 subgenomic replicon (SGR-JFH1) cell lines were constructed in Huh7 and Huh7.5 backgrounds by transfecting in vitro transcribed SGR-JFH1 replicon RNA prepared from linearized pSGR-JFH1 into Huh7 or Huh7.5 and selecting with 800 µg/mL G418. Single colonies were selected and expanded. The clones expressing the highest level of HCV protein by western blot were designated SGR-JFH1 (7) and SGR-JFH1 (7.5). Following selection, cells were maintained in 400 µg/mL G418 (Cellgro).

Name	Description	Selection
GL	Produces JFH1 virions from stably integrated, ribozyme modified genome	5ug/mL Blasticidin
HepG2	human hepatoma line	
HepG2-CD81	HepG2-CD81 transgenic	400ug/mL Hygromycin
HP	High passage genotype 1b HCV replicon in Huh7 with multiple adaptive mutations	200µg/mL G418
HP cured	HP cured of replicon by IFN-a treatment	
Huh7	human hepatoma line	
Huh7.5	human hepatoma with T55I mutant RIG-I	
IHH	immortalized human hepatocytes from Ranjit Ray genotype 1b HCV replicon in Huh7 with single adaptive mutation	200µg/mL G418
K2040	K2040 cured of replicon by IFN-a treatment	
K2040 cured	primary hepatocyte line	
PH5CH8		
SGR-JFH1 (7)	JFH1 subgenomic replicon in Huh7	200µg/mL G418
SGR-JFH1 (7.5)	JFH1 subgenomic replicon in Huh7.5	200µg/mL G418
TR3772	LDL-R overexpressing cell line from Jin Ye	400µg/mL G418

Table 2-1. Cell lines used in this study

Construction of HepG2-CD81 cell line

HepG2-CD81 cells were constructed by transfecting HepG2 cells with Addgene plasmid 11588 (Addgene) which expresses the human CD81 cDNA under the control of a cytomegalovirus promoter. Cells were selected with 400 ug/mL hygromycin B (Invitrogen). Single colonies were picked, expanded, and screened by flow cytometry for CD81 cell surface expression. The clone with the highest CD81 expression was designated HepG2-CD81.

IFNs, cytokines, and bioactive chemicals

IFN- α -2a was purchased from PBL. IFN- β -1a (Avonex®) is from Biogen Idec. The sterol response element binding protein (SREBP) antagonist 25-hydroxycholesterol (25-HC) was obtained from Jin Ye. The microsomal triglyceride transferase protein (MTP) inhibitor BMS-2101038 (137) was synthesized by Chuo Chen at UT Southwestern Medical Center. The NS3/4A protease inhibitor ITMN-C was obtained from InterMune.

DNA protocols

Molecular cloning techniques

Polymerase chain reaction (PCR) was carried out using TaKaRa ExTaq (Takara Bio) enzyme and buffer according to the manufacturer's protocol in a BioRad MyCycler thermocycler and primers ordered from Integrated DNA Technologies. PCR products were purified by agarose gel electrophoresis and extracted with the QIAquick gel extraction kit (Qiagen). Restriction digests were performed in 20-50ul reactions using enzymes and buffers from Promega or New England Biolabs according to the manufacturer's protocol. Ligation of sticky ends was done using a 3:1 molar ratio of insert:vector in a 20uL reaction with T4 DNA ligase (NEB) at room temperature for 1 hour or overnight at 16°C. Ligation reactions were transformed into One Shot® TOP 10 or MAX Efficiency® DH5 α chemically competent E. coli cells (Invitrogen) by incubating 1 μ l of ligation reaction with 50 μ l cells on ice for 30 minutes, heat shocking at 42°C for 30 seconds and then incubating on ice for an additional 2 minutes. Cells were

plated on Luria-Bertani (LB) media containing the appropriate selective marker and incubated at 37°C. Plasmid stocks were prepared by inoculating a single colony into 50mL of LB broth, growing overnight at 37°C with shaking at 225rpm, and extracting plasmid DNA with the GenElute Endotoxin-free Plasmid Midiprep Kit (Sigma). DNA concentration was determined using NanoDrop spectrophotometry. Plasmid stocks were stored at -20°C and transformed bacteria stocks were stored at -80°C in 10% DMSO or 50% glycerol.

Sequencing and sequence data analysis

DNA sequencing was performed by the McDermott Center Sequencing Core at UT Southwestern or the University of Washington Biochemistry DNA Sequencing Facility. Both facilities used 1200ng of plasmid template and 8pmol primer in a 12ul volume and were amplified using Big Dye Terminator 3.1 chemistry and analysed by capillary electrophoresis (ABI). Trace files for manual base-calling and verification were examined using Chromas software (Technelysium). Sequence data was analysed, annotated, and otherwise manipulated and explored using Vector NTI software (Invitrogen).

Cloning JFH1 expression constructs

Plasmids expressing the JFH1 nonstructural proteins were constructed by PCR amplifying the nonstructural genes from the pJFH1 template using primers containing a NotI site engineered in the 5' primer and an XbaI site in the 3' primer. (Primers are listed in Table 2-2). PCR products were digested in a NotI XbaI double digest. These products

were ligated into pFLAG-CMV-HA which had also been digested with NotI and XbaI and treated with alkaline phosphatase. This vector creates a 5' Flag-HA tagged fusion protein under the control of a CMV promoter. The resulting constructs were called pNS3/4A (JFH1), pNS4A/B (JFH1), pNS4B (JFH1), pNS5A (JFH1), and pNS5B (JFH1). Constructs were verified by restriction digest and sequencing using primers M13-21 (5'-TGTAACGACGGCCAGT-3') and M13-REV (5'-CACACAGGAAACAGCTATGACCAT-3'). Expression was confirmed by transfecting these constructs into Huh7 cells and immunoblotting for HA reactive protein of the expected size.

#	Name	Sequence	Description
662	JFH 2781 a	TTAGGCATAAGCCTGCCGGGGCAGTG	3' primer to clone structural proteins Core-P7
663	JFH351s	GTAGACCGTGCACCATGAGCA	5' primer to clone structural proteins Core-P7
668	NS3/4A_JFH1_NotI	GCGGCCGCTGCTCCCATCACTGCTTATGC	5' primer to clone NS3/4A
669	NS3/4A_JFH1_XbaI	TCTAGACTAGCATTCTCCATCTCATCAAAGC	3' primer to clone NS3/4A
670	NS4AB_JFH1_NotI	GCGGCCGCTAGCACGTGGGTCCTAGCTG	5' primer to clone NS4AB
671	NS4AB_JFH1_XbaI	TCTAGACTAGCATGGGATGGGGCAGTC	3' primer to clone NS4AB
672	NS4B_JFH1_NotI	GCGGCCGCTGCCTCTAGGGCGGCTCTCATC	5' primer to clone NS4B (use w/ #671)
673	NS5A_JFH1_NotI	GCGGCCGCTTCCGGATCCTGGCTCCGC	5' primer to clone NS5A
674	NS5A_JFH1_XbaI	TCTAGACTAGCAGCACACGGTGGTATC	3' primer to clone NS5A
675	NS5B_JFH1_NotI	GCGGCCGCTTCCATGTCATACTCCTGGACCG	5' primer to clone NS5B
676	NS5B_JFH1_XbaI	TCTAGACTACCGAGCGGGGAGTAGGAAG	3' primer to clone NS5B

Table 2-2. Primers for cloning JFH1 protein expression vectors.

Cloning interferon- λ promoter luciferase constructs

In order to study the transcriptional activation of interferon- λ (Type 3 interferons), Promoter luciferase constructs containing the 2kb region upstream of the transcription start site of the interferon- λ 1 or interferon- λ 3 genes was cloned into pGL3-Basic (Promega), a plasmid which expresses firefly luciferase under the control of an inserted promoter of interest. To construct pIFN- λ 1luc, template DNA was isolated from a human blood sample using the Qiagen genomic DNA extraction kit. IFN- λ 1 (also called IL-29) promoter was amplified from this template in a PCR reaction using primer IL-29 fwd (5'-GAAGATCTCAAGTCACTTTGCCTTCCTATGCC-3') which contains a BglII site and IL-29 rev (5'-CTGCAGCCATGGCTAAATCGC-3') which contains an NcoI site. The resulting PCR product and PGL3-Basic vector were digested with these enzymes and ligated together to form pIFN- λ 1luc. Due to the high homology between IFN- λ 2 and IFN- λ 3 (also called IL-28A and IL28B, respectively), IFN- λ 3 could not be efficiently amplified from genomic DNA, so a BAC containing the appropriate sequence, CTC-246B18 (ResGen) was used as the template for PCR. Primer IL-28B fwd (5'-CCCAAGCTTCGCAGCCTTGGGCCTGAC-3') which contains a HindIII site and primer IL-28B rev (5'-GACGACTCATGACTGTGTGCACAGAGAGAAAGGGAGC-3') which contains a BspHI site were used to amplify the IFN-L3 promoter, digested, and then ligated into pGL3-Basic which had been digested with HindIII and NcoI (compatible with BspHI) to create pIFN-L3luc. These constructs were verified by sequencing with: RVprimer 3 (5'-CTAGCAAAATAGGCTGTCCC-3'), GLprimer2 (5'-CTTTATGTTTTTGGCGTCTTCCA-3'), and IL-29revseq (5'-TCTCAGCTACTCAGGAGGC-3').

RNA protocols

In vitro transcription of HCV RNA

In vitro transcription was used to prepare infectious HCV JFH1 RNA for transfection to produce virus particles or as a control for RT-qPCR assays. 10ug of pJFH1 was linearized by digestion with XbaI in a 50ul reaction overnight at 37°C in order to ensure that the RNA transcript would contain the correct 3' end. XbaI activity was inactivated by incubation at 65°C for 2 hours. The reaction was then treated with 0.5ul mung bean nuclease (Promega) for 1 hour at 37°C to remove any overhanging ends. To remove protein, 20ul of the reaction was treated with 0.5ul 20% SDS and 0.5ul of 1mg/mL proteinase K and incubated at 50°C for 1 hour. DNA was then precipitated by adding 1/20 volume 0.5M EDTA, 1/10 volume 5M sodium acetate, and 2 volumes 100% ethanol and chilling at -20C for \geq 15 minutes. DNA was pelleted by centrifugation, washed with 70% ethanol, dried, and resuspended in 9ul water.

4ug of this DNA was then used as a template for in vitro transcription using the Megascript T7 kit (Ambion) in a 20ul reaction containing 2ul reaction buffer, 2ul of each ribonucleotide and 2ul of enzyme mix. In vitro transcription was carried out at 37°C for 3 hours, an additional 2ul of enzyme mix was added, and the reaction was incubated for an additional 2 hours at 37°C. Template DNA was removed by incubation with 1ul RNase free DNase1 at 37°C for 1 hour. To precipitate RNA, 25ul of RNase free water was added along with 25ul lithium chloride precipitation solution (7.5M LiCl, 50mM EDTA) and then the reaction was incubated at -20C for \geq 30 minutes. RNA was pellet by centrifugation at maximum speed in a microcentrifuge for 15 minutes. The pellet was

washed once with 70% ethanol, resuspended in 50ul nuclease free water, and stored at -80°C.

RNA extraction

For relative quantitation of cellular mRNAs or HCV RNA, cells were washed with PBS and detached with 0.05% trypsin (Gibco). Trypsin activity was neutralized by the addition of media containing 10% FBS. Cells were pelleted at 35,000 rpm for 1 minute, washed with PBS and lysed in 540ul Buffer RLT (Qiagen). Lysates were homogenized by passing 5 times through a 20 gauge needle or by using Qiasredder columns (Qiagen) in the case of infectious samples. The RNeasy kit (Qiagen) was used according to the manufacturer's protocol to extract RNA, with the addition of an on-column DNase digestion step. RNA was eluted in 40uL of nuclease free water and concentration determined by NanoDrop spectroscopy. RNA samples were stored at -80°C.

For quantitation of HCV RNA in cell free supernatants or pellet fractions of immunoprecipitation reactions, HCV RNA was extracted from 140uL of supernatant or agarose bead slurry using the QIAamp viral RNA mini kit (Qiagen) according to the manufacturer's protocol and eluted in 80uL of water to allow 25uL of RNA to be used in triplicate for real time (RT)-PCR reactions.

SYBR green relative RT-PCR

RNA samples were diluted with nuclease-free water to prepare 10ng/uL stocks of each sample. 25uL RT-PCR reactions were set up in triplicate using 12.5ul SYBR green

master mix (ABI), 1ul 1.25uM primer mix, 0.25ul RNase inhibitor, 6.125ul water, and 5ul (50ng) RNA sample, and 0.125ul reverse transcriptase. For each sample, GAPDH control reactions were set up in parallel to the gene(s) of interest. “No template” controls were prepared for each primer set and “no reverse transcriptase” controls were prepared for each RNA sample. Reactions were prepared in 96 well plates, sealed, and centrifuged at 300g for 2 minutes. Plates were run in an Applied Biosystems 7300 Real Time PCR system using a 30 minute reverse transcription step at 48°C and a 10 minute step at 95°C, followed by 40 cycles of [95°C for 15 seconds, 60°C for 60 seconds]. Cycle threshold (Ct) values were exported to Microsoft Excel and then fold change in mRNA expression was calculated by the formula $\text{fold change} = 2^{-ddCt}$, where $dCt = (Ct(\text{gene of interest}) - Ct(\text{GAPDH}))$ and $ddCt = dCt(\text{experimental sample}) - dCt(\text{control sample})$. The primers used to amplify genes of interest are show in Table 2-3.

#	Primer	Sequence
013	IFNbeta_r 5'	CAGCAATTTTCAGTGTGTCAGAAGCT
014	IFNbeta_r 3'	TCATCCTGTCCTTGAGGCAGTAT
017	GAPDH_4 5'	CTG GGC TAC ACT GAG CAC CAG
018	GAPDH_4 3'	CCAGCGTCAAAGGTGGAG
087	JFH1S	TGCGGAACCGGTGAGTACAC
088	JFH1A	GGGCATAGAGTGGGTTTATCCA
091	hIFN-b forward	TGCTTCTCCACGACAGCTCTTT
092	hIFN-b reverse	CCCATTCAATTGCCACAGGA
095	HCVTaqS	cgggagagccatagtg
096	HCVTaqAS	agtaccacaaggccttgcg
123	IFN-L1 fwd	CACGCGAGACCTCAAATATGTG
124	IFN-L1 rev	AGGGTGGGTTGACGTTCTCA
125	IFN-L2/3 fwd	GCCACATAGCCCAGTTCAAGTC
126	IFN-L2/3 rev	GGCATCTTTGGCCCTCTTAAA
127	Human IL-28A	Superarray
128	Human IL-29	Superarray
131	Human IL-18	Superarray
132	Human IL-1B	Superarray

Table 2-3. Primers for RT-PCR assays.

Taqman quantitative RT-PCR

Quantitative RT-PCR (RT-qPCR) reactions to determine HCV levels in terms of absolute genome copy number per volume were set up using the GeneAmp EZ rTth RNA PCR kit (ABI), primers HCVTaqS and HCVTaqAS (Table 2-3), and Taqman probe (ABI). Triplicate 50uL reactions were set up using 25ul RNA extracted with the QIAamp Viral RNA minikit (Qiagen) and 2x the volumes of components listed in the manufacturer's protocol for a 25ul reaction. A standard curve using in vitro transcribed HCV RNA was set up in duplicate or triplicate at 10^8 , 10^6 , 10^5 , 10^4 , 10^3 , 10^2 , and 10^1 genome copies per well based on the length of 9.6kb length of the HCV genome and base pair mass of RNA such that 48.8ng HCV RNA= 10^{10} genome copies. Plates were run in an Applied Biosystems 7300 Real Time PCR system using a 30 minute reverse transcription step at 60°C and a 5 minute step at 95°C, followed by 40 cycles of [95°C for 20 seconds, 62°C for 60 seconds]. Genome copies per well were converted to genome copies per mL by multiplying by a factor of 7.14 (RNA extracted from 140ul/1000uL, divided into 1/3 wells).

siRNA knockdown

Previously described siRNA duplexes targeting CD81 (UGAUGUUCGUUGGCUUCCU), SR-BI (GCAGCAGGUCCUUAAGAAC), and Claudin-1 (UAACAUUAGGACCUUAGAA) were purchased from Dharmacon. The member of the siGENOME ON-TARGETplus SMART pool (Dharmacon) targeting the LDL receptor, which resulted in the greatest knockdown of *Ldl-r* mRNA expression, was identified (GGACAGAUUCAUCAACGA). 0.4nmols of these siRNA duplexes were

transfected into 1×10^5 Huh7.5 cells using RNAiMAX transfection reagent (Invitrogen). Cells were analyzed for knockdown or used for infection at 3 days post transfection.

Microarray analysis

For microarray analysis of response to HCV infection, Huh7 and Huh7.5 cells were infected at MOI=2 and samples were collected at 4, 12, 24, 36, and 72 or in a separate experiment 72, 96, and 120 hours post infection. RNA was extracted using the RNeasy kit. Fluorescent Cy3 and Cy5-labelled cRNA were synthesized from total RNA using the Agilent Low RNA Input Fluorescent Linear Amplification Kit according to the manufacture's specifications. Fluorescent cRNA targets were purified using Qiagen RNeasy mini spin columns and then evaluated using the NanoDrop Spectrophotometer. Human 1A Oligo Microarray (V2), which contains over 20,000 60-mer probes corresponding to over 18,000 human genes, were purchased from Agilent. Hybridisation and washing of slides was performed according to Agilent's protocols. Spot quantitation, normalization and application of a platform-specific error model was performed using Agilent's Feature Extractor software and all data was then entered into a custom-designed database, Expression Array Manager, and then uploaded into Rosetta Resolver System 4.0.1.0.10 (Rosetta Biosoftware, Kirkland, WA) and Spotfire Decision Suite 7.1.1 (Spotfire, Somerville, MA). A single experiment comparing two samples, one from a HCV-infected cells and one from the mock infected cells, was performed with four replicate arrays using the dye label reverse technique, thus providing mean ratios between the expression levels of each gene in the analyzed sample pair, standard deviations, and *P* values.

Protein protocols

Western blot

For immunodetection of proteins, cells were washed with PBS and detached with .05% trypsin. Trypsin activity was neutralized by the addition of media containing 10% FBS. Cells were pelleted at 3,500 rcf for 1 minute, washed with PBS and lysed with 100uL of cell lysis buffer consisting of 25mM Tris, 150mM NaCl, 1% TritonX-100, 1mM EDTA supplemented with 1ul okadaic acid, 10ul aprotinin (Sigma) and 10ul Sigma protease inhibitor cocktail per mL. Lysates were incubated on ice for 10 minutes and then pelleted at 12000g for 10 min. Supernatants were transferred to a new tube and protein levels quantitated by Biorad assay using 1 ul of sample in 200ul of reagent. Protein concentrations were determined by comparison to a standard curve prepared with a known concentration of BSA.

20-100ug of protein was mixed with an appropriate volume of 2x or 4x SDS loading buffer and boiled at 100°C for 5 minutes. Samples were separated by SDS-PAGE and transferred to nitrocellulose membranes. Membranes were blocked with 5% milk in PBST. After a brief rinse with PBST, membranes were probed with primary antibody for ≥ 1 hour at the dilutions listed below in Table 2-4. Blots were washed and incubated with 1:10,000 peroxidase-conjugated secondary antibody (Jackson Immunoresearch) for 1 hour (conventional) or 10 minutes (SnapID system, Milipore). Membranes were washed 3 x 5 minutes in PBST and developed using ECL reagent (GE Healthcare). For multiple probings, blots were washed in PBST for 5 minutes, water for 5 minutes and then stripped in 0.2M NaOH for 5 minutes at room temperature or β -

mercaptoethanol stripping buffer (25mM Tris, 100mM β -ME, 1% SDS) for 30 minutes at 55°C, followed by a 5 minute water wash and 2 x 5 min washes with PBST.

Relative densitometry analysis was performed using ImageJ software (NIH) and the formula (mean intensity experimental band – mean intensity background) / (mean intensity control band – mean intensity background).

Antibody	Animal	Source	WB	IFA
α 1-antitrypsin	sheep	Biodesign International	1:2000	
Actin	goat	Santa Cruz	1:500	
ApoB	sheep	Biodesign International	1:1000	
ApoE	goat	Calbiochem	1:2000	1:1000
α -Tubulin	mouse	Sigma	1:5000	
Claudin-1 (2H10D10)	mouse	Zymed	1:500	
GAPDH	goat	Santa Cruz	1:1000	
HA	mouse	Sigma	1:5000	
HCV Core	mouse	Affinity BioReagents		1:500
IPS-1	rabbit	James Chen	1:1000	
ISG-56	rabbit	Ganes Sen	1:4000	
LDL-R (HL-1)	mouse	Jin Ye	1:2000	
LDL-R (C7)	mouse	Jin Ye	1:500	
NF κ B p65	rabbit	Upstate	1:1000	
Serum A	human	Will Lee	1:2000	1:3000
Serum F	human	Will Lee	1:1000	
SR-B1 (ab396)	rabbit	Abcam	1:2000	
IKBa	rabbit	Santa Cruz	1:1000	
IRF3	rabbit	Michael David		1:500

Table 2-4. Antibodies used in this study.

Immunoprecipitation

For recovery of immunocomplexes, up to 500uL of HCV-containing supernatant was incubated with the indicated antibody for 1 hour and then 50uL of Protein G Plus Agarose Suspension (Calbiochem) was added. Tubes were rocked at 4°C overnight and then centrifuged at 1000g for 2min. Supernatant was removed and used for infection,

RNA extraction, or mixed with SDS sample buffer for western blotting. Pellets were washed 3 times with PBS and then used for RNA extraction or western blotting.

Virology assays

Infection

For infections with HCV at a defined MOI, concentrated virus stocks were diluted with an appropriate amount of DMEM and incubated with Huh7.5 cells for 1.5 hours. Cells were washed 1 time with PBS and then maintained in DMEM containing 10% FBS and analyzed 48 hours post infection, unless otherwise indicated. Infections with Sendai virus (Cantrell strain, Jackson Labs) were performed at 100 hemagglutination units (HAU) per mL by diluting a 4,000 HAU/mL stock in serum free media and incubating cells with virus for 1 hour, washing 1 time with PBS, and then maintaining cells in DMEM containing 10% FBS for up to 24 hours.

Virus production

HCV was collected from the supernatant of an Huh7 derived cell line that constitutively produces genotype 2a strain JFH1 RNA from a ribozyme-modified HCV genome integrated into the host genome (kind gift from George Luo). For large scale virus preps, these cells were incubated with DMEM containing 2% FBS for 48 hours and then the HCV containing supernatant was filtered through a .22uM filter and concentrated 100x using Centricon 100,000MW cut-off filters (Millipore). Alternatively, high titer virus stocks were prepared by seeding 1×10^6 Huh7.5 cells in a T-75 flask and

infecting on the following day with 2×10^4 FFU of a passaged cell-culture adapted strain of HCV JFH1 prepared by Andrea Erickson and propagated by Courtney Wilkins. This yields an MOI of ~ 0.01 . Cells are then expanded to several 15cm dishes. At 4 days post infection media was changed to 2% FBS media and harvested when cytopathic effects became evident. These sups were then filtered and concentrated as described above. Virus stocks were stored at -80°C .

Focus forming unit assay

100uL of virus sample were used to infect 2×10^4 Huh7.5 cells in triplicate in a 48 well dish. After 48 hours, plates were washed with PBS and fixed for 30 minutes in 3% paraformaldehyde. Cells were permeabilized with 0.2% TritonX-100 in PBS for 15 minutes. Cells were then blocked in 10% FBS for 10 minutes and stained using 1:1500 human α -HCV polyclonal serum for 1 hour, followed by 1 hour of 1:500 peroxidase-conjugated donkey α -human antibody (Jackson ImmunoResearch). Infected foci were visualized using the Vector VIP peroxidase substrate staining kit according to the manufacturer's protocol (Vector Labs) and counted by light microscopy on a Nikon Eclipse TE2000-E microscope.

Gradient fractionation

To fractionate HCV virions by density, 5-50% iodixanol gradients (Optiprep) were prepared in DMEM buffered with HEPES and equilibrated overnight at 4°C . 0.5mL of virus sample was loaded on the top of the 10mL gradient and then spun in an Sw40Ti ultracentrifuge rotor at 40,000rpm for 6 hours. 1mL fractions were removed by pipetman

from the top of the gradient into pre-massed microcentrifuge tubes. Mass of the tube subtracted from the mass of the tube + fraction yielded the density in g/mL of each fraction. Fractions were then used for infection, RNA extraction, immunoprecipitation, or frozen at -80°C for later use.

Interferon bioassay

A bioassay of interferon activity present in conditioned media was carried out on the basis of ability to block vesicular stomatitis virus (VSV) infection. 2×10^4 cells were seeded per well in a 96 well plate format. (Note: each sample to be tested in duplicate requires 24 wells). Conditioned media to be tested was treated with UV to inactivate virus infectivity. 2-fold serial dilutions of conditioned media or 1000 U/mL IFN- β control were prepared and incubated with cells for 12 hours. This media was removed and then cells were infected with VSV at MOI=5 in a volume of 50ul/well (diluted in DMEM) for 1 hour. Virus was removed and then cells were incubated in normal media for an additional 12 hours before staining with crystal violet. Interferon activity in experimental samples was measured by comparing the dilution cutoff where cells remain uninfected (purple- cells present, clear- cells lysed by infection) to the standard curve.

Cellular assays

Luciferase

In order to measure IFN- β or IFN- λ promoter activity, pIFN- β luc, pIFN-L1luc, pIFN-L2H, or pIFN-L3 were transfected into cells at a 4:1 molar ratio with pCMV-

Renilla. For infection assays, cells were infected 24 hours post transfection and then analysed 16-24 hours post infection (Sendai virus) or 24-48 hours post infection (HCV). At this time samples were lysed in 60ul passive lysis buffer/well. Triplicate 25 ul samples were measured using 25ul Luciferase Assay Substrate (firefly) and 25ul Stop & Glo Substrate (renilla) (Promega) dispensed and read by a Berthold Centro LB960 luminometer. Data was collected using MikroWin2000 software and exported to Microsoft Excel for analysis. Relative luciferase units (RLU) were calculated by the formula $RLU = [\text{ratio experimental sample (firefly/renilla)}] / [\text{ratio control sample (firefly/renilla)}]$.

LDL-R function assay

Uptake of 3'-prenylmethyl-23,24-*dinor*-5-cholesterol-22-oate-3 β -ol (PMCA) oleate, a blue fluorescent cholesterol analog, was used to assess endocytic activity of the LDL-R (68). Cells were incubated for 16 hours in media containing 1 $\mu\text{g}/\text{mL}$ PMCA oleate and assessed by fluorescence microscopy or by flow cytometry on the Pacific Blue channel of an LSRII flow cytometer (BD Biosciences).

25-hydroxycholesterol treatment

To modulate LDL-R expression, cells were treated for 16 hours in DMEM containing 10% NCL-PPS (newborn calf lipoprotein deficient serum), 50uM compactin, 50uM mevalonate, 10uM geranylgeraniol, 10ug/mL cholesterol and the indicated amount of 25-hydroxycholesterol. We note that 25-HC treatment of cells suppresses the synthesis of geranylgeraniol, a prenyl lipid that is essential for HCV replication (136;141). Thus, in

order to retain HCV replication competence of cells all treatments with 25-HC were carried out in the presence of 10uM geranylgeraniol.

Microscopy

Immunofluorescence staining

Cells analysed by immunofluorescence were seeded in 4 well chamber slides (LAB-TEK) and fixed with 3% PFA for at least 30 minutes at room temperature, but more commonly overnight at 4°C. Cells were permeabilized with 0.2% Triton-X in PBS for 15 minutes followed by a PBS wash and blocking in 10% FBS in PBS. Primary antibodies were prepared in 10% FBS in PBS and incubated in a volume of 250uL/well for one hour. Slides were washed 3 times with PBS and incubated in the dark for one hours with Alexa488 or Alexa594 secondary antibodies (Molecular Probes) and 4',6-diamidino-2-phenylindole (DAPI) or propidium iodide for nuclear staining. Slides were washed 3 times with PBS, and then coverslips mounted over Vectashield (Vector Labs) and the edges of slides sealed with clear enamel (Revlon). Slides were stored in the dark at room temperature for short term storage or at 4°C for extended storage/archive. Slides were examined on a Nikon Eclipse TE2000-E microscope. Images were captured using NIS Elements software (Nikon).

Flow cytometry

Intracellular staining of HCV

To determine the percentage of HCV-infected cells within in vitro cultures, 2×10^5 - 1×10^6 infected cells were trypsinized, washed with PBS, and fixed with 3% PFA. Cells were stained for intracellular HCV protein following the Current Protocols in Immunology intracellular staining protocol using 1:2000 human polyclonal α -HCV serum A and 1:2000 Alexa Fluor 488 Goat α -human secondary (Molecular Probes).

Surface CD81 expression

CD81 expression was measured using PE-conjugated α -human CD81 antibody according to the manufacturer's protocol (BD Pharmingen). Cells were analyzed on a FACScan2 flow cytometer and data was collected using Cell Quest Pro (Becton Dickson). Data was analyzed using FlowJo (Tree Star, Inc.).

Statistics

Error bars in the figures presented here represent standard deviation from 3 or more measurements and are calculated using Microsoft Excel's stdev function. Tests of statistical significance employ Student's t-test and were calculated using the online t-test calculator available at www.graphpad.com/quickcalcs/ttest1.cfm.

CHAPTER 3: THE JFH1 CULTURE MODEL

Introduction

Although HCV was discovered in 1989, an infectious cell culture system would not be developed until 15 years later. Attempts to infect tissue culture cell lines with virus isolated from patients did not result in productive infection, so studies of the full virus lifecycle were confined to the chimpanzee model. Due to the high cost and limited access to this model system, an alternative would be needed to facilitate studies on a scale proportional to the burden of disease. These limitations were partially overcome by Volker Lohmann with the development of the HCV replicon system in which an HCV RNA is able to produce proteins and form a viral replicase complex that supports persistent viral replication, but does not produce infectious particles (78). Replicons can be constructed with a full length genome or as a subgenomic replicon where the HCV IRES drives expression of a selectable marker such as neomycin resistance and the HCV nonstructural proteins are expressed under the control of an EMCV IRES.

Several such subgenomic replicons were constructed by researchers in Japan using HCV genome sequences isolated from patients with fulminant hepatitis. One of these subgenomic replicons, SGR-JFH1 was found to replicate without the need to acquire cell culture adaptive mutations. This was unusual as most subgenomic replicons require adaptive mutations for efficient cell culture replication. Intrigued, Wakita and colleagues constructed the full length HCV JFH1 genome and transfected it into human hepatoma cells. Surprisingly, this genome was able to produce HCV particles which were

released into the supernatant of transfected cells and could be used to infect cells in a second round of infection. This discovery meant that a system was now available for studying the complete virus lifecycle in tissue culture. We received plasmids pJFH1 and pSGR-JFH1 encoding the complete virus genome and subgenomic replicon, respectively, from Takaji Wakita. I used these tools to begin developing assays and protocols for studying HCV infection in the Gale laboratory as described in this chapter and the previous chapter.

Results & Discussion

Identifying JFH1 reactive antibodies

Many techniques including immunoblot, immunofluorescence microscopy, and immunohistochemistry rely on access to an antibody that is able to recognize and bind to the protein of interest. In order to identify an antibody which could be used for studying infection with the JFH1 strain of HCV, I screened sera from HCV infected patients. Serum samples from 8 patients infected with genotype 2 HCV were obtained (with informed consent) from Dr. William Lee at UT Southwestern. These sera were designated Serum A-H in order to protect patient confidentiality. Sera were treated with 1% Triton-X in order to neutralize any HCV infectivity.

Huh7.5 cells were transfected with in vitro transcribed JFH1 RNA. Lysates from these cells or mock transfected cells were separated by SDS page and transferred to nitrocellulose membranes. These membranes were probed with serum A, B, C, D, E, F, G, and H (each antibody on its own membrane) at a 1:1000 dilution. Two sera, A and F, detected multiple HCV proteins (Fig. 3-1A). In order to identify the proteins detected by Serum A and Serum F, constructs expressing HA-tagged nonstructural proteins NS3/4A, NS4A/B, NS5A, and NS5B were transfected into Huh7 cells. All constructs expressed HA-reactive protein of the expected size. Serum A was found to detect at least NS3/4A, NS4A/B, and NS5A. Serum F was found to detect NS3/4A and NS4AB. Since Serum A had the greatest sensitivity (based on the strength of signal at 1:1000 dilution) and range of detected proteins, it was used in the development of subsequent immunoassays described in Chapter 2.

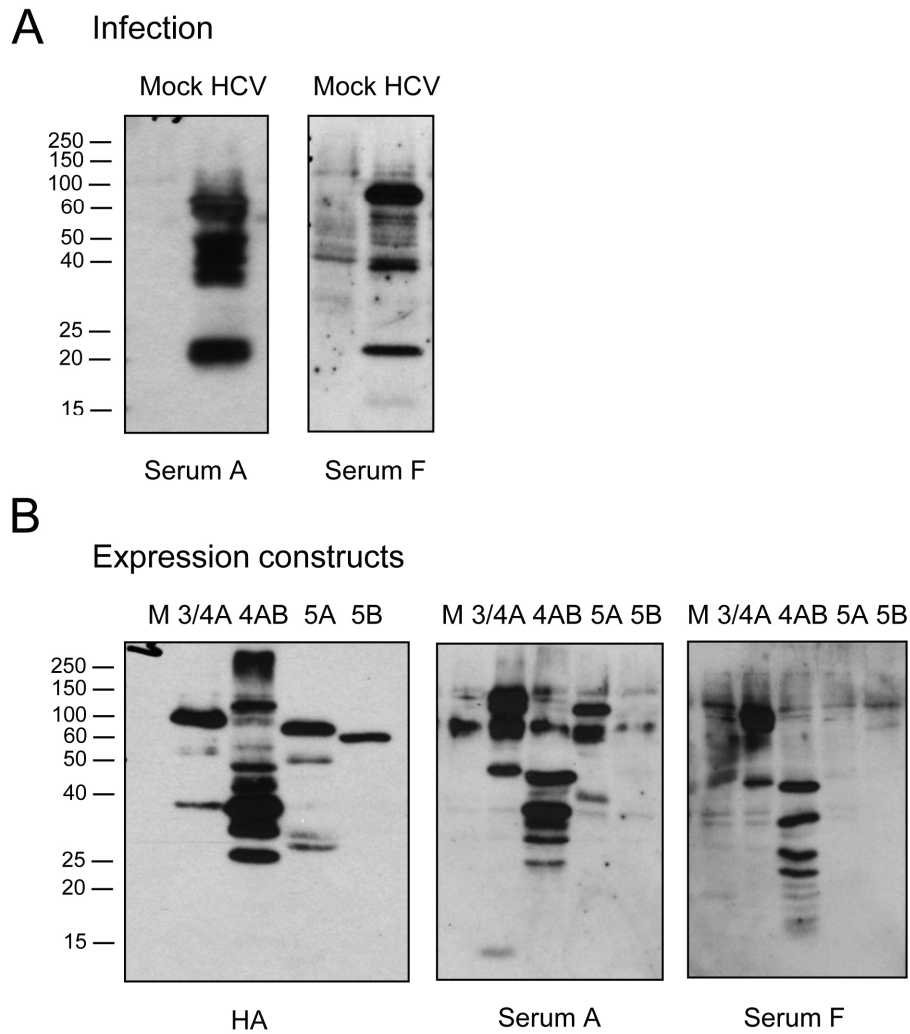


Figure 3-1. Identification of HCV JFH1 immunoreactive human sera. A) Lysates from HCV infected Huh7.5 cells were immunoblotted with sera from HCV infected patients. B) Huh7.5 cells were transfected with constructs expressing HA-tagged HCV nonstructural proteins and immunoblotted with sera from HCV infected patients.

Virus infection parameters

In order to design interpretable experiments it is important to understand the normal kinetics of virus entry, replication and release. In order to determine the amount of time virus should be incubated with cells in infection experiments, 2×10^4 Huh7.5 cells were seeded in 4 well chamber slides. HCV was incubated with cells at $\text{MOI}=0.5$ in a volume of 250ul for 5, 30, 60, 180, or 240 minutes at 37°C . Cells were then washed with PBS and incubated at 37°C in normal media for an additional 48 hours. Slides were fixed with 3% PBS and then stained for intracellular HCV. The number of HCV positive and negative cells in a representative field of view was counted manually from saved images to calculate % infected (Fig 3-2A). The percent infected reached a maximum at 60 minutes of incubation indicating that any diffusion or entry processes which can be disrupted by PBS wash have been completed by 1 hour. After the intracellular staining protocol for flow cytometry had been developed, this experiment was repeated by infecting 1×10^5 Huh7.5 cells at $\text{MOI}=0.5$ in 6 well dish in a volume of 0.5mL (Fig. 3-2B). In this experiment the maximum number of cells was infected within 30 minutes of incubation. The difference likely reflects a lower diffusion barrier due to a greater fraction of the virus containing media being in contact with the cells. Virus was incubated with cells for a minimum of 1.5 hours in all future infections to ensure sufficient virus-cell contact.

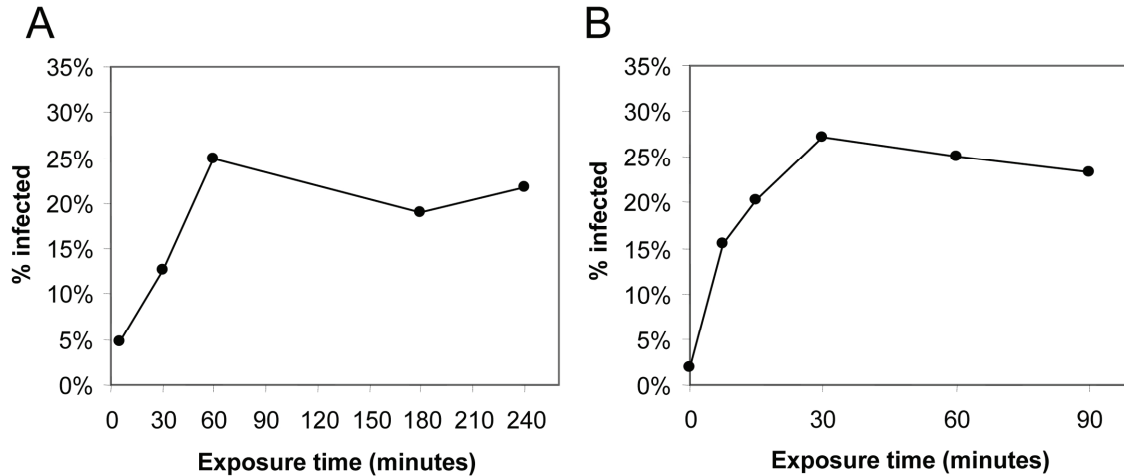


Figure 3-2. HCV JFH1 entry kinetics. Huh7.5 cells were incubated with HCV at MOI=0.5 at 37° for the indicated time, washed once with PBS, then incubated in media for an additional 48 hours and fixed with PFA. A) Results from infection in a chamber slide counted by IFA. B) Results from infection in a 6 well dish analysed by flow cytometry.

To accurately measure virus titer or the effects of a treatment on a single round of infection, it is important to pick a time point that allows infection to progress long enough for infected cells to produce HCV protein, but not so long that results are significantly confounded by multiple rounds of infection. The kinetics of virus production can be determined by a one step growth experiment in which infection is performed at a sufficiently high MOI such that all cells are initially infected and the effects of virus spread are minimized. I conducted a 1 step growth curve in Huh7.5 cells by infecting at MOI=2 and measuring the amount of virus released at 12 hour intervals following infection (Fig. 3-3). These results show that virus production reaches a peak at 48 hours post infection. As such, virus entry experiments and titer assays were measured at 48 hours post infection.

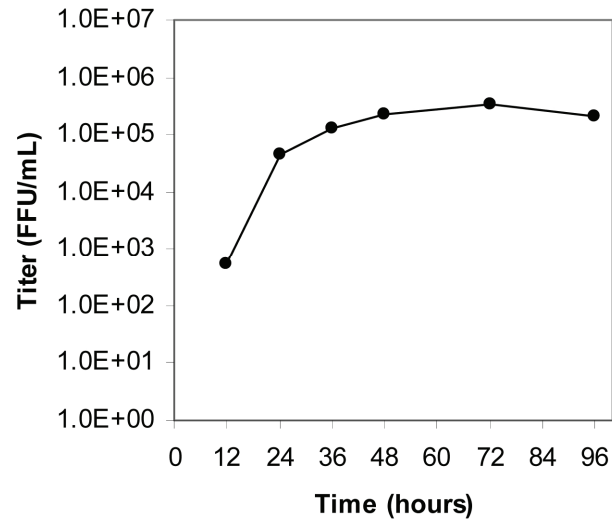


Figure 3-3. HCV JFH1 one step growth curve. Huh7.5 cells were infected with HCV at MOI=2 and samples were collected for titer every 12 hours.

Virus stability

Estimates of exposure risk, safety procedures, and confidence in the results of one's experiments can all be enhanced by a sense of the physical characteristics and hardiness of a virus. Towards this end I examined the effect of heat or UV stress on the HCV virion in order to assess the thermal and UV stability of HCV infectivity. Although virus stocks were stored at -80°C to ensure long term viability, I did not observe a significant decline in infectivity in unconcentrated virus supernatants stored at 4°C for up to a week. In order to assess virus stability at higher temperatures I measured infectivity of virus incubated at room temperature or at 37°C (Fig 3-4). In both cases, about 20% of infectivity remained after 24 hours. Although there are not enough data points to draw a

firm conclusion, the fact that 80% of infectivity remains after 6 hours at 37°C suggests an approximately linear decline in infectivity with time.

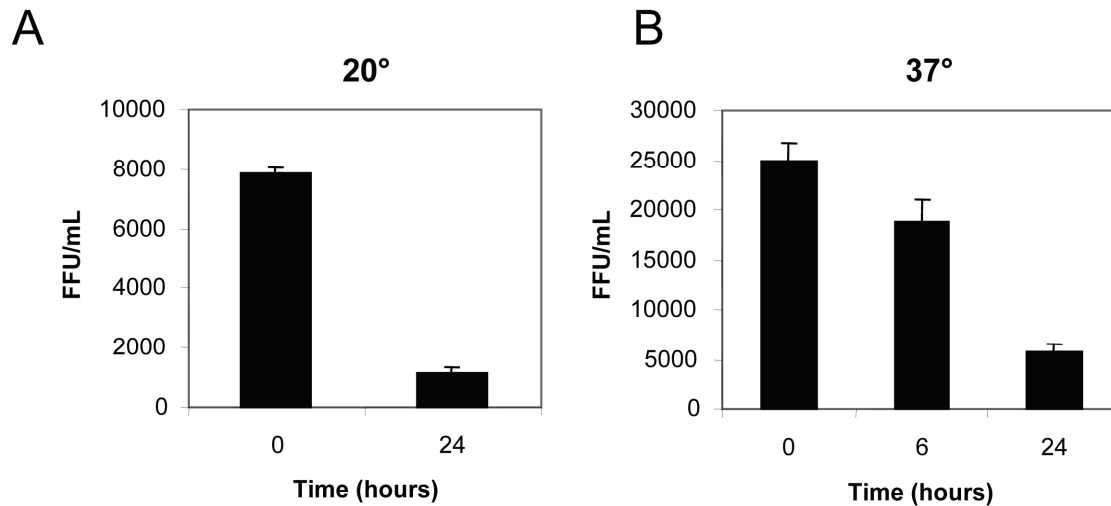


Figure 3-4. Temperature stability of HCV JFH1. HCV was incubated at A) room temperature or B) 37°C for the indicated amounts of time. (Note: 0 hour sample was incubated at 4°C)

Gale lab safety protocols include an ultraviolet (UV) irradiation step in the clean-up protocol after working with HCV in biological safety cabinets as UV is able to inactivate virus infectivity by crosslinking proteins and damaging genetic material. In order to quantify the effects of UV on virus infectivity I carried out a UV killing curve. 0.5mL samples of HCV containing supernatant in a 12 well dish were exposed to the UV light in a biological safety cabinet and samples were removed for titer after 1, 2, 3, 5, and 10 minutes of exposure (Fig 3-5). Infectivity declined rapidly with UV exposure with less than 1% remaining after 5 minutes of exposure.

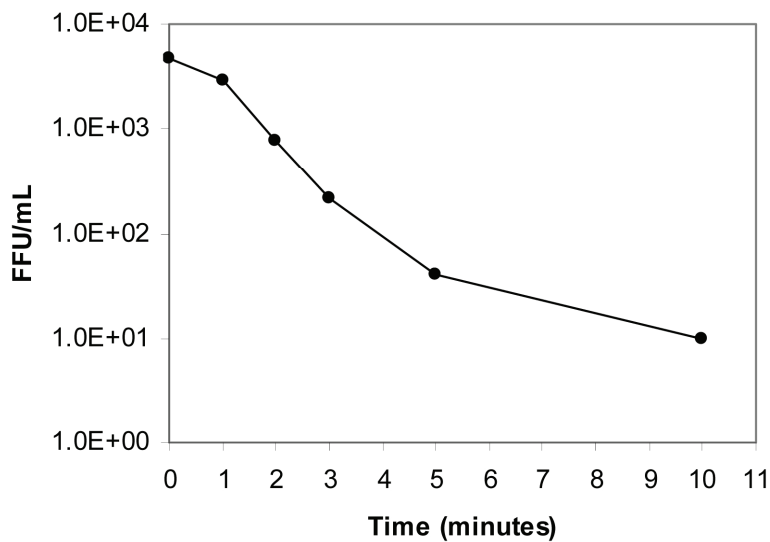


Figure 3-5. HCV JFH1 sensitivity to UV light. 0.5mL samples of media containing HCV were exposed to UV light in a biological safety cabinet for the indicated times in a 12 well dish.

Interferon sensitivity

Patients infected with genotype 2 strains of HCV have a much greater likelihood of successful outcomes with IFN- α therapy with 80% of patients achieving a sustained virologic response (SVR) compared to a 40% SVR in patients infected with genotype 1 strains. As JFH1 is a genotype 2 virus I was interested in studying the sensitivity of this virus to interferon and then finding a low dose of interferon which could be used to select for interferon resistant virus and sequence the mutations conferring interferon resistance. Towards this end I determined the 50% inhibitory concentration (IC₅₀) of IFN- α on HCV RNA replication. Huh7.5 cells were infected at MOI=1. 48 hours post infection, cells were treated with 0, 0.5, 5, 10, or 50 U/mL IFN- α for an additional 48 hours. RNA was extracted and relative HCV RNA levels were measured by RT-PCR (Fig 3-6). The IC₅₀ value was determined to be 5 U/mL. Attempts to select IFN resistant virus were not

pursued further due to limitations of the study design (IFN treated cells did not produce enough infectious particles to sustain a passing strategy) as well as potential safety concerns about creating a virus that would be more resistant to therapy in the case of an accidental exposure.

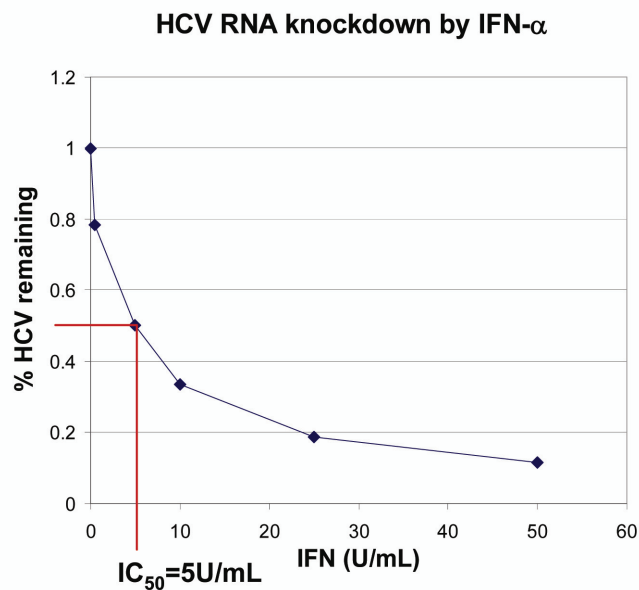


Figure 3-6. HCV JFH1 sensitivity to IFN- α . Huh7.5 cells were infected at with HCV at MOI=1. After 48hs of infection, cells were treated with IFN- α at 0, 0.5, 5, 10, 25 or 50 U/mL for an additional 48 hours. Intracellular HCV RNA was measured by RT-PCR and normalized to untreated levels.

Susceptible cell lines

Initial experiments with HCV conducted in human hepatoma (Huh7) derived cell lines revealed that there are variations in permissiveness for infection among these lines. Huh7.5 cells are a daughter cell line of Huh7 which have been cured of an HCV replicon by interferon treatment. This line contains a defect in the innate immune response which

renders them more permissive for infection than the parent Huh7 cell line (discussed in more detail in Chapter 5). However other Huh7 derived cured replicon lines were found to be less permissive for infection. Huh7, Huh7.5, HP cured, and K2040 cured cells were infected at MOI=1 or MOI=7.5 and stained for intracellular HCV at 48 hours post infection (Fig 3-7A). K2040 cured cells were much less permissive for infection than Huh7, although a proportionally higher percentage of cells was infected at MOI=7.5 than MOI=1. This suggests that K2040 cured cells may have a deficiency (though not complete absence) of some entry or replication factor supporting initial infection. Conversely, HP cured cells could not be infected even at MOI=7.5 which may suggest a complete lack of an essential entry or replication factor. The defects in K2040 cured and HP cured infection were not pursued further; however it would be interesting to determine whether these observations represent entry or replication defects. Such a question could be addressed by experiments measuring cell associated HCV RNA at an early time post infection and/or by transfecting HCV RNA to avoid entry defects.

In addition to hepatoma derived cell lines, it would be desirable to study infection in other non-cancer hepatocyte cell lines. I infected Huh7.5 or Immortalized Human Hepatocytes (IHH) at MOI=1 and stained for intracellular HCV protein at 48 hours post infection (Fig 3-7B). I was unable to detect any HCV positive IHH cells. I was similarly unable to infect PH5CH8 cells at MOI=1, although a visiting fellow in the Gale Lab, Junichi Tanabe, was able to infect this line using MOI=10.

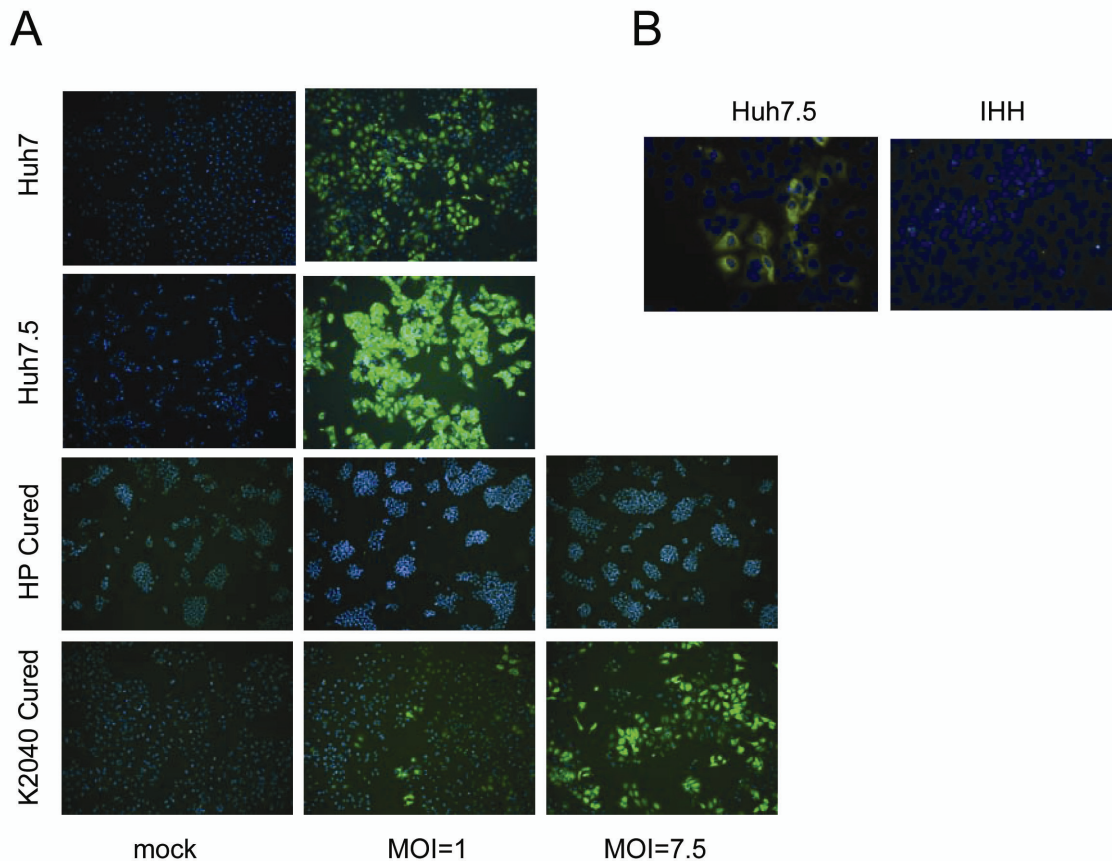


Figure 3-7 Cell line susceptibility to HCV JFH1 virus. A) Huh7, 7.5, K2040 cured and HP cured cells were infected at MOI=1 or 7.5 and stained for presence of virus at 48 hours post infection. B) Huh7.5 or IHH cells infected at MOI=1

In a further attempt to establish another hepatocyte culture model of infection, I constructed a HepG2-CD81 transgenic cell line (Fig 3-8) to rescue the HepG2 lack of the essential HCV entry factor CD81. I attempted to infect this cell line at MOI=1 but did not detect any HCV positive cells by IFA. The fact that only a limited subset of hepatocyte cell lines support HCV JFH1 infection highlights the complex interplay between virus

and host and the multiple barriers- entry, host replication factors, and innate immune evasion- that the virus must overcome to establish persistent infection.

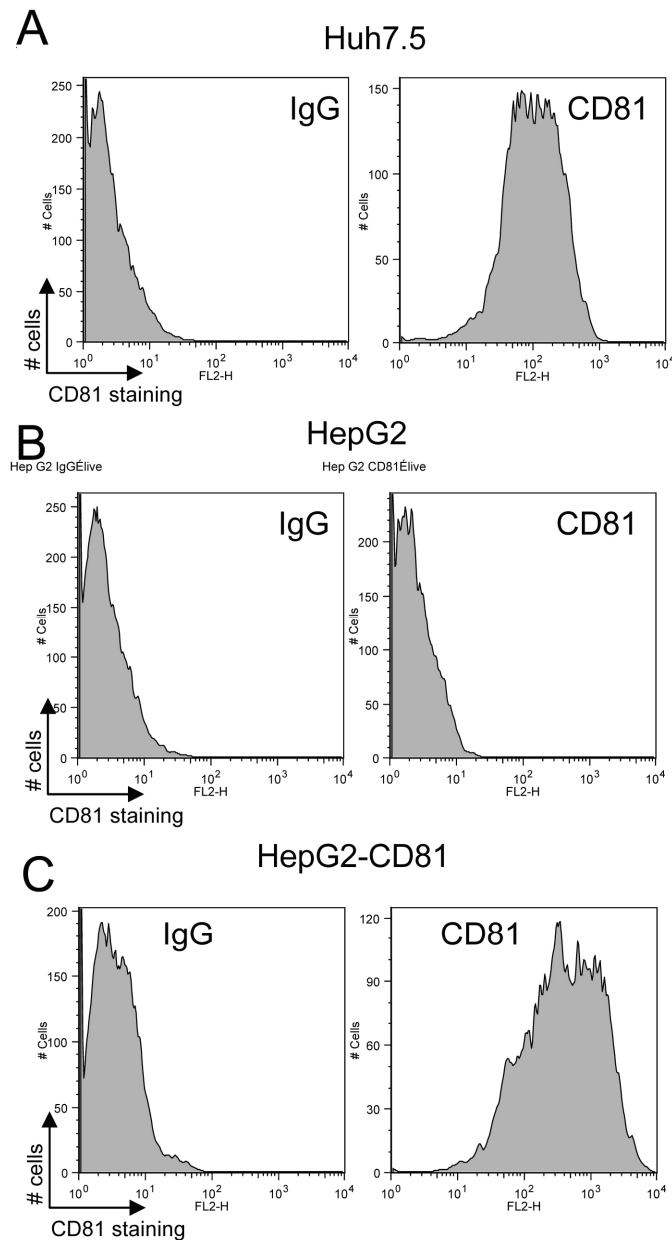


Figure 3-8. CD81 expression in HepG2 cells. A) Huh7.5 cells were stained with PE-conjugated anti-CD81 antibody or isotype control and analysed by flow cytometry. B) CD81 expression in wildtype HepG2 cells. C) CD81 expression in a HepG2-CD81 transgenic cell line.

CHAPTER 4: HCV ENTRY VIA LIPOPROTEIN INTERACTIONS

Introduction

The process of cell interaction with the HCV virus particle, and the mechanisms of cell entry by HCV are incompletely understood. However, several HCV co-receptors have been identified using soluble envelope protein binding assays and HCV pseudoparticles expressing E1 or E2 (12). These receptors include CD81, SR-BI, claudin-I, and occludin (13;28;144). CD81 is a member of the tetraspanin family of membrane proteins. The high density lipoprotein (HDL) receptor, SR-BI, also binds E2 and is required for cell entry by HCV pseudoparticles, while blocking antibodies against SR-BI reduce HCV entry into cultured hepatoma cells (19;62). Claudin-I is a tight junction protein that is required for HCV entry into cells expressing CD81 and SR-BI, and may facilitate direct cell to cell virus spread during infection (129). Recently another tight junction protein, human occludin, has been identified as an HCV entry factor and may play a role in restricting species specificity of HCV infection (109).

The low density lipoprotein receptor (LDL-R) has also been proposed to function as a co-receptor for HCV entry wherein LDL-R-HCV interaction would be facilitated through virus association with host lipoprotein components (20;36;52;96;128). Indeed, in previous studies to assess in vitro binding of patient-derived HCV particles to cultured hepatocytes, virus binding was strictly associated with the levels of LDL-R expression despite high expression of CD81 and SRBI on the target cells (84;138). Cell entry of HCV RNA of patient-derived virus isolates was also dependent on LDL-R expression by

the primary hepatocyte target cells (3;95). However primary hepatocytes and virtually all HCV clinical isolates studied to date do not support efficient productive infection in vitro, thereby limiting our understanding of LDL-R/virus/lipoprotein interactions in HCV infection.

The development of a tissue culture system for productive HCV infection based on genotype 2a strain JFH1 (134) has afforded the possibility of testing the role of these interactions in productive infection using virus particles resembling those produced in vivo. Recent studies using this HCV cell culture infectious system indicate a role for HCV/lipoprotein interactions in HCV infection. The HCV replicase has been shown to localize to sites of very low density lipoprotein (VLDL) assembly within infected cells, from which release of infectious virus is dependent on the microsomal transfer protein (MTP) and secretion of apolipoproteins apoB and apoE (20;36;52;103). Importantly, hepatocytes secrete VLDL particles which are composed of a hydrophobic core of triglycerides and cholesteryl esters surrounded by a surface coat containing phospholipids, free cholesterol and two predominant lipoproteins, apoB (present in a single copy) and apoE (multiple copies). Nascent VLDL particles released into plasma are not ligands for LDL-R. However, upon processing by lipoprotein lipase which hydrolyzes the triglycerides in the core of the lipoprotein particles, a large proportion (~70%) of the resulting intermediate density lipoproteins (IDL), is efficiently removed from plasma by LDL-R on hepatocytes. This process depends on the interaction between LDL-R and apoE located on IDL. The remaining IDL in the circulation is converted to LDL by a reaction catalyzed by hepatic lipase, which further reduces the amount of triglycerides in the lipoprotein particles (21). β -VLDL is a class of lipoprotein particles

enriched in cholesteryl ester that is similar to IDL in that cellular uptake of β -VLDL is dependent on the interaction between LDL-R and apoE associated with the lipoprotein particles. β -VLDL is frequently used as a substitute for IDL to study LDL-R-mediated endocytosis as it can be easily isolated from animals fed with diet enriched in cholesterol, while IDL is difficult to isolate. Once formed from either IDL or VLDL, LDL is taken up by LDL-R on hepatic as well as nonhepatic cells in a process that relies on interaction between the receptor and apoB associated with LDL. Thus, HCV interaction with host lipoproteins, and formation of HCV/lipoprotein particles, could explain the low density of HCV particles present in patient sera and may define a role for HCV/lipoprotein particles in infection.

In the present study we examined HCV/lipoprotein interaction and function in HCV infection *in vitro*. Our observations present a role for the LDL-R in mediating HCV entry of cultured cells through an apoE-dependent process of HCV/lipoprotein complexes.

Results

HCV interacts with lipoprotein metabolism

Our interest in the interaction between HCV and lipoprotein metabolism grew out of collaborations with Dr. Jin Ye's laboratory. A former postdoc in the Gale lab, Dr. Chunfu Wang discovered a geranyl-geranylated host protein, FBL2, required for HCV replication (136;141). This led to a search for other host factors which might contribute to HCV replication. An understanding of how such host factors support HCV replication would be expected to yield potential therapeutic targets for the treatment of HCV.

Towards this end an assay was designed in which the HCV replicase complex was immunoprecipitated with anti-NS5A antibody and the associated host proteins were identified by mass spectrometry. Several proteins involved in the synthesis of lipoprotein particles including apoE, apoB, and microsomal triglyceride transfer protein (MTP) were among those identified (52). This observation was particularly interesting in the context of the early reports showing association between HCV RNA and lipoprotein particles. It suggested that the basis of this interaction may lie in a deliberate exploitation of the lipoprotein synthesis machinery by HCV as opposed to incidental interactions between secreted virus and secreted lipoproteins occurring in serum.

To explore the link between lipoprotein metabolism and HCV replication I sought to perturb the lipoprotein synthesis machinery and examine the effect on release of HCV. In order to determine the effect of blocking MTP activity on HCV release I conducted a dose response experiment with the MTP inhibitor BMS-2101038 (137). Huh7.5 cells were infected at MOI=1 and then changed to NCL-PPS media containing the MTP

inhibitor compound at 0, 5, 50, or 500nM. Release of infectious HCV measured at 48 hours showed an approximate 2/3 decline relative to untreated cells at all concentrations examined (Fig 4-1A). Based on this dose curve I selected 10nM as the dose to use in a time course experiment to examine at what time point post infection MTP inhibition was affecting HCV release. Huh7.5 cells were infected at MOI=1 and then samples from untreated or 10nM MTP inhibitor treated cells were collected over 72 hours for titering. MTP resulted in an approximate 50% decline in release of infectious HCV at all time points indicating that effects of MTP inhibitor on HCV release were relatively constant and the virus was not able to overcome this blockade at late time points (Fig. 4-1B). Since HCV was still released even in the presence of MTP inhibitor, this suggests that either a portion of infectious HCV does not depend on MTP activity, or that blockade of HCV/VLDL release was not complete as inhibitor was not added until 3 hours after initial exposure of cells to HCV. In order to address the second possibility, GL cells which secrete infectious HCV without the need of an infection step, were pretreated for 16 hours with 100 or 500nM MTP inhibitor. At time 0 cells were washed with PBS and then fresh NCL-PPs media containing MTP inhibitor at 100 or 500 nM was added. Infectivity, HCV RNA release, and hepatic protein secretion were measured (Fig. 4-1 C,E,D). 500nM MTP inhibitor was able to completely block the release of HCV infectivity (Fig. 4-1C), RNA (Fig. 4-1D), and VLDL release as measured by immunoblotting for secreted apoB (Fig. 4-1E) without affecting the release of another liver secreted protein, a1-antitrypsin and without affecting intracellular HCV RNA levels.

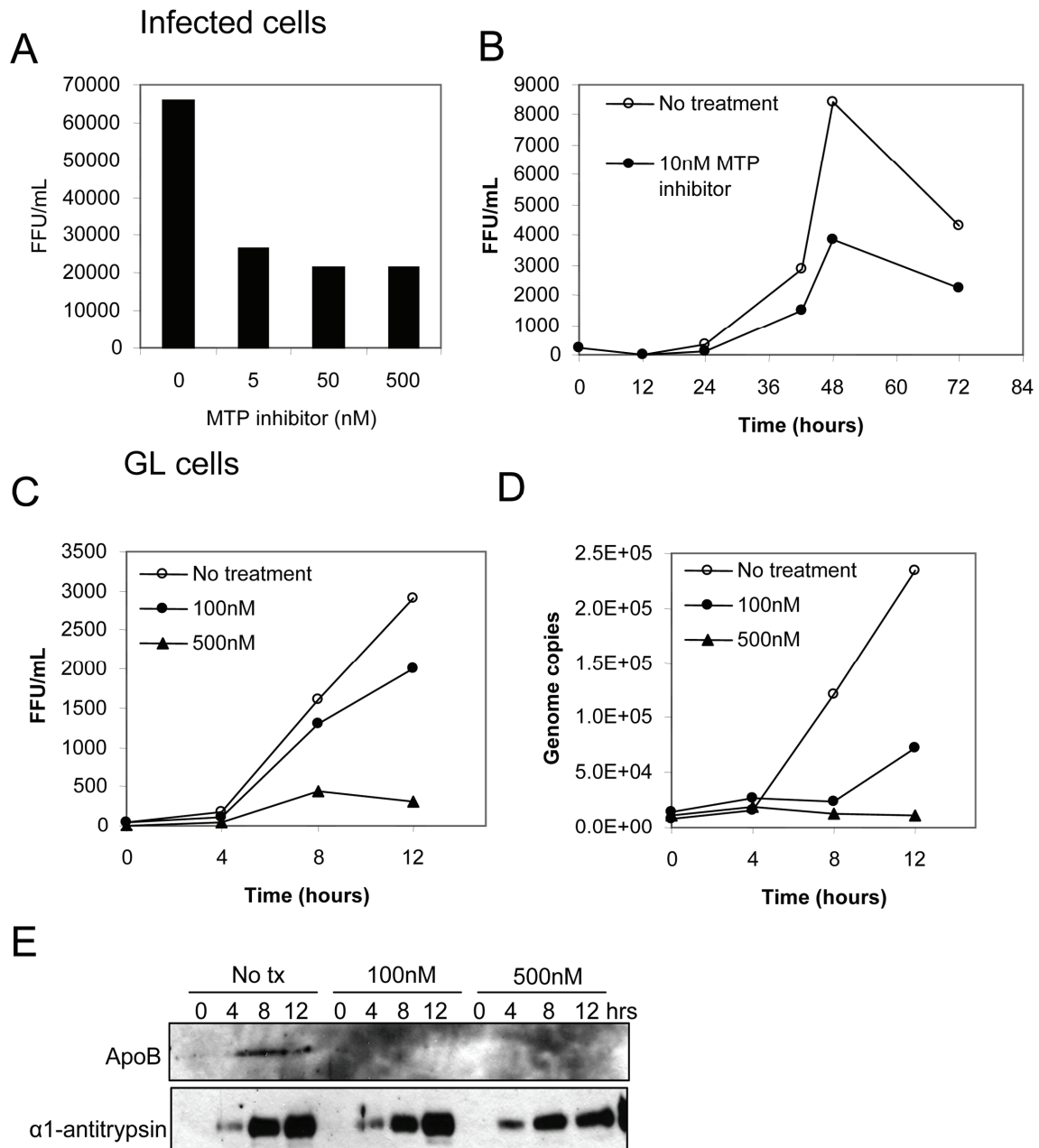


Figure 4-1 Microsomal triglyceride transferase activity required for efficient HCV release. A) Huh7.5 cells were infected at MOI=1 for 3 hours, then changed to NCL-PPS media containing MTP inhibitor BMS-2101038 at the indicated concentration. HCV release 48 hours post treatment is quantified by focus forming unit assay. B) Infectious particle release from Huh7.5 cells maintained in media with or without 10nM inhibitor following infection at MOI=1. C) GL cells were pretreated for 16 hours with MTP inhibitor and then changed to fresh NCL-PPS media containing inhibitor at the indicated concentration. Release of HCV infectious particles or D) HCV RNA is presented. E) Immunoblot of hepatic proteins released into the supernatant of GL cells.

We reasoned that if blocking lipoprotein synthesis decreased HCV release, perhaps delivering excess lipid to hepatocytes by LDL or free oleate could stimulate VLDL production and therefore enhance HCV secretion. 2×10^4 Huh7.5 cells seeded in a chamber slide were infected at MOI=0.5 in the presence of 0, 50, 150 or 300 ug/mL LDL and maintained in media containing these concentrations of LDL for 48 hours and then stained for intracellular protein (Fig. 4-2B). Rather than enhancing HCV replication this treatment seemed to inhibit replication, although later experiments would show that this was due to an effect on entry. An alternative method for delivering lipid to hepatocytes is direct supplementation with oleate. Huh7.5 cells were infected at MOI=0.5 and then maintained in media containing 0, 100, 200, or 500ug/mL oleate for 48 hours (Fig 4-2A). Oleate treatment led to a significant decline in the release of HCV. While this was not the direction of the effect predicted, it still supports a link between alterations in lipoprotein metabolism and the HCV lifecycle.

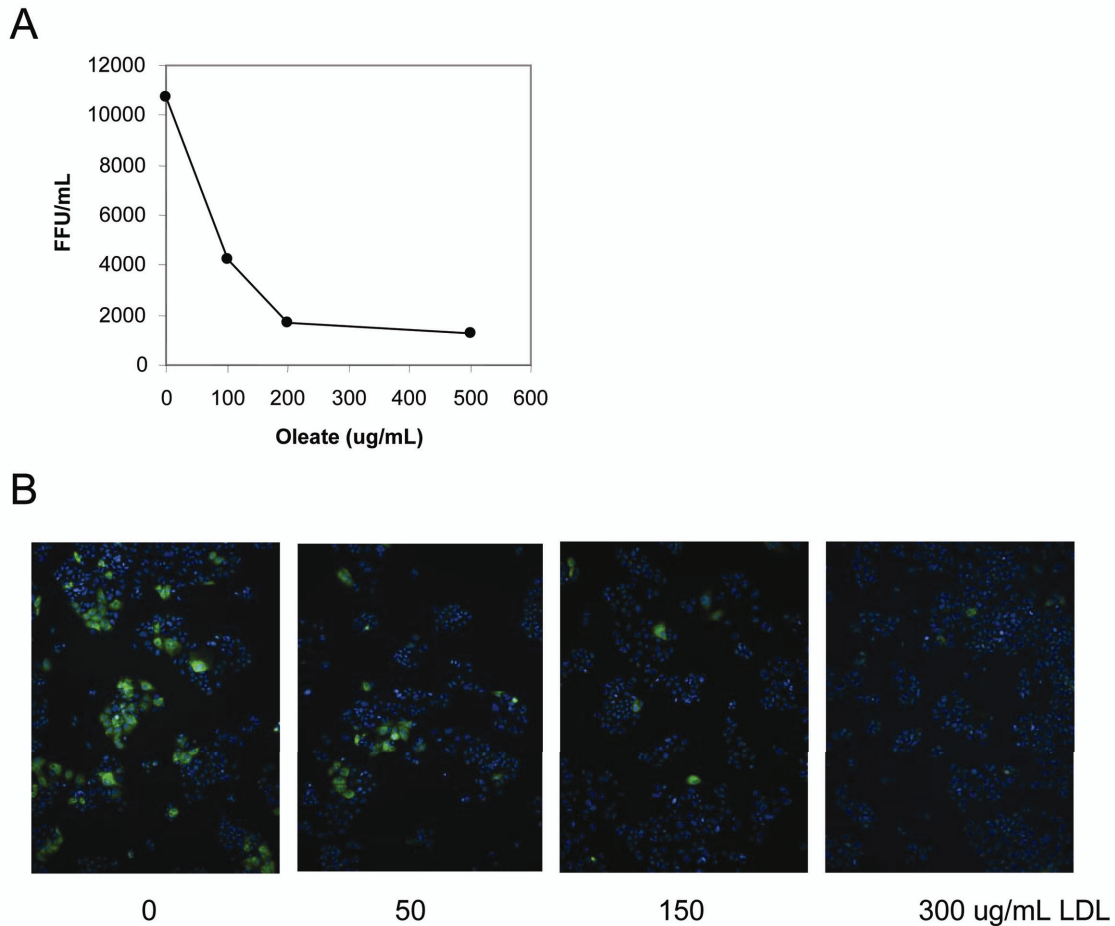


Figure 4-2 Lipid modulation affects HCV lifecycle. A) Huh7.5 cells were infected at MOI=0.5 and then maintained in media containing the indicated amounts of oleate for 48 hours. HCV released into the supernatant is quantitated by focus forming unit assay. B) Huh7.5 cells were infected at MOI=0.5 in the presence of LDL at the indicated concentration and maintained in media containing the indicated concentration for an additional 48 hours.

β -VLDL blocks HCV infection via apoE

If the infectious HCV virion is a hybrid lipoviral particle which depends on the VLDL synthesis machinery for release, one might expect that it would contain components of normal lipoprotein particles and perhaps compete with these particles for uptake by hepatocytes. To assess the effect of exogenous lipoproteins on HCV infection

with putative HCV/lipoprotein particles we infected Huh7.5 cells with HCV at MOI = 0.5 in the presence of increasing concentrations of HDL, LDL, or β -VLDL. The percentage of infected cells were then determined via flow cytometry assay. When added to cultures prior to HCV infection, β -VLDL reduced the number of infected cells by approximately 60%. In contrast, LDL treatment of cells only moderately reduced the percentage of HCV infected cells, while HDL treatment had no effect on infection (Fig. 4-3A and B). HDL is a complex containing apolipoproteins AI-AIII that serve to bind SR-BI. β -VLDL and LDL particles both contain apoB and bind to the LDL-R, but β -VLDL particles also contain the higher affinity LDL-R ligand apoE (21).

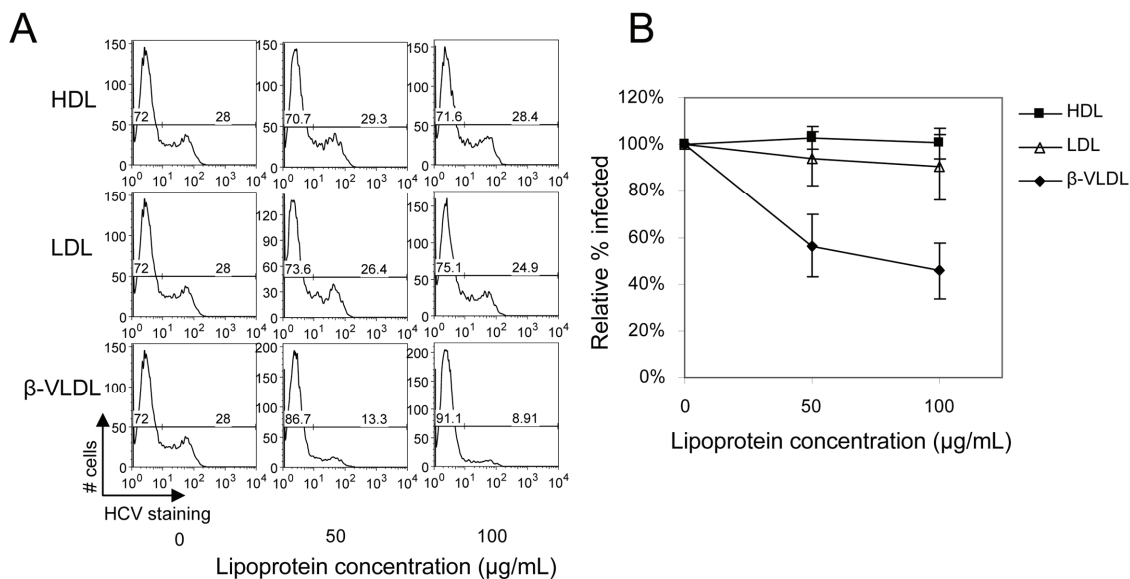


Figure 4-3. β -VLDL competes with apoE for HCV binding and entry. A) HCV supernatants from infected Huh7.5 cells were mixed with increasing concentrations of HDL, LDL, or β -VLDL and were incubated with Huh7.5 cells at MOI=0.5 for 90 minutes at 37°. After washing with PBS, cells were cultured for an additional 48 hours and intracellular HCV protein was detected by flow cytometry. Data are presented from a single representative experiment (out of three total experiments). B) The percentage of cells infected with HCV in the presence of increasing concentrations of indicated lipoprotein relative to mock-treated cells as determined by flow cytometry. The mean and standard deviation from 3 separate experiments are shown.

That β -VLDL blocked HCV infection indicates that apoE could preferentially compete for cell binding with HCV/lipoprotein particles. To test this idea, we infected cells in the presence of increasing concentrations of goat polyclonal apoE or sheep polyclonal apoB antibody or nonimmune control antibodies. The presence of apoE but not apoB antibodies rendered a dose-dependent block of HCV infection (Fig. 4-4). These results suggest that apoE plays an important role in HCV infection.

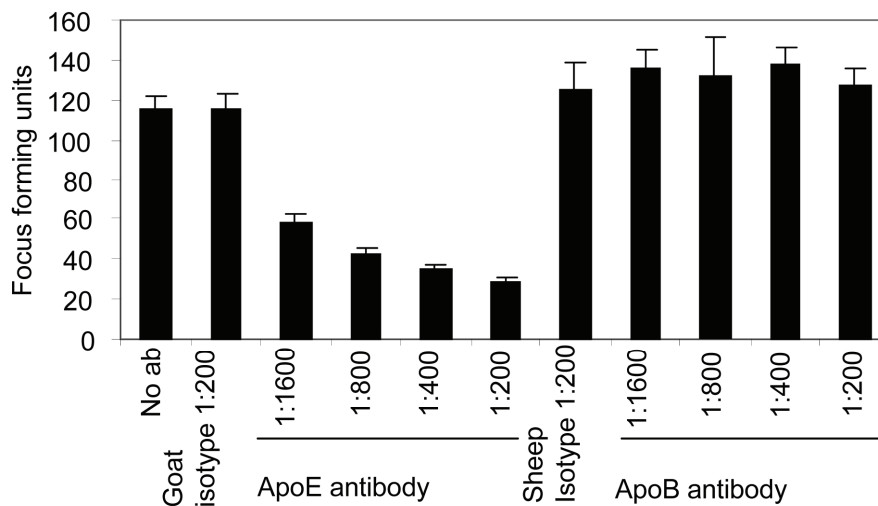


Figure 4-4. ApoE is an HCV entry factor. Huh7.5 cells were infected in the presence of increasing concentrations of α -apoE, α -apoB, or isotype control antibodies and the relative number of infected cells was quantified by focus forming unit assay 48 hours later.

Infectious HCV particles contain apoE

To determine if apoE was physically associated with infectious HCV particles we examined protein, HCV RNA, and overall infectivity of apoE or apoB-associated virus. Immunocomplexes were recovered from immunoprecipitation reactions of cell culture supernatant from HCV-infected Huh7.5 cells using polyclonal antibodies specific for

apoE, apoB, or Sendai virus (unrelated virus negative control). The components of the unbound, supernatant fractions and the immunocomplex (pellet fractions) of each immunoprecipitation reaction were then examined in parallel. Anti-apoB or anti-apoE but not anti-Sendai virus antibodies removed the apoB or apoE containing particles from the supernatant fraction and were recovered in the pellet fraction (Fig. 4-5A). Analysis of the relative amount of HCV RNA associated with each of these samples demonstrated an approximate 65% recovery of the total input HCV RNA within the anti-apoE immunocomplex. Small amounts HCV RNA were recovered from anti-apoB immunocomplexes, but only background levels of HCV RNA were present in anti-Sendai virus antibody immunocomplexes (Fig. 4-5B). The number of infectious HCV particles remaining in the supernatant after each immunoprecipitation reaction were quantified using a sensitive focus-forming unit assay of infected Huh7.5 cells. Supernatants from anti-apoE but neither anti-Sendai virus nor anti-apoB immunoprecipitation reactions exhibited an approximate 65% reduction in infectivity (Fig. 4-5C, bottom panel). This reduction paralleled the relative amount of both apoE-associated HCV RNA (Fig. 4-5B) and the reduction of HCV infectivity achieved when infection was carried out in the presence of β -VLDL or apoE antibody (Fig. 4-3, 4-4). These results indicate that apoE is a component of the infectious HCV particle and forms a stable virion complex that serves to support or enhance virus particle infectivity. These properties of apoE are relatively specific for HCV, as infection with Sendai virus, another enveloped RNA virus, was reduced by immunoprecipitation of infectious supernatant with anti-Sendai virus antibodies but not by anti-apoE antibodies (Fig. 4-5C, top panel). It was somewhat unexpected that immunoprecipitation using anti-apoB antibodies did not result in

recovery of significant amounts of HCV RNA since β -VLDL particles contain both apoB and apoE. However this observation is consistent with results shown in Fig. 4-5A in which anti-apoB did not deplete apoE from virus supernatants, suggesting that within β -VLDL particles the single apoB molecule may be relatively inaccessible to antibody.

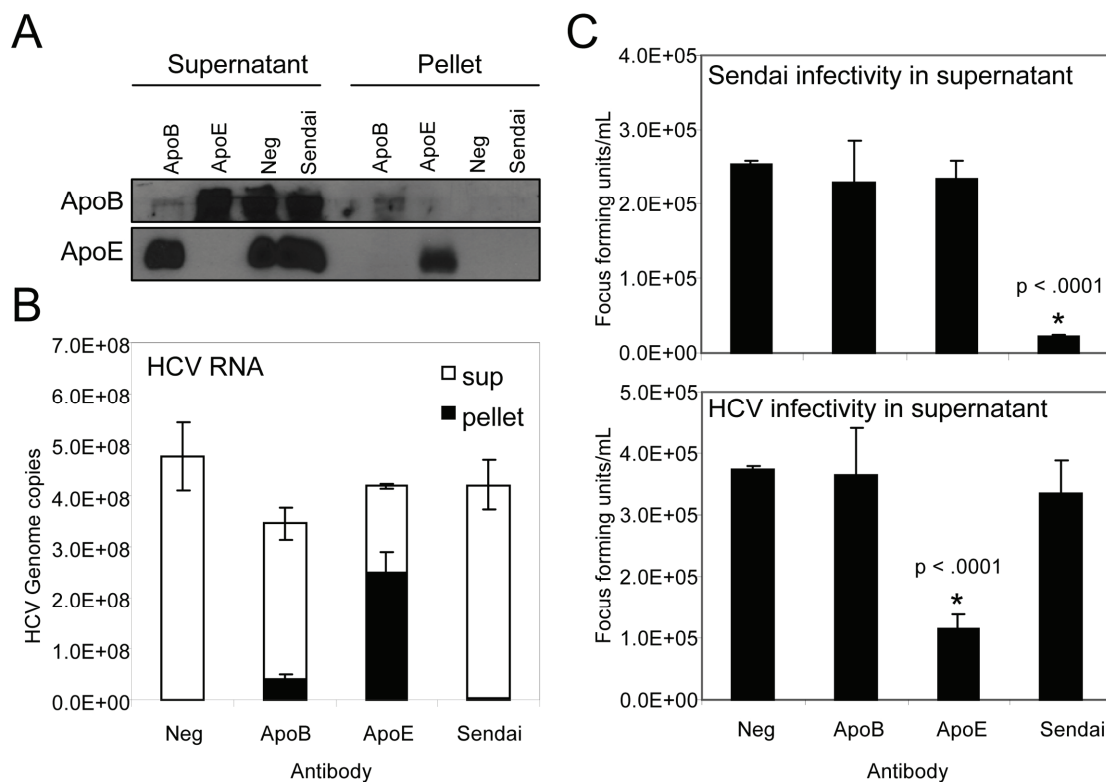


Figure 4-5. ApoE associates with HCV RNA and infectious HCV particles. A) Immunoblot analysis of immunocomplexes or residual supernatants recovered from the indicated immunoprecipitation reactions. B) Supernatant from JFH1 infected cells was immunoprecipitated with antibody to apoB, apoE, or Sendai virus. RNA was extracted from the resulting pellet fractions or residual supernatant, and HCV genome copies were quantified by RT-qPCR. C) The number of infectious virions remaining in the supernatant after immunoprecipitation was determined by focus forming assay after infection of Huh7.5 cells (bottom panel). Similar immunoprecipitation reactions in media containing Sendai virus were also assessed by focus forming unit assay (top panel). P values were determined by Student's t-test comparison against negative control (beads, no antibody).

LDL-R is a co-receptor for HCV

The presence of apoE within β -VLDL and IDL confers greater affinity for LDL-R binding than LDL (21), and the increased ability of β -VLDL or apoE antibody to block HCV infection compared to LDL or apoB antibody implicates the LDL-R as a possible common binding site on hepatocytes for both β -VLDL particles and infectious HCV virions. Since HCV infection was dependent on access to apoE binding site(s) on target cells, we sought to determine if LDL-R participates in the HCV-host cell interaction. We therefore modulated LDL-R expression using Huh7.5 cells in which LDL-R expression is regulated by sterol response element binding protein (SREBP) or TR3772 cells (hereafter referred to as LDL-R1), an Huh7.5 derived cell line from Jin Ye's laboratory which stably expresses LDL-R under the control of a CMV promoter. 25-hydroxycholesterol (25-HC), an antagonist of the SREBP pathway, blocks the expression of the LDL-R by suppressing *Ldl-r* promoter activity within treated cells (2). We note that 25-HC treatment of cells also blocks the synthesis of geranylgeraniol, a prenyl lipid that is essential for HCV RNA replication (136;141). Thus, in order to retain HCV replication competence of cells all treatments with 25-HC were carried out in culture media supplemented with 10uM geranylgeraniol, which supports HCV replication in the presence of high levels of 25-HC (136;141).

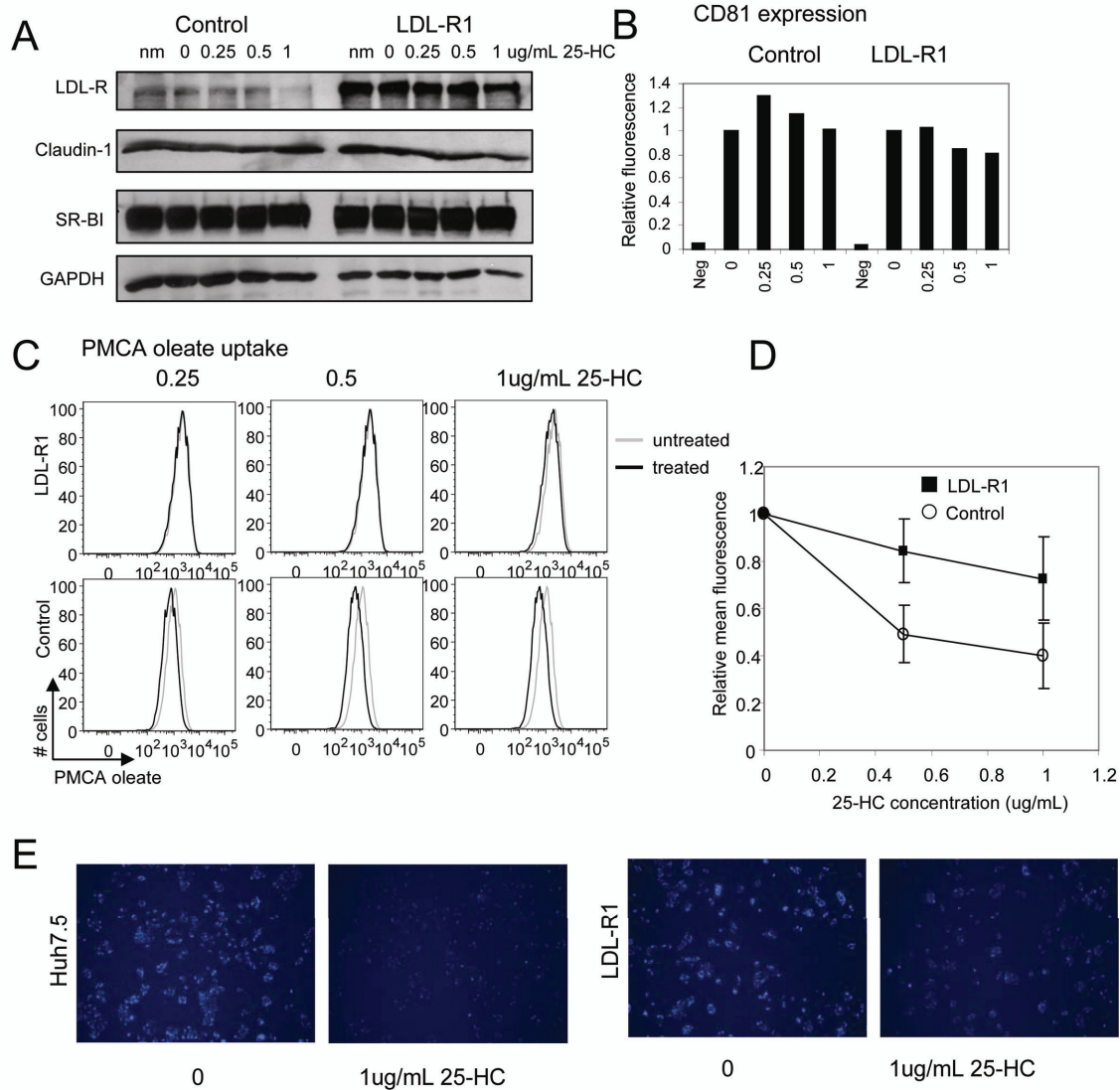
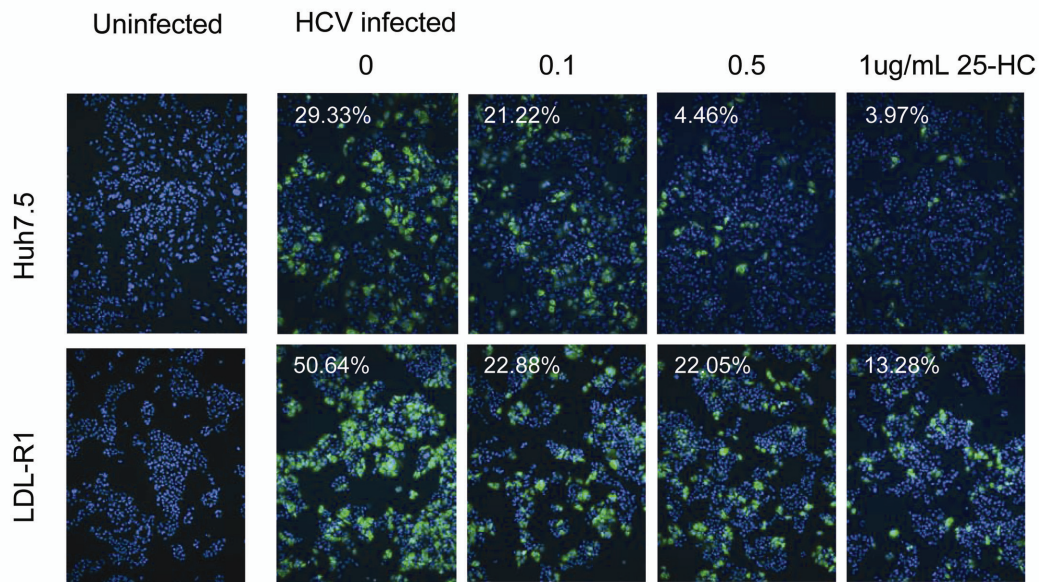


Figure 4-6. 25-hydroxycholesterol specifically inhibits LDL-R expression and function. Control cells and an LDL-R overexpressing stable cell line (LDL-R1) were treated for 16 hours with increasing amounts of 25-HC (shown above each lane) and analysed for protein expression, PMCA oleate uptake, and HCV infection. NM, normal media. A) Immunoblot analysis of LDL-R and HCV co-receptor abundance. B) CD81 expression was measured by flow cytometry and is presented as mean fluorescence relative to untreated cells. C) Uptake of PMCA oleate, a fluorescent LDL analogue, was measured by flow cytometry. Graphs show the fluorescence peaks of treated (black line) versus untreated (0 μ g, gray line) cells from a representative experiment. D) Mean PMCA oleate uptake by control and LDL-R1 cells treated with increasing 25-HC. Graph shows relative mean fluorescence from five separate experiments. E) Fluorescence microscopy of PMCA oleate (blue) uptake in Huh7.5 or LDL-R1 cells.

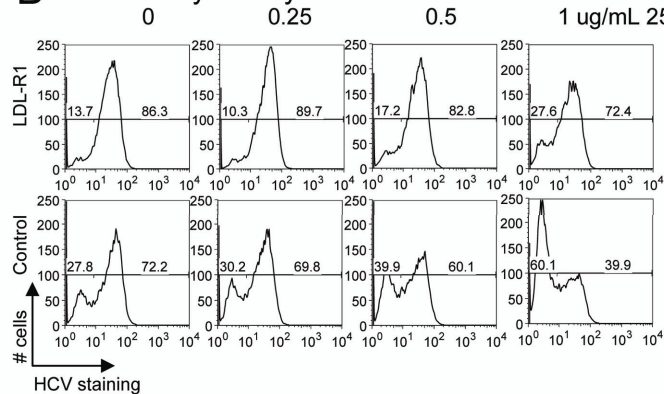
25-HC treatment resulted in a dose-dependent decrease in the expression of the LDL-R within control cells but not in LDL-R1 cells (Fig. 4-6A). 25-HC did not affect the expression levels of claudin-1, SR-BI or CD81 (Fig. 4-6A and B). To assess the functional impact of 25-HC treatment on ligand uptake by the LDL-R we measured the uptake of PMCA oleate, a fluorescent LDL analogue, in treated cells (68). Increasing concentrations of 25-HC had no significant effect on PMCA oleate uptake by LDL-R1 cells, but uptake was reduced by approximately 60% in control cells (Fig. 4-6C, D, E).

Importantly, when 25-HC-treated cells were challenged with HCV (at MOI=0.5-1.0) we observed an approximate 60% reduction in the frequency of HCV-infected cells (Fig. 4-7) that mirrored the reduction in ligand binding and uptake by the LDL-R (Fig. 4-6). The reduction in HCV infection paralleled that mediated by the β -VLDL competition and anti-apoE immunoprecipitation experiments (Figs. 4-3 and 4-5, respectively). The effect of 25-HC on HCV infection was specific for the HCV entry process, as treatment with up to 1 μ g/mL 25-HC had no effect on intracellular HCV replication and viral protein expression in cells harboring an HCV subgenomic replicon (Fig. 4-8).

A Immunofluorescence



B Flow cytometry



C

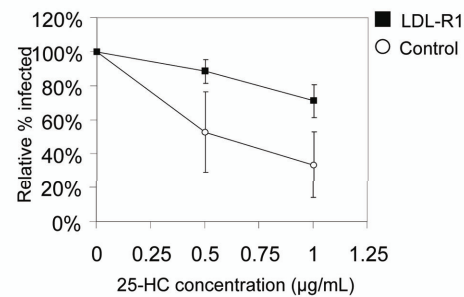


Figure 4-7. Inhibition of HCV infection through suppression of LDL-R expression and function. A) Control cells and an LDL-R overexpressing stable cell line (LDL-R1) were treated for 16 hours with increasing amounts of 25-HC (shown above each lane) in lipoprotein deficient serum and analysed for HCV infection. B) Cells treated with 25-HC as above were infected with HCV at MOI=1. Graphs show the percent of HCV positive cells as measured by flow cytometry staining for intracellular HCV proteins. Data are from a representative experiment. C) The mean relative percentage of infected cells from five combined experiments as described in B.

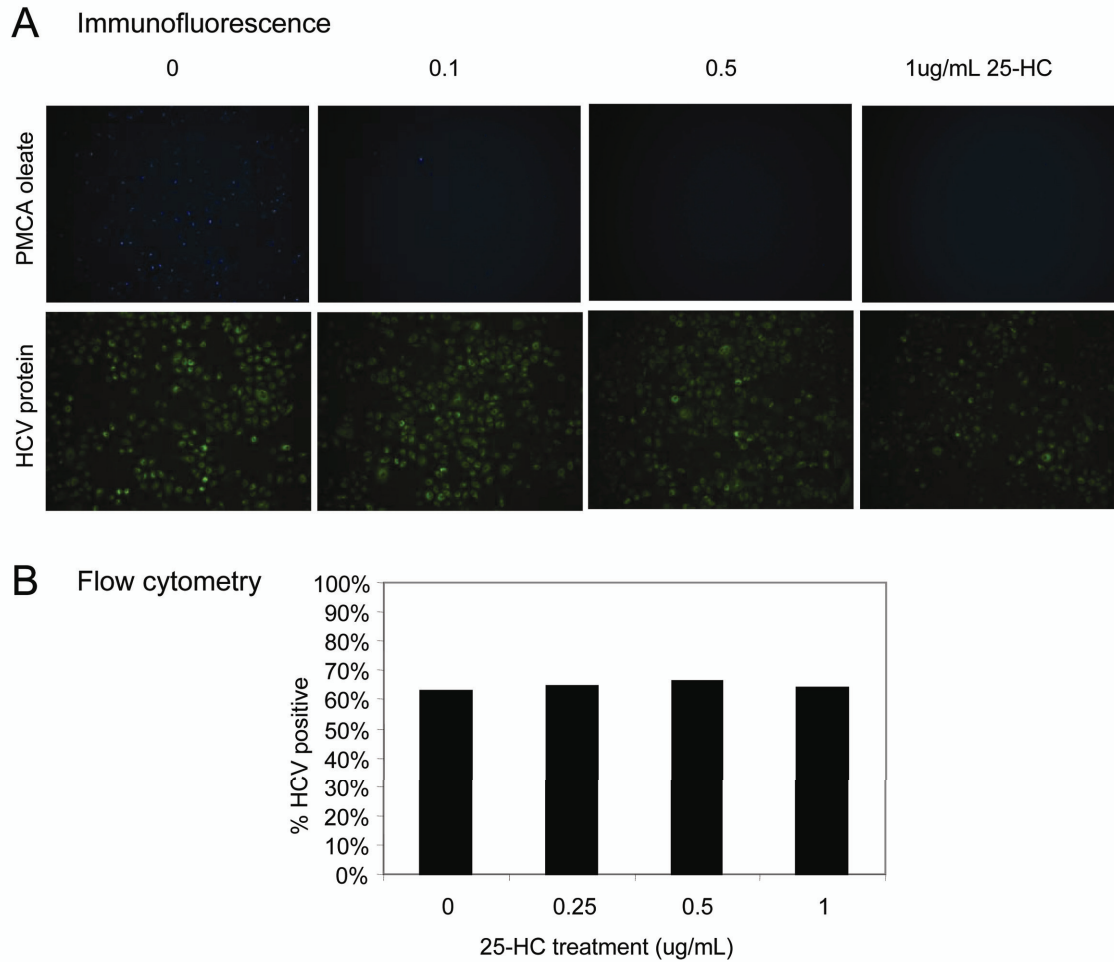


Figure 4-8. 25-hydroxycholesterol inhibits LDL-R function but not HCV replication. SGR-JFH1 cells which contain a stably replicating HCV replicon but do not produce infectious particles were treated with 25-HC. A) PMCA oleate uptake (blue) and HCV protein (green) were visualized by fluorescence microscopy. B) The percentage of cells staining HCV positive as analysed by flow cytometry.

In order to define the potential role of the LDL-R in cell binding and entry by HCV, and to compare LDL-R functions to the various HCV co-receptors, we conducted expression knockdown experiments using siRNA targeting the LDL-R, CD81, claudin-I or SR-BI. Knockdown of each receptor target was verified by immunoblot analysis (Fig. 4-9A) or flow cytometry assay of treated cells (Fig. 4-9B). We achieved a level of knockdown of CD81 or claudin-1 expression (Fig. 4-9C) that significantly reduced HCV infection, consistent with their known function as HCV co-receptors. Importantly, siRNA knockdown of LDL-R expression also reduced the frequency of infected cells and suppressed infection by approximately 30-40% overall in independent experiments (Figs. 4-9D and 4-9E). This effect was less than the 60% reduction of HCV infection that occurred in cells treated with β -VLDL or 25-HC (Figs. 4-3 and 4-7), likely reflecting the background level of HCV infection resulting from less than 100% siRNA transfection efficiency in the target cells. Knockdown of SR-BI expression by more than 90% (Fig. 4-9C) did not significantly affect HCV infection in our studies. Taken together, our results indicate that LDL-R can function as a co-receptor for HCV infection to facilitate cell binding and/or entry processes through interactions with an HCV/lipoprotein virion complex.

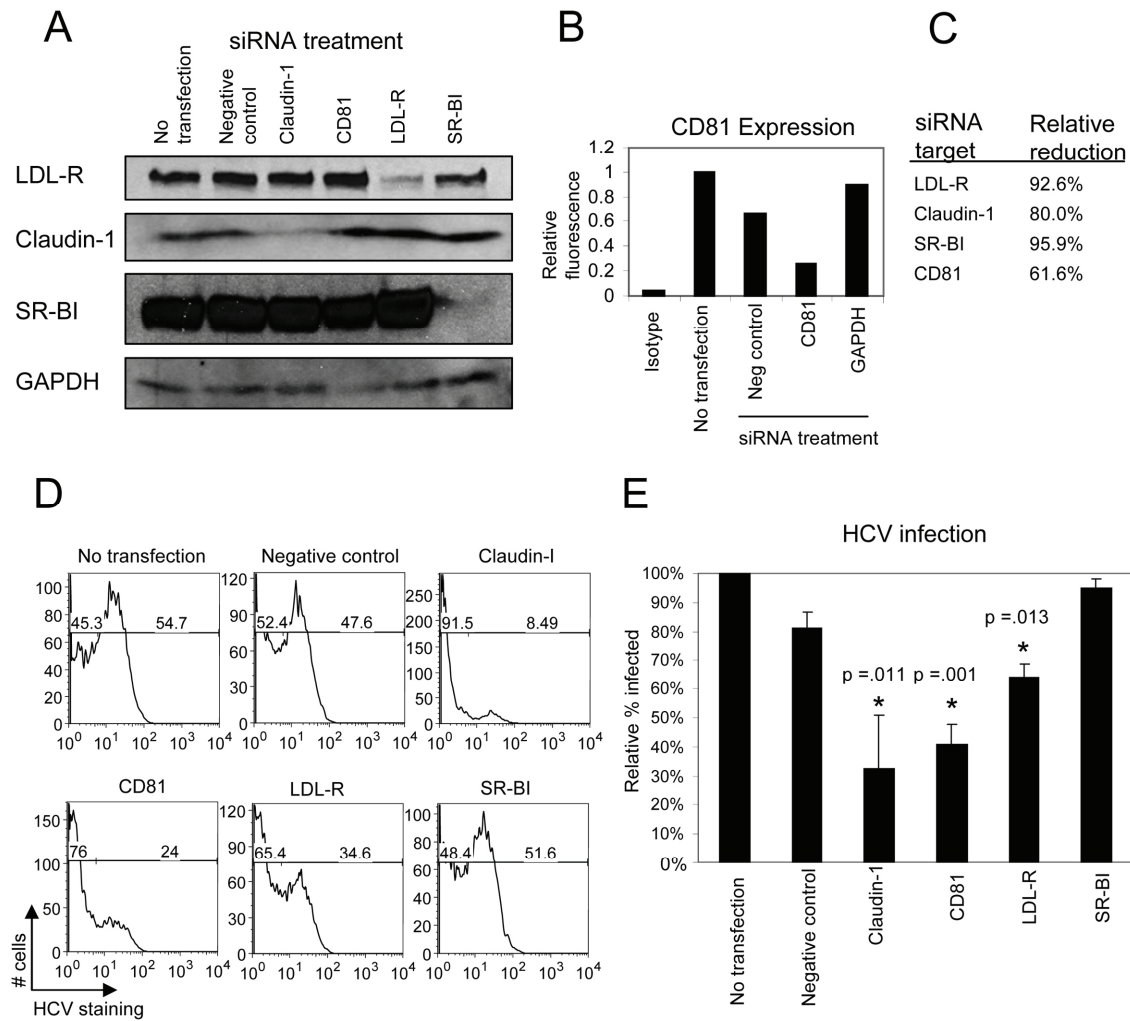


Figure 4-9. Knockdown of LDL-R expression decreases HCV infection. Huh7.5 cells were treated with 0.4nM of siRNA targeting the indicated mRNAs or a negative control siRNA. In each case we achieved 60-80% transfection efficiency of target cells as measured by parallel transfection of fluorescently labeled control siRNA and immunofluorescence microscopy analysis of the transfected cells. A) Immunoblot analysis of cells harvested three days after siRNA transfection. B) CD81 expression in siRNA-treated cells was measured by flow cytometry. Data are presented as mean fluorescence relative to non-transfected control cells. C) Reduction of targeted protein expression relative to negative control siRNA treated cells as measured by quantitative densitometry from immunoblot (LDL-R, Claudin-1, SR-BI) or mean fluorescence signal (CD81) D) siRNA-treated Huh7.5 cells were infected with HCV at MOI = 0.5. Two days later the percentage of HCV-infected cells was determined by flow cytometry assay. Data are shown from a representative experiment. E) Combined HCV infection results from three separate experiments as described in C. P values were determined by Student's t-test comparison against siRNA control-treated cells.

Characteristics of HCV infectious particles

In order to determine if the HCV virions that associate with apoE are the same as those which depend on LDL-R for virus binding and/or entry of target cells, we carried out density fractionation and infectivity studies of virus supernatant from HCV-infected cells. Infectious cell supernatants were subject to ultracentrifugation through iodixanol density gradients from which fractions were collected and subjected to immunoprecipitation with anti-apoE or nonimmune control antibodies. We measured the relative level of HCV RNA present in the immunocomplex recovered from each fraction or that remained in the non-bound supernatant from each reaction. In parallel we measured the infectivity of the immunoprecipitation supernatant and input material from each gradient fraction. RNA analysis of the supernatant and pellet from each fraction demonstrated a peak of apoE-associated HCV RNA within the 1.06 g/mL fraction (Fig. 4-10A). The HCV RNA association with apoE was specific since only nonsignificant levels of HCV RNA were recovered within the respective control immunocomplexes. (Fig. 4-10B).

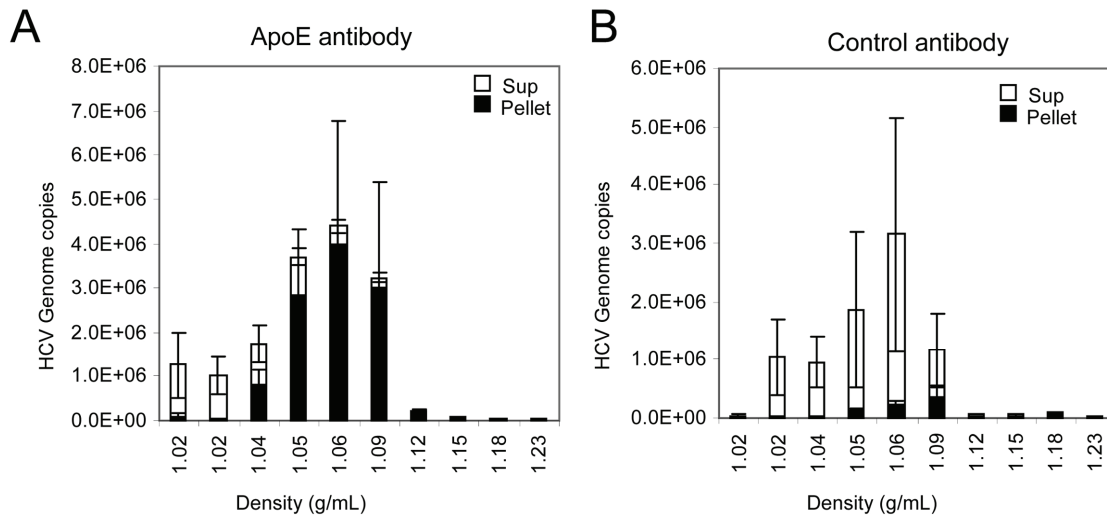


Figure 4-10. ApoE is a component of low density infectious HCV particles. Supernatant from HCV-infected Huh7-5 cells was ultracentrifuged through a 5-50% iodixanol gradient. 1mL fractions were collected from the gradient and used in immunoprecipitation reactions. A) 0.5mL of each fraction was immunoprecipitated with apoE antibody. HCV RNA recovered within the pellet or residual supernatant of each fraction was determined by RT-qPCR. B) 0.5mL of each fraction immunoprecipitated with isotype control antibody and analysed by RT-qPCR.

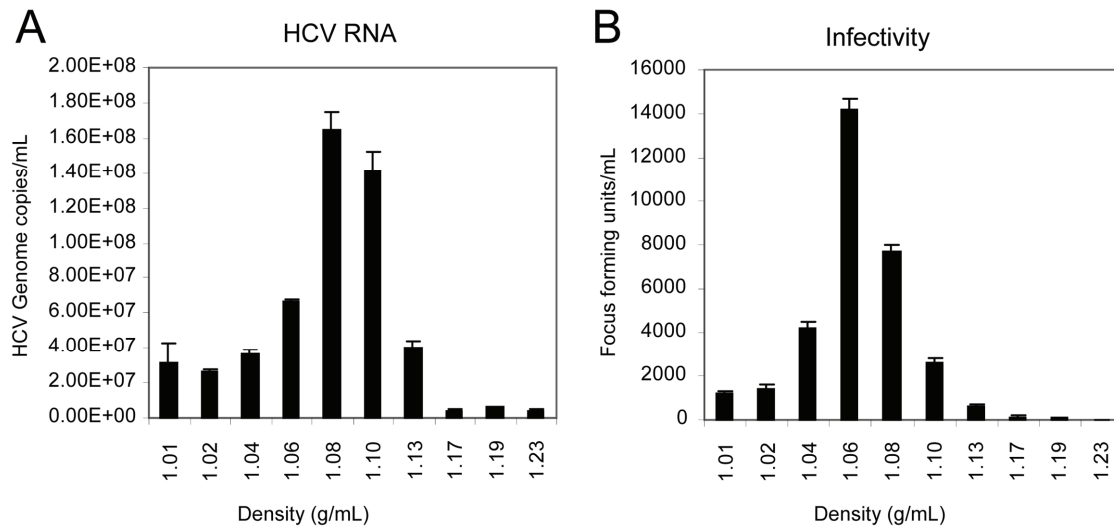


Figure 4-11. HCV peak infectivity occurs at low density. Supernatant from HCV-infected Huh7-5 cells was ultracentrifuged through a 5-50% iodixanol gradient. 1mL fractions were collected from the gradient and analysed. A) Total HCV RNA within each gradient fraction was quantified by RT-qPCR. B) Infectivity of gradient fractions.

We found that the peak of total HCV RNA present within the gradient had a density of approximately 1.09-1.10 g/mL (Fig 4-11A), whereas the peak of infectious HCV particles occurred at a density of 1.06 g/mL, corresponding to the density of the peak apoE-associated HCV RNA (compare 4-11A with Fig4-10A). To determine if the 1.06 g/mL apoE-associated, infectious HCV was dependent on the LDL-R for cell entry, we divided infectious HCV supernatant between two sets of gradients and subjected each to separation by ultracentrifugation. The resulting fractions were then recovered and used to infect Huh7.5 cells alone or cells that had been pretreated for 16 hours with 1 μ g/mL 25-HC to reduce LDL-R expression. In untreated cells the peak of infectivity occurred at a similar density of 1.06 g/mL (Fig. 4-12A). The corresponding 1.06 g/mL peak recovered from the parallel gradient was significantly reduced in its infectivity when used to infect 25-HC treated cells, indicating that HCV virions of this density are dependent on

LDL-R for infection (Fig. 4-12B). Thus the HCV virions exhibiting a density of approximately 1.06 g/mL are associated with apoE and mediate high infectivity that is dependent on the LDL-R.

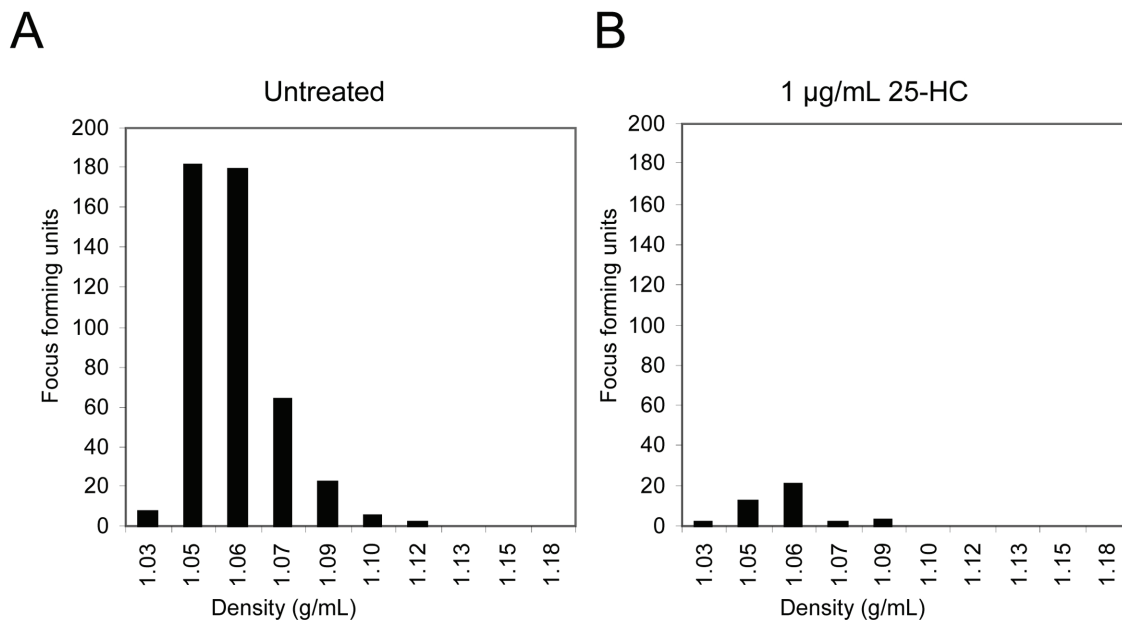


Figure 4-12. LDL-R modulation blocks entry of low density infectious HCV particles. 1 ml each of a common HCV supernatant stock were separated by ultracentrifugation through 10-40% iodixanol density gradients. A) The resulting fractions were used to infect Huh7.5 cells that were cultured alone or B) pretreated for 16 hours with 25-HC to suppress LDL-R expression. HCV infection of cells was quantified 48 hrs later by focus forming unit assay.

Discussion

Our studies reveal that cell culture produced HCV JFH1 infectious virions contain apoE which allows them to productively infect hepatocytes through interactions with the LDL-R. These observations confirm and extend the observations of Chang, et al., who demonstrated that apoE antibody was able to block the entry HCV RNA from cell culture derived virus into Huh7.5 cells (20). Our results reveal that anti-apoE antibody blocks an HCV entry pathway of productive infection. We also showed that apoE antibody was directed against infectious particles, as infectivity was reduced following immunoprecipitation of particles containing apoE and HCV RNA. Although primary hepatocytes do not efficiently support productive infection with patient HCV isolates, it has been demonstrated that entry of patient derived HCV RNA depends on expression of LDL-R in cultured hepatocytes (95). Similarly, we observed that modulating LDL-R levels with 25-HC, siRNA or by LDL-R overexpression controlled productive infection with HCV. Collectively, these results support the idea that HCV entry contributed through the LDL-R pathway leads to productive virus infection as opposed to nonspecific uptake of lipoprotein associated virions.

Early studies of the physical properties of HCV virions derived from patient sera demonstrated a lower than expected density (1.08g/mL) compared to other flaviviruses (93). It was subsequently determined that this low density was due to HCV association with β -lipoproteins which include LDL and VLDL (128). Prince et al. found that most of the patient derived HCV RNA was in the VLDL fraction (111). Other studies have demonstrated that HCV RNA contained within the VLDL and LDL serum fractions of

HCV patients was able to be endocytosed by target cells and that this apparent virus entry activity could be blocked by anti-LDL-R and anti-apoE antibodies (3). Consistent with these observations, we observed that infectious HCV fractionated at a similar density (1.06g/mL) in vitro and importantly was associated with apoE. Furthermore, pretreatment of cells with the LDL-R ligands, β -VLDL (50ug/mL treatment) and to a lesser extent LDL (100ug/mL treatment), reduced subsequent HCV infection. These observations agree with other reports that pretreatment of cultured cells with either VLDL (50-62.5 μ g/mL treatment) or with LDL (125-200 μ g/mL treatment), but not HDL, blocked binding of patient-derived HCV to cultured human fibroblasts (9;37;96). Thus patient-derived and cell culture derived HCV particles can compete with LDL and VLDL/ β -VLDL for binding to human cells. Our studies indicate that cell binding by HCV may more closely resemble the VLDL/IDL interaction with target cells than the LDL interaction inasmuch as highly infectious virus contains apoE and is most sensitive to competition for target cells by exogenous VLDL.

VLDL is produced in hepatocytes wherein lipids stored in droplets within the endoplasmic reticulum (ER) are transferred to a growing apoB core through the actions of microsomal transfer protein (MTP) (54). The growing lipoprotein particle acquires additional triglycerides, cholesterol, and apoE, and is secreted from the cell through the golgi apparatus. HCV core protein localizes to the surface of lipid droplets and is able to interact with viral structural proteins assembled on the ER (94). Furthermore, intracellular membranes containing the HCV replicase are enriched in MTP, apoB and apoE (52), and inhibition of the expression or activity of either of these factors blocks the release of infectious HCV (20;36). Thus, the release of infectious HCV is dependent on

virions being packaged as a VLDL-like particle, which ultimately facilitates infection efficiency through LDL-R interactions of target cells expressing the full complement of HCV co-receptors.

We propose a model in which HCV is secreted from hepatocytes as a VLDL-like lipoviral particle (LVP) containing at least HCV core, RNA, E1, E2 apoB and apoE. In common with natural VLDL derived particles, the HCV LVP could bind initially to cell surface glycosaminoglycans, such as heparin sulfate, in a relatively non specific interaction mediated by either E2 or apoE as both have been shown to bind heparin sulfate (99;114). In terms of the LDL-R, these initial interactions with the target cells could permit the LVP to a specific interaction between apoE and/or apoB and the LDL-R. Such an interaction could depend the processing/lipid removal of the LVP by lipoprotein lipase, which has also been reported to be involved in HCV entry (10). By this model the infectious virus particle could mediate a stable interaction with the target cell that promotes the E2-CD81 interaction, subsequent endocytosis, pH-dependent fusion, and the final entry steps directed by claudin-1 and occludin (28;109). Whereas apoE- LDL-R interaction is probably not essential for entry in vitro since infection was not completely blocked by excess β -VLDL, apoE antibody, or LDL-R knockdown, and because viral E2 protein can interact directly with surface expressed receptors, we propose that efficient and perhaps natural HCV infection are supported by the LVP/LDL-R interaction on target cells during the initial processes of cell binding by the virus. Indeed our siRNA knockdown experiments confirm that both CD81 and claudin-1 function in HCV entry, and recent studies define human occludin as the species-specific factor that is essential for HCV infection (109). While we did not observe any defects in HCV entry upon

knockdown of the majority of SR-BI expression, it is possible that only a small amount of SR-BI is required to facilitate infection or that virions containing sufficient lipid do not require the putative HDL enhancement/membrane modulating function of SR-BI. SR-BI may additionally represent an alternative pathway for entry possibly involving E2 or apoE binding since antibodies against SR-BI have been reported to reduce HCV cell entry (19;62;81). Interestingly, a mutation in E2 has been reported which shows decreased dependence on SR-BI and increased dependence on CD81 for entry, indicating that SR-BI usage by HCV is conditional and might be modulated by viral adaptive mutations (39). Variations in E2 have also been reported to influence HCV genotype differences in SR-BI dependent entry of HCV pseudoparticles (72).

The production of HCV as an LVP may serve as a mechanism to both enhance infection and escape immune detection by co-opting the host lipid delivery system. It may also help to explain the hepatotropism of HCV, as apolipoproteins regulate the recycling of lipid particles to the liver. Moreover, the nature of the HCV virion as a VLDL derived LVP implies that modulating lipoprotein metabolism could play a role in the treatment or management of HCV infection. Indeed, microsomal transfer protein and long chain acylCoA synthetase-3 have already been identified as enzymes required for efficient release of HCV from infected cells (52;140). The grapefruit flavonoid naringenin has also been shown to reduce HCV release from cells by interfering with lipid metabolism, which could possibly alter the composition of the LVP (103). Omega-3 fatty acid supplementation alters lipid metabolism and reduces VLDL production in humans (14). Together these observations suggest that therapeutic or dietary modulation

of specific lipid could be considered as an avenue to regulate LVP production and impart control of HCV infection.

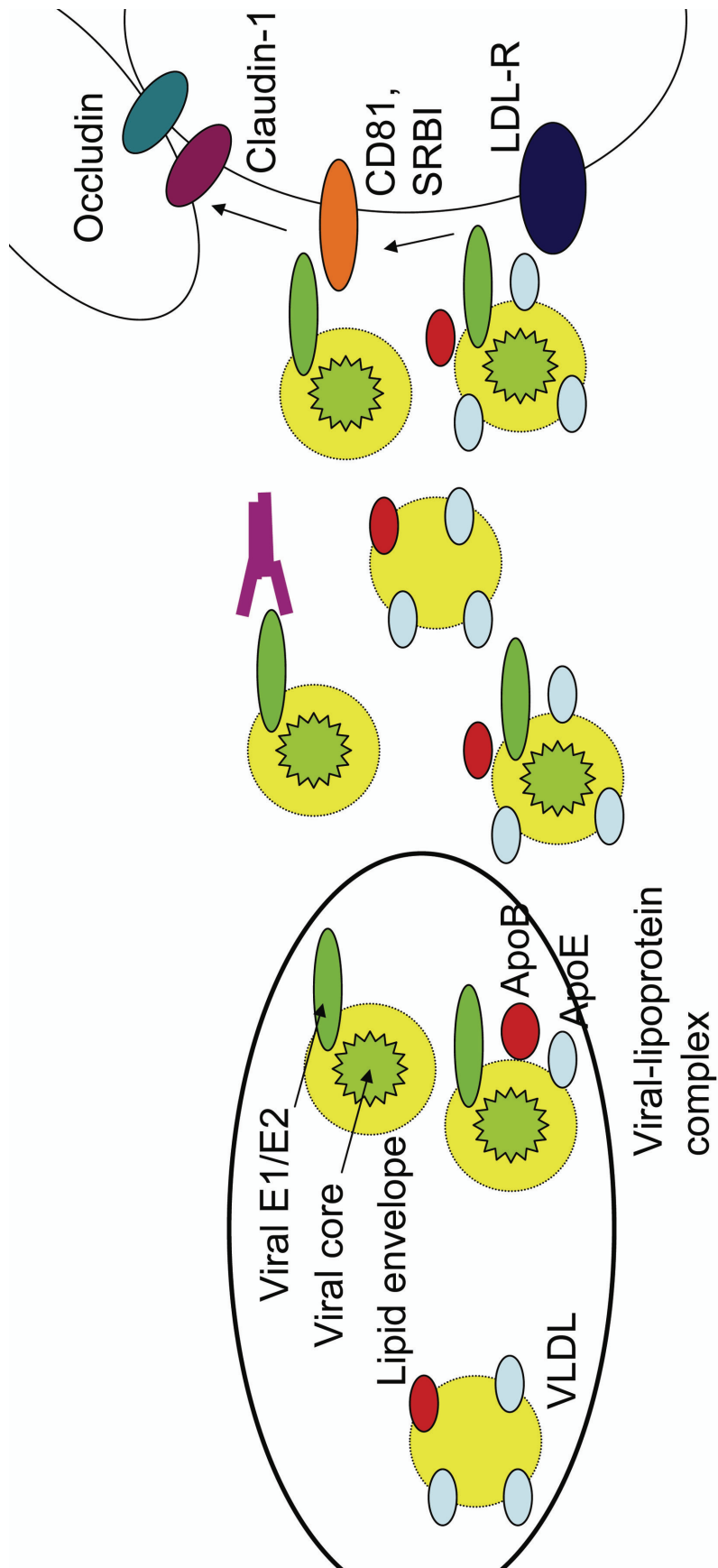


Figure 4-13. Model of HCV entry

CHAPTER 5: HCV ENGAGEMENT OF HOST INNATE IMMUNE DEFENSES

Introduction

After a virion has entered a cell, it is susceptible to the innate immune defenses. Activation of type I interferons represent the first line of defense in the immune response to virus infection. Pattern recognition receptors (PRRs) including the RIG-I like receptors (RLRs) and Toll-like receptors (TLRs) activate downstream signaling cascades leading to activation of the transcription factors interferon regulatory factor-3 (IRF3) and NF κ B which in turn lead to the production of type I interferons (α/β) and inflammatory cytokines. Interferon α/β is then able to signal in an autocrine and paracrine manner through the type I interferon receptor leading to the production of interferon stimulated genes (ISGs) with antiviral activities. Consequently there is a selective pressure driving viruses to evolve strategies for evading these defenses.

Studies in the Gale lab have elucidated many of the key events in innate immune recognition of HCV and subsequent evasion of this response by HCV. Initial studies by Sumpter et al. defined a human liver carcinoma cell line (Huh7.5) that showed enhanced permissiveness for HCV RNA replication (124). This observation did not appear to be an HCV-specific enhancement to viral RNA replication, but rather a defect in innate immune control. Genetic and biochemical studies traced the defect to a single amino acid mutation (T55I) in the N-terminal CARD domain of RIG-I. This mutation turns RIG-I into a dominant-negative protein, thus abolishing its signaling. IFN- β induction by HCV RNA in Huh7.5 cells could be rescued by ectopic expression of a wild-type form of RIG-

I (124). In order to identify the region of the HCV genome recognized by RIG-I, Saito et al. performed an extensive mapping study and found that RIG-I efficiently recognized an unstructured region within the 3' UTR (117). Based on prior understanding of RIG-I recognition, which included the requirements of a 5' triphosphate and dsRNA structure, it was assumed that dsRNA replication intermediates or stem-loop structures within the 5' and 3' UTR regions would contain the RIG-I ligand. However, it was discovered that the most potent IFN- β inducing regions corresponded to an unstructured polyU/UC-rich region within the 3' UTR. Furthermore, the replication intermediate of this region consists of a polyA/AG sequence also activate RIG-I signaling, suggesting that poly-adenosine and poly-uridine regions are substrates of RIG-I. The RIG-I-dependency of the HCV PAMP RNA was confirmed through studies which showed loss of signaling when the RNA was transfected into RIG-I $-/-$ cells. On the other hand, no effect on the potency of the HCV PAMP RNA to trigger IFN β induction was observed in MDA5 $-/-$, MyD88 $-/-$, and TRIF $-/-$ cells, demonstrating that MDA5 and TLR signaling were not required for triggering type I IFN in response to the HCV PAMP RNA (117). Additionally, In Huh7 derived cell lines the TLR3 pathway is defective, suggesting that any innate immune reponse observed in these cells would be TLR3 independent (110). These studies highlight the importance of RIG-I in HCV RNA detection leading to IFN- β signaling. However, HCV also encodes mechanisms to block IFN- β signaling.

Studies by Foy et al. revealed the ability of HCV NS3/4A to disrupt induction of type I interferon. Ectopic expression of NS3/4A could block Sendai virus induced phosphorylation, dimerization and nuclear translocation of IRF-3 (32). This blockade was dependent on the protease activity of NS3/4A and could be reversed by treatment of cells

with a pharmacological inhibitor of the protease function of NS3/4A or by mutating the active site within the NS3/4A protease domain (32). Subsequently, it was shown that NS3/4A acted downstream of RIG-I as IFN- β induction was blocked by co-expression of NS3/4A with a constitutively active form of RIG-I (N-RIG) (31). NS3/4A was found to act upstream of the IRF-3 activating kinases TBK1 and IKK ϵ , as the activity of these signaling molecules were not affected by co-expression with NS3/4A (18). When IPS-1 was identified as the adaptor molecule bridging RIG-I to these downstream signaling components, it was also found to be the target of NS3/4A-mediated blockade.

While these studies provided compelling evidence for RIG-I dependent initiation of innate immunity to HCV and subsequent evasion of these pathways by HCV NS3/4A protease, the outcome of these opposing detection and evasion activities in the context of live virus infection as well as the existence/importance of alternative signaling pathways stimulated by HCV infection remained unexplored. Such studies are the focus of this chapter.

Results

HCV infection induces an antiviral response

In order to determine the kinetics of HCV activation of the innate immune response, Huh7 cells seeded in chamber slides were infected with HCV at MOI=0.5 and fixed for immunofluorescence analysis at 12 hour intervals. IRF3 localization was examined as a marker of innate immune activation with redistribution of IRF3 from a cytoplasmic localization to a nuclear localization indicating activation. HCV infected cells with nuclear IRF3 could be detected by 36 hours post infection (Fig. 5-1). In Huh7.5 cells no nuclear IRF3 was observed at times points up to 48 hours.

One of the target genes downstream of IFN stimulation is the transcription factor IRF7. Upon activation/phosphorylation, IRF7 translocates to the nucleus where it drives expression of IFN- α species, thereby facilitating an IFN amplification loop. In order to determine if HCV infection was capable of activating IRF7, Huh7 or Huh7.5 cells were transfected with HA-tagged constructs expressing IRF7. These cells were fixed at 12 hour intervals post infection with HCV at MOI=1 and examined for IRF7 localization by immunofluorescence. Nuclear IRF7 could be detected in the Huh7 cells but not the Huh7.5 cells by 36 hours post infection. This suggests that HCV infection is capable of phosphorylating IRF7 and supporting an interferon amplification loop that may be RIG-I dependent.

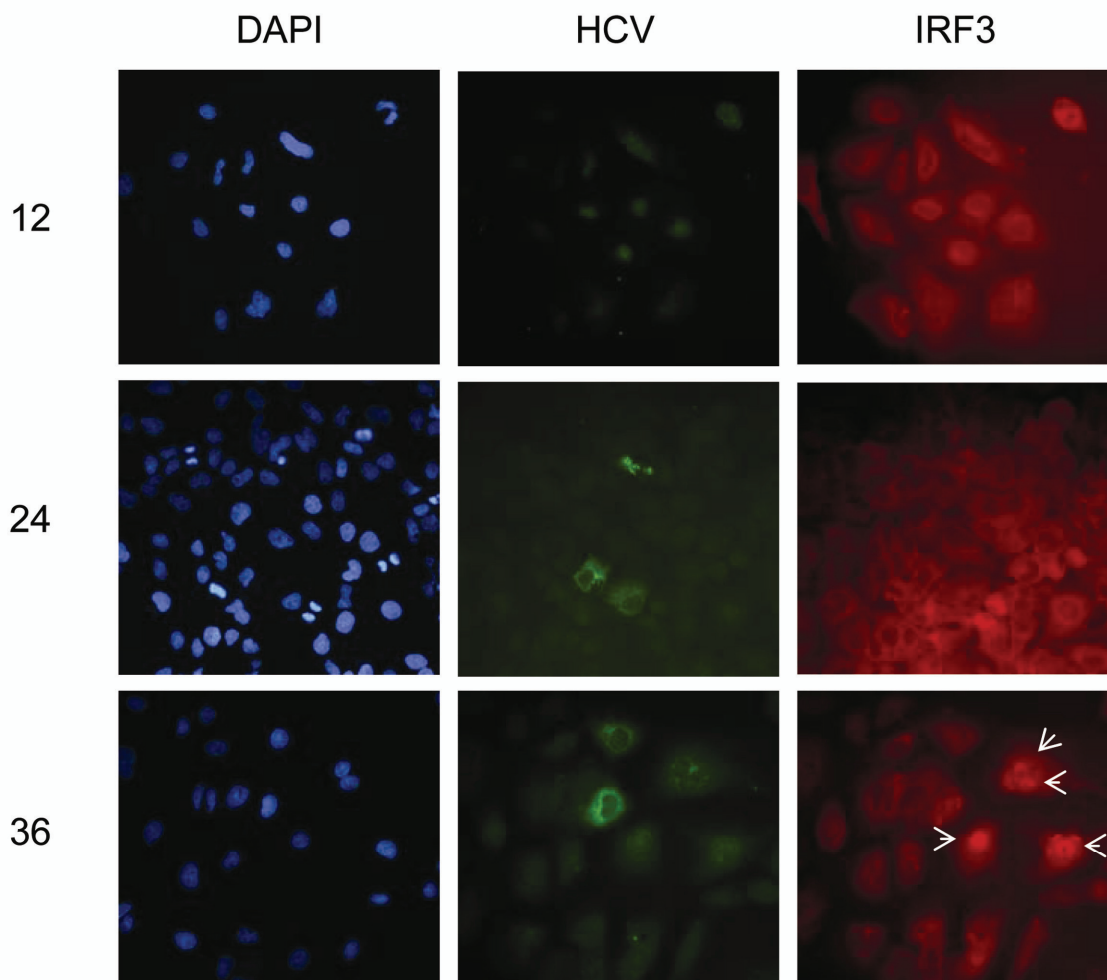


Figure 5-1. HCV infection activates IRF3. Huh7 cells infected with HCV at MOI=0.5 show nuclear IRF3 localization by 36hrs post infection.

These results provide evidence for HCV mediated activation of innate immune response, but do not address the efficacy of this response against HCV. In order to determine if HCV products were capable of stimulating a response with antiviral activity against HCV, I tested the interferon/antiviral activity released into the supernatant of cells transfected with HCV PAMP RNA. Huh 7 cells were transfected with the HCV PAMP RNA (PUC), an HCV derived negative control RNA (X region), or a host negative control RNA (tRNA). Serial dilutions of condition media (supernatants) from these cells were prepared by diluting sample in fresh media. An IFN- β control was similarly prepared by serial dilution in normal media. Antiviral activity of these preparations was assessed by looking at their ability to block HCV infection in a pretreatment experiment or inhibit HCV RNA replication in a post-treatment experiment (Fig. 5-2). In the pretreatment experiment Huh7.5 cells were treated with dilutions of the conditioned media or IFN- β for 12 hours, washed with PBS, infected with HCV in a 48 well plate at 150 FFU/ well, and then incubated in normal media for an additional 48 hours when the number of infected foci was quantified. Similar to the IFN- β positive control, conditioned media from HCV PAMP (PUC) treated cells was able to completely prevent HCV infection, while conditioned media from HCV X region or tRNA treated cells had no effect on infection. In the post-treatment experiment Huh7.5 cells were infected at MOI=1. 24 hours post infection these cells were treated with the conditioned media or IFN- β for an additional 24 hours and relative HCV RNA levels were quantified by RT-PCR. Both IFN- β and PUC treated cells showed a 75% decline in HCV RNA levels while there was no effect on HCV levels in the negative control treated cells. These data

indicate that recognition of the HCV PAMP can lead to at least a partially effective antiviral response against HCV in infected and neighboring cells.

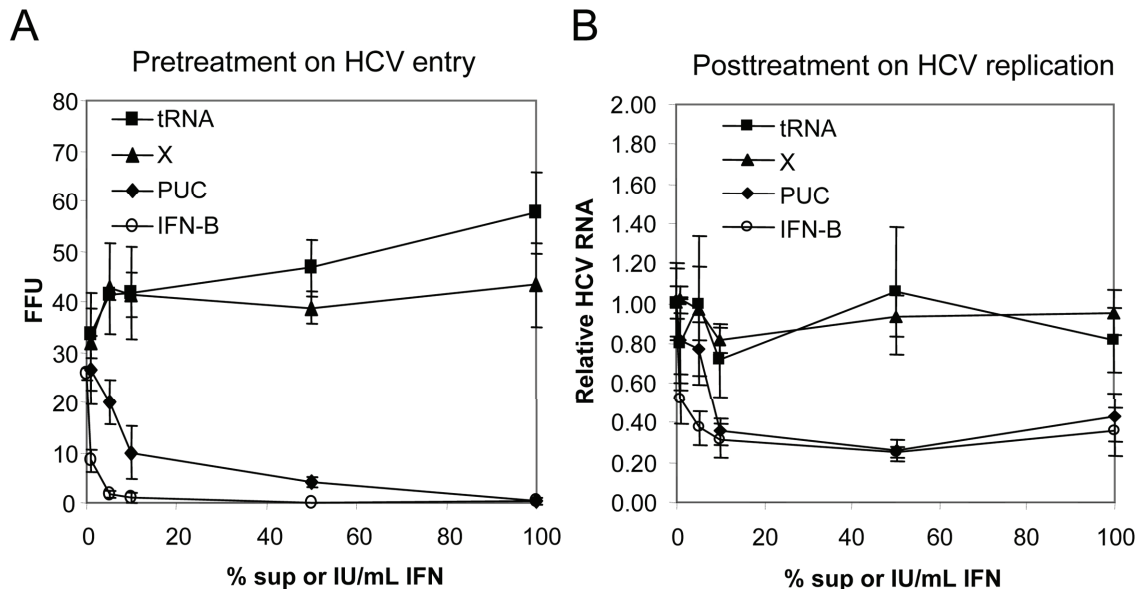


Figure 5-2. Antiviral activity in supernatant of HCV RNA treated cells. Human IFN- β or supernatant collected from Huh7 cells 24 hours post transfection with tRNA, PUC, or X RNA was diluted in DMEM and A) added to naïve Huh7.5 cells 12 hours prior to infection to assess effect on HCV entry, or B) 24 hours post infection to assess effect on relative HCV RNA present 48 hours post infection.

RIG-I is a key mediator of HCV control

Prior work with the replicon system suggested that RIG-I may be an important mediator of the innate response to HCV. In order to test the ability of RIG-I to control initial infection, Huh7 (wildtype RIG-I) or Huh7.5 (RIG-I mutant) cell lines were infected with HCV and their relative permissiveness was measured over a time course of infection. A one step growth curve experiment was carried out by infecting Huh7 or Huh7.5 cells with HCV at MOI=2 and then measuring the titer of HCV released into the

supernatant over time (Fig. 3A). Virus was detectable in the supernatant of Huh7.5 cells at an earlier time point post infection (24 hours) compared to Huh7 (36 hours) and at higher titers during the first 36 hours of infection. However, by 72 hours post infection the amount of virus present in the supernatant of both lines had equalized.

To visually assess RIG-I mediated control of HCV, Huh7 and Huh7.5 cells were seeded on glass slides and infected at MOI=1. Slides were fixed and stained for intracellular HCV protein every 12 hours post infection for 2 days (Fig. 5-3B). Consistent with the growth curve experiment, HCV infected cells were readily detectable by 24 hours in Huh7.5 cells. HCV positive cells were also detectable in the Huh7 line by 24 hours, although the percentage of HCV positive cells lagged behind the Huh7.5 line. By 48 hours almost all cells were infected in both lines suggesting that RIG-I dependent control of HCV is most pronounced in the early hours of infection. However RIG-I may continue to play a role in suppressing virus replication levels at later time points since the intensity of protein staining was diminished in Huh7 cells at 48 hours despite similar numbers of cells being infected.

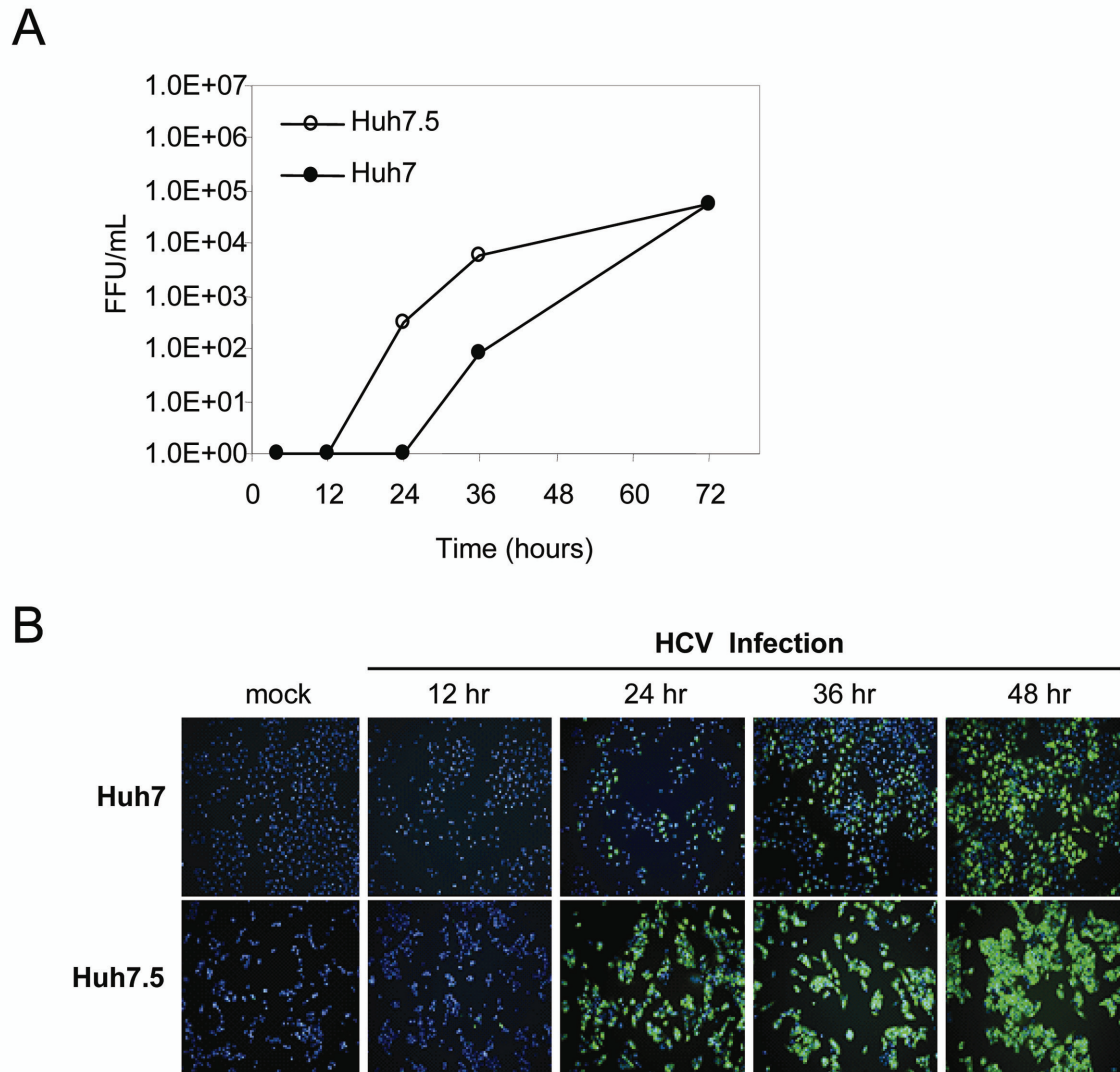


Figure 5-3. RIG-I controls early HCV infection. A) Huh7 or Huh7.5 (RIG-I deficient) cells were infected at MOI=2 and supernatant was collected for titer at the indicated time points. B) Huh7 or Huh7.5 cells were infected at MOI=1 and fixed for intracellular HCV staining every 12 hours.

HCV cleaves IPS-1 to disrupt innate immunity

In 2005 several groups reported on a signaling molecule linking RIG-I to downstream IRF3 activation. While all groups identified the same protein, it was given a unique name by each group and called IPS-1, MAVS, VISA, or Cardif. This molecule was also independently identified in the Gale lab and initially termed Signaling Transducer to Interferon (STI). I will use each group's terminology here to describe their findings, but refer to the protein as IPS-1 elsewhere throughout this work after the nomenclature of the first accepted paper. Kawai et al. showed that overexpression of IPS-1 led to ISG expression through activation of IRF3, IRF7, and NF- κ B. They further showed that IPS-1 contained a CARD domain which mediated binding to RIG-I and MDA5, and that knockdown of IPS-1 reduced type 1 interferon response to viral infection (66). Seth et al. confirmed these findings and showed that MAVS contained a transmembrane region targeting it to the mitochondria. They also showed that MAVS functions downstream of RIG-I and upstream of TBK-1 (120). Xu et al. again showed that overexpression of VISA activates IFN- β and NF- κ B, and that knockdown blocks virus-induced signaling. They showed that VISA forms a complex with RIG-I and IRF3, and mapped sites of VISA interactions with TRIF and TRAF6 (139). Meylan et al. confirmed these findings for Cardif, and additionally showed that the protein could be cleaved by the HCV NS3/4A protease at position 508 (91). Before I joined the Gale lab, studies by Ming Loo and Cindy Johnson had similarly established that expression of HCV NS3/4A from a transfected plasmid or by an HCV replicon could cleave IPS-1 at amino acid position 508, resulting in a faster migrating form detectable by western blot. In collaboration with Ming Loo I carried out studies to determine at what time during the

course of HCV infection IPS-1 was cleaved, and what effects this cleavage may have on the HCV lifecycle.

Huh7 cells were mock infected or infected with HCV at MOI=2 and then lysates were collected for immunoblot analysis at 6, 12, 24, and 48 hours post infection. The faster migrating cleaved form of IPS-1 could be detected at 48 hours post infection coincident with detection of HCV NS3 (Fig.5-4A). In a parallel series of immunofluorescence experiments, the 48 hour time point associated with IPS-1 cleavage correlated with the loss of detectable nuclear IRF3. These observations are consistent with an NS3/4A mediated blockade of IPS-1 dependent signaling to the IRF3 innate immune program. Despite using a high MOI to ensure that all cells were infected, quantification of activated cells showed a maximum of 15% nuclear positive cells which was observed at the 36 hour time point. This suggests that IRF3 activation is either a very transient phenomenon or that in many cells HCV is able to cleave IPS-1 and block IRF3 activation even before there are sufficient levels of HCV RNA to trigger RIG-I dependent signaling. Results from an interferon bioassay experiment favor the latter hypothesis.

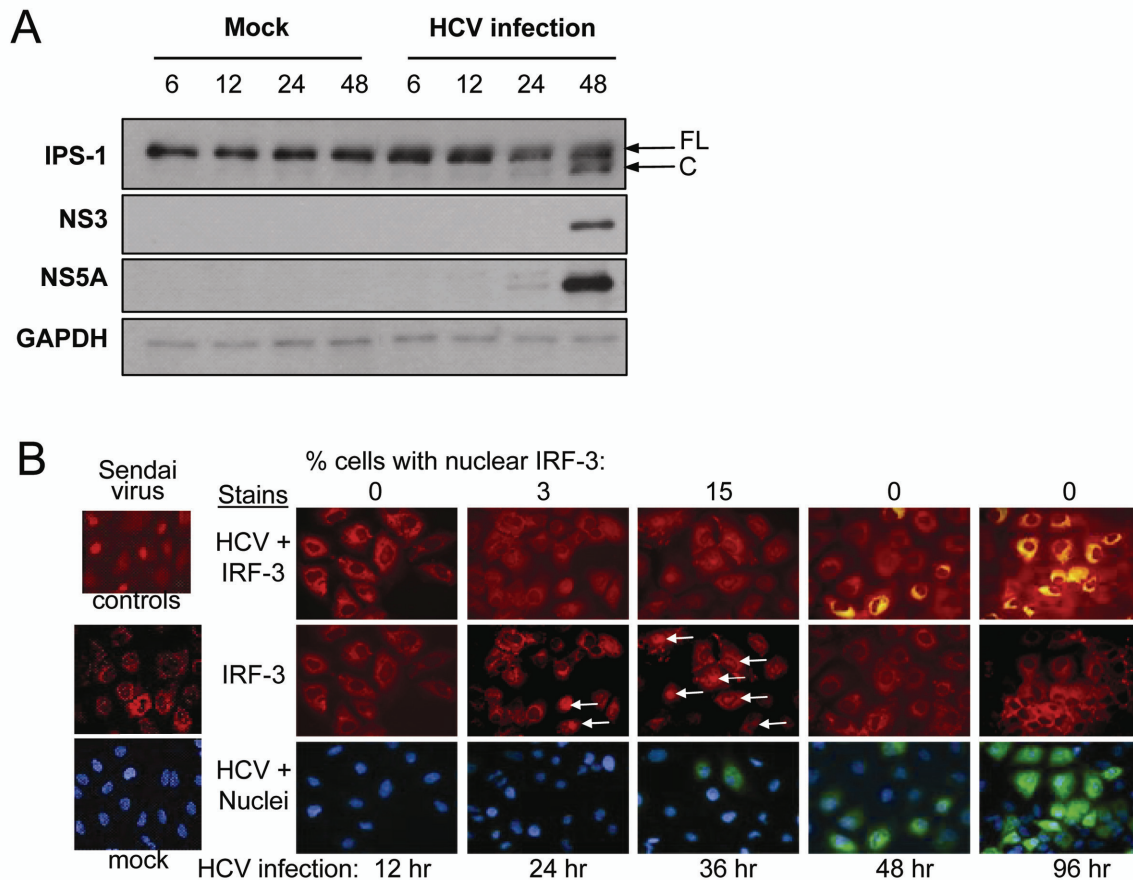


Figure 5-4. HCV cleaves IPS-1 to block innate immune signaling. A) Huh7 cells were mock treated or infected with HCV at MOI=2. Cell lysates were collected at the indicated time points and analysed by immunoblot.(FL, full length, C, cleaved) (Infection experiment by David Owen, immunoblot by Ming Loo) B) Huh7 cells were infected with HCV at MOI=2 or Sendai virus (control). Slides were fixed and IRF-3 and HCV proteins detected by immunofluorescence. The percentage of cells with nuclear IRF-3 localization based on counting multiple fields is presented above each time point. (Infection experiment by David Owen, immunostain and microscopy by Ming Loo)

Although HCV PAMP RNA transfection leads to the secretion of interferon activity into the media (Fig. 5-2), similar experiments using supernatant from HCV infected cells did not show significant antiviral activity. Huh7 or Huh7.5 cells were infected with HCV at MOI=1 and then conditioned media was collected at 1, 2, 3, or 4 days post infection for measurement of interferon activity by VSV bioassay (described in

methods). None of the samples showed interferon activity greater than the assay's limit of detection of 1-2 U/mL. IFN- β expression was also below the limit of detection in HCV infected Huh7 or Huh7.5 cells as measured by luciferase assay or RT-PCR. This suggests that despite initial low levels of HCV-triggered IRF3 activation and the differences observed in Huh7 and Huh7.5 infection kinetics, HCV is able to very efficiently evade this pathway via IPS-1 cleavage.

If HCV cleavage of IPS-1 by NS3/4A is the major factor blocking an innate immune response, then preventing NS3/4A cleavage with a specific protease inhibitor would be expected to restore innate immune signaling. To test this hypothesis I infected Huh7 cells with HCV at MOI=1. At 48 hours post infection cells were washed and then incubated with fresh media containing the HCV NS3/4A protease inhibitor ITMN-C. Cells were collected at 0, 24, 36, or 48 hours post treatment and analysed by immunoblot (Fig 5-5C). ITMN-C treatment resulted in an accumulation of full length IPS-1 protein by 24 hours post treatment and induction of interferon stimulated gene-56 (ISG-56), suggesting restoration of the IPS-1 dependent innate immune response. IPS-1 integrity and ISG-56 expression were similarly restored in the genotype 1b K2040 replicon cell line upon treatment with ITMN-C (Fig. 5-5A and B). In both cases treatment was associated with a decline in the levels of HCV protein. Thus therapy with NS3/4A protease inhibitors may have a dual efficacy in inducing an innate immune response in addition to the direct effects on polyprotein processing.

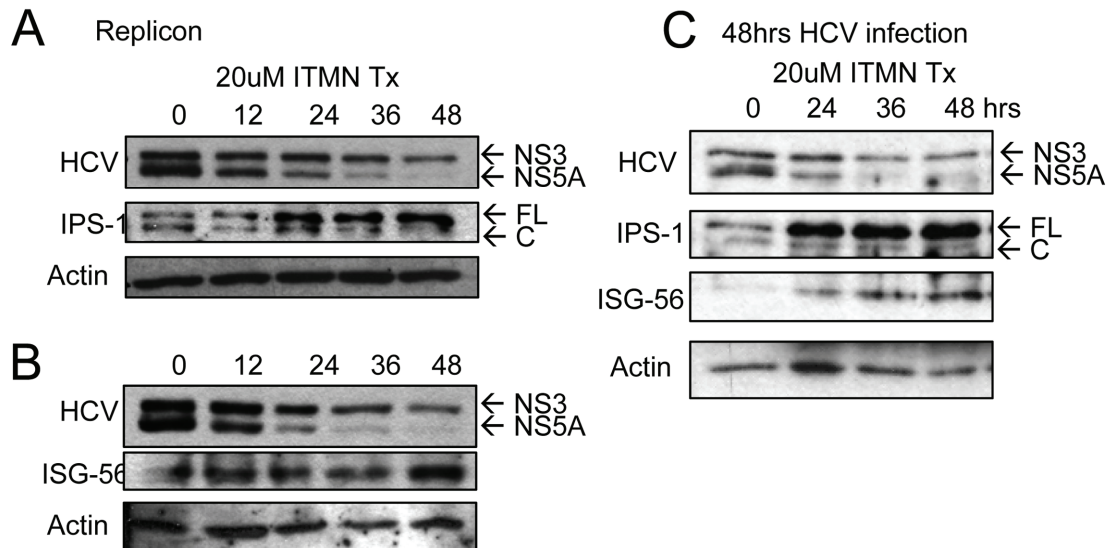


Figure 5-5. NS3/4A protease inhibitor restores innate immune response. Huh7 cells containing the JFH1 replicon (A and B) or Huh7 cells 48hrs post HCV infection at MOI=1 (C) were treated with 20uM ITMN-C for an additional 0, 12, 24, 36 or 48 hours. Western blot analysis shows a decline in HCV protein levels associated with protection of IPS-1 from cleavage and induction of ISG-56 expression.

HCV induces RIG-I independent innate immunity

In addition to characterizing HCV infection with respect to the known pathways predicted to be important in innate immune response, we wanted to explore the global response to HCV infection using a microarray approach. In particular we were interested in identifying potential RIG-I independent pathways of HCV detection. Towards this end we included analysis of Huh7.5 cells alongside Huh7. These cells were infected in triplicate at MOI=2. RNA was extracted at 4, 12, 24, 36, and 72 hours post infection and analysed by microarray in collaboration with the Katze lab at the University of Washington.

269 genes were identified which were statistically significantly regulated at least 2 fold up or down in at least one of the time points in at least one of the cell lines (Fig 5-6A and Appendix A). Overall, more genes were regulated by HCV infection in Huh7.5 cells than in Huh7 (Fig. 5-6B). Number of genes regulated correlated with HCV RNA copy number (compare Fig. 5-6B and 5-6C). This may indicate a host program of gene expression activated in response to detection of higher levels of HCV RNA by a pattern recognition receptor (PRR). Alternatively, elevated HCV RNA may just be a surrogate marker for generally higher levels of HCV replication, protein, and associated virus perturbation of host metabolism. Interestingly in the Huh7.5 cells at late time points (36 hours and later) post infection, genes that are member of an ISG bioset were upregulated. When infection was extended to 96 or 120 hours in a follow-up experiment, these genes were even more strongly induced (Fig. 5-6D). This suggests the existence of pathways leading to a RIG-I independent interferon response to HCV infection. The interferon species (if any) leading to the induction of these interferon stimulating genes is unknown. However a type 3 interferon, IFN- λ 3 (IL-28B) was upregulated at 36 hours along with a component of the type 3 interferon receptor (IL28RA). Several inflammatory cytokines were also induced, particularly at 3 days and later post infection (Fig. 5-6D, right panel).

Figure 5-6. HCV stimulates a RIG-I independent host response. Huh7 or Huh7.5 cells were infected in triplicate with HCV at MOI=2. At the indicated time points post infection RNA was extracted for microarray analysis. A) Cluster analysis of genes that were at least 2 fold upregulated or downregulated in at least 1 sample condition. B) Total number of differentially regulated genes as described above for each sample condition. C) HCV genome copies per ng of cellular RNA as determined by RT-qPCR. D) Expression profiles of selected immune-associated genes in Huh7.5 (RIG-I deficient) cells. (Infection experiment by David Owen, microarray and gene analysis by Kathie Walters)

To determine the relevance of the interferon lambda finding I made interferon lambda promoter luciferase constructs for IFN- λ 1 and IFN- λ 3 in which the 2kb region immediately upstream of the translation start site was cloned into the PGL3 Basic luciferase plasmid backbone. In preliminary experiments to characterize these constructs I found that Sendai virus infection readily activates IFN- λ 1 in a RIG-I dependent manner. Sendai virus infection or constitutively active IRF3 (IRF3-5D) did not induce IFN- λ 3 promoter activity, but it could be induced by cotransfection with a constitutively active form of IRF7, IRF7-2D. When IFN- λ promoter luciferase activity was examined at 24 or 48 hours post HCV infection, no induction of either the IFN- λ 1 or IFN- λ 3 promoter was observed. Efforts to detect IFN-L expression by RT-PCR were also unsuccessful. Thus I was unable to confirm a role for interferon lambda signaling in response to HCV infection. It should also be noted that IFN- β was not among the genes at least 2 fold regulated, even in Huh7 cells at early time points. This again underscores the efficient evasion of IFN- β activation by HCV.

Many of the inflammatory cytokines upregulated in the microarray contain NF κ B binding sites in their promoters. In order to look for evidence of NF κ B activation during the course of infection, Huh7 or Huh7.5 cells were infected with HCV at MOI=2. Cell lysates were collected at late time points on days 2, 3, and 4 post infection and analysed

by immunoblot (Fig. 5-7A). As expected there were higher levels of HCV protein present in the RIG-I deficient Huh7.5 cells. Huh7.5 cells also showed the loss of inhibitor of NF κ B (I κ Ba) consistent with activation of NF κ B signaling. Differences between mock and infected Huh7 cells were less pronounced, but there also appeared to be a reduction in I κ Ba levels. No ISG-56 was detected suggesting that the IFN- β pathway remained blocked and that any NF κ B activation was occurring independently of the IFN inducing pathway. Direct evidence of NF κ B activation was also sought by looking directly for the presence of the NF κ B p65 subunit in the nucleus of infected cells. Huh7 or Huh7.5 cells were seeded on chamber slides and infected with HCV at MOI=1 or treated with 10ug/mL TNF- α as a positive control to activate NF κ B. Nuclear p65 staining was observed at 48 hours and later in both infected Huh7 and Huh7.5 cells (Fig. 5-7B and C). The presence of nuclear p65 in Huh7.5 cells which lack RIG-I and in Huh7 at times post IPS-1 cleavage argues for the existence of a RIG-I/IPS-1 independent pathway of NF κ B activation and subsequent inflammatory cytokine production.

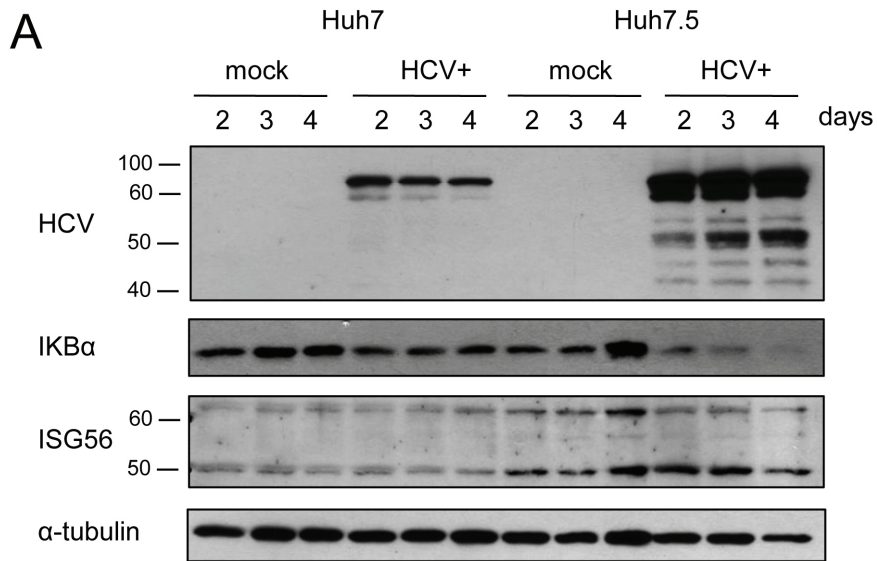
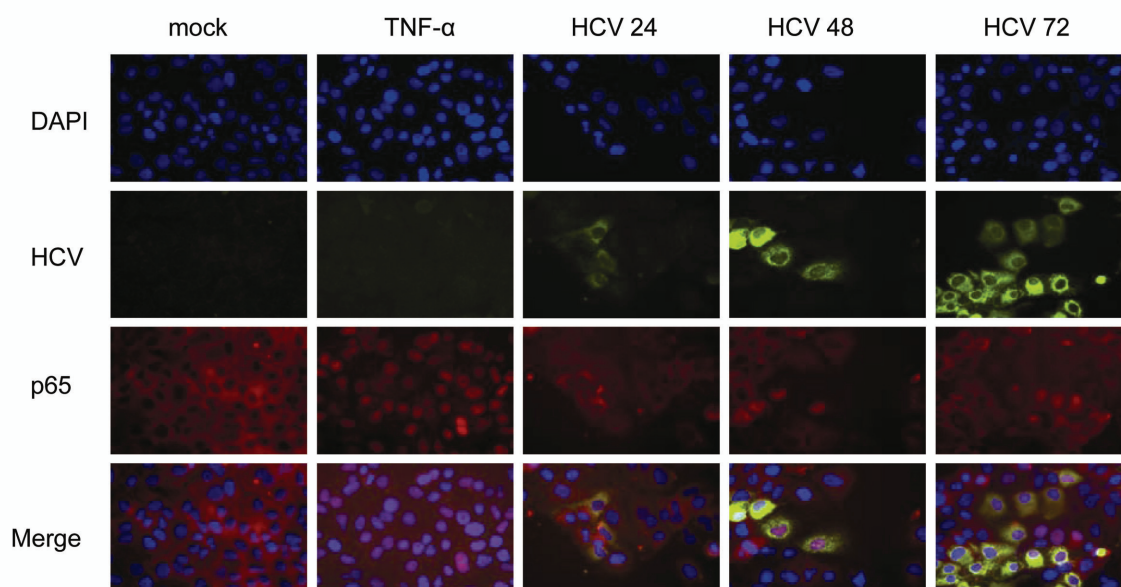
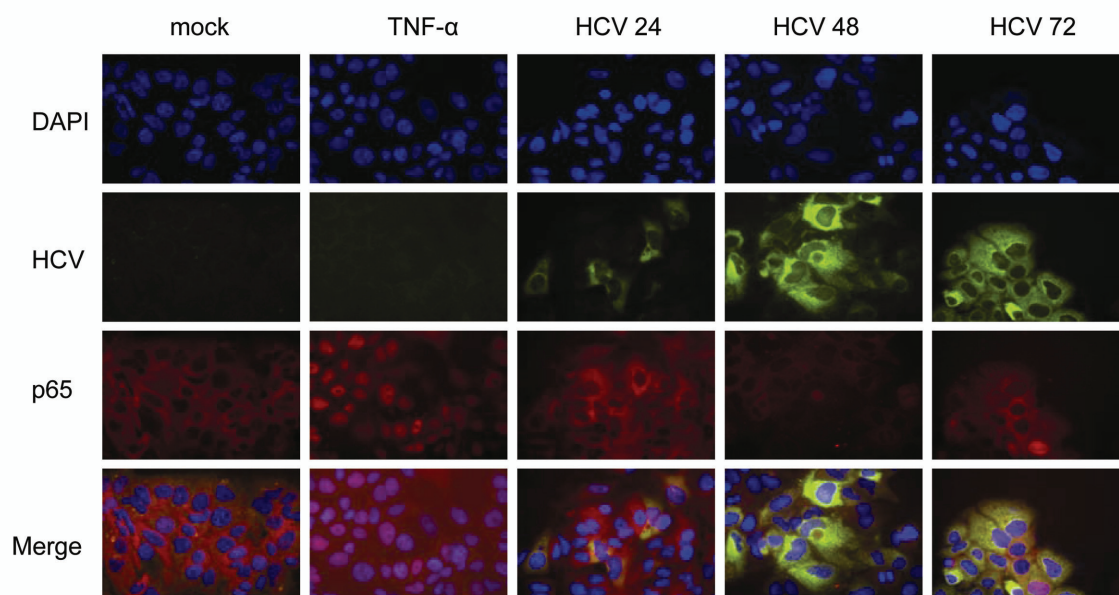


Figure 5-7. HCV activates NFκB. A) Huh7 or Huh7.5 cells were infected with HCV at MOI=2. Cell lysates were collected 2, 3, or 4 days post infection and analysed by immunoblot for NFκB activation (loss of IκBα) or interferon activation (ISG56). B) (next page) Huh7 or C) Huh7.5 cells were treated with 10ng/mL TNF-α or infected with HCV at MOI=2 and stained for intracellular HCV protein (green) or NFκB p65 (red).

B Huh7**C** Huh7.5

Discussion

These data show that HCV is capable of inducing RIG-I dependent activation of an innate immune response mediated through IRF3 and/or IRF7 leading to the production of interferon species with anti-HCV antiviral activity. This response is transient however as cleavage of IPS-1 during HCV infection occurs between 24 and 48 hours post infection leading to a loss of IRF3 signaling and a blockade of the innate immune response. These tissue culture observations are likely to reflect what occurs during human disease as cleavage of IPS-1 has also been observed in liver tissues from chronically infected patients (79). Prior studies to define the minimal components of NS3/4A required for the blockade found that a single-chain protease, consisting of the NS3 protease domain covalently linked to NS4A, was sufficient for IPS-1 cleavage (58). Interestingly, the closest relative to HCV, GB virus B, also mediates cleavage of IPS-1 by NS3/4A (22). As HCV and GB viruses cause persistent infection in humans, this suggests the importance of disrupting IPS-1 signaling through viral protease actions in establishing a persistent viral infection. Indeed we observed that treatment with an NS3/4A protease inhibitor led to a restoration of ISG induction which correlated with a decline in HCV protein levels.

In addition to cleavage of IPS-1, HCV has been suggested to evade type I IFN induction through a variety of alternative strategies. NS3/4A has been shown to cleave the TLR3 adaptor molecule TRIF, thus blocking TLR3 dependent signaling, though this has not yet been demonstrated in vivo (75). Others have shown that HCV NS3, NS3/4A, NS4B, and NS5A inhibit MyD88-dependent TLR signaling in a murine macrophage cell line (1). This study found that NS5A directly binds MyD88 and inhibits the recruitment

of interleukin-1 receptor-associated kinase 1 (IRAK1) to MyD88, thus blocking MyD88-dependent signaling. The NS5A-MyD88 interaction was found to be mediated by the interferon sensitivity-determining region (ISDR) located between amino acids 204 to 280 within NS5A, as demonstrated by studies in which expression of a mutant NS5A lacking this region partially restored Myd88-dependenet signaling (1). HCV is also able to antagonize type I IFN signaling by inducing the expression of a negative regulator of JAK/STAT signaling. Expression of the HCV core protein in the human hepatocellular liver carcinoma cell line, HepG2, induced the expression of suppressor of cytokine signaling (SOCS)-3 (16). SOCS-3 expression has been observed in liver biopsies of HCV-infected patients undergoing IFN therapy (135). While SOCS3 inhibits cytokine signaling by preventing the activation of STAT proteins, the mechanism by which HCV core induces SOCS-3 expression has yet to be determined. In addition to the HCV core induction of SOCS-3 expression, HCV NS5A has been shown to disrupt the function of the IFN-inducible gene PKR (34). The study found that amino acids 2209 to 2274 of HCV genotype 1b NS5A directly binds to PKR and inhibits dimerization, thus disrupting PKR activity. These mechanisms of immune evasion are outlined in Figure 5-8.

While HCV is quite effective at blocking pathways leading to type 1 IFN production, our microarray studies show that alternative signaling pathways exist leading to the activation of NF κ B and the expression of inflammatory cytokines. The identity of the upstream sensor(s) leading to this activation remain unclear. Also unresolved is the nature of the stimulus- whether a specific virus PAMP, or an altered cellular state arising from uncontrolled virus replication. An interesting target for future investigation in this area is the NOD-like receptor (NLR) family of proteins. The original family members

NOD1 and NOD2 were identified as activators of NF κ B signaling in response to bacterial PAMPs. Other family members form caspase-1 activating complexes termed inflammasomes. The NLRP3 inflammasome has been shown to play a role in the innate immune response to influenza infection (6;55;127) as well as a variety of other cell stress or “danger” stimuli (reviewed in (15)). Only a few of the 23 family members have been characterized. It would be interesting to construct vectors expressing these proteins and screen for their ability to enhance NF κ B signaling in response to HCV. There is also evidence for crosstalk between the RLR and NLR pathways as NLRX1 has been shown to interact with IPS-1 although reports conflict as to whether it acts as a positive or negative regulator of innate immunity (97;126).

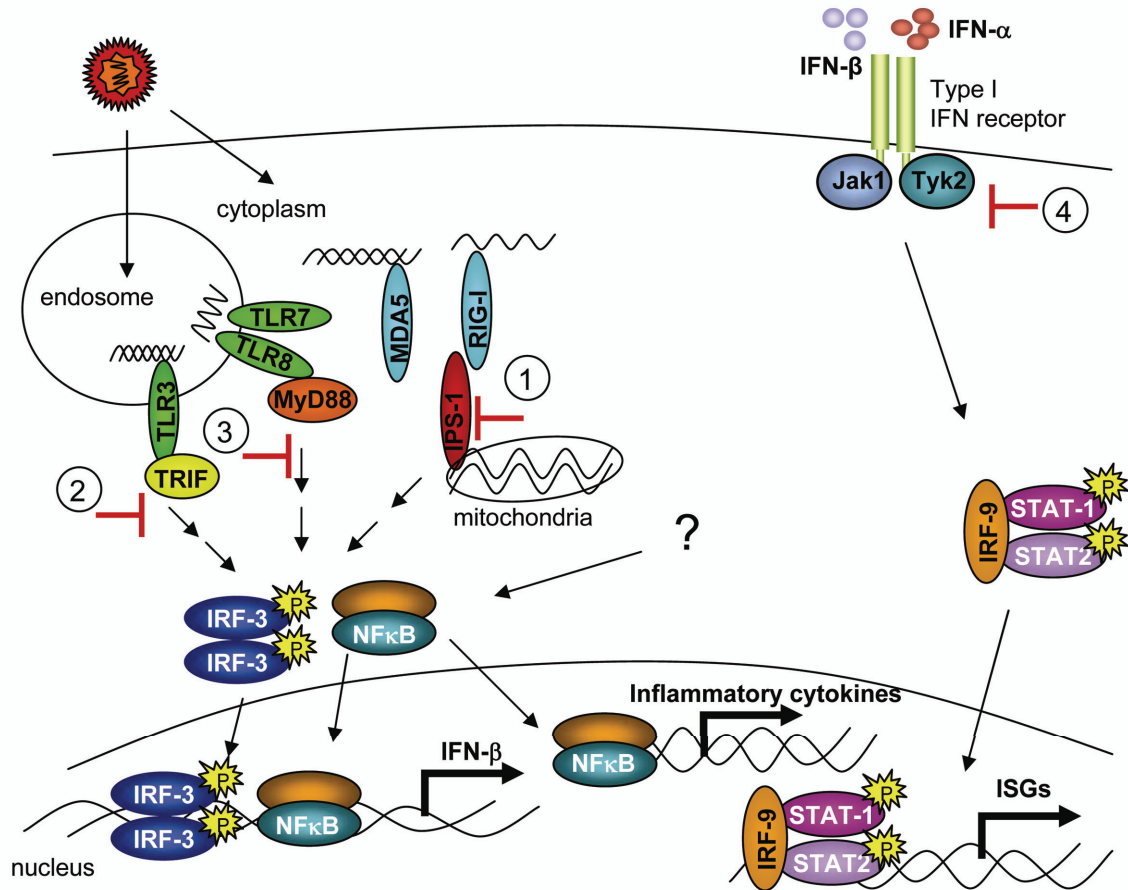


Figure 5-8. Model of HCV interaction with innate immune system. In order to evade activation of ISGs in response to detection of virus products, HCV employs a number of strategies including 1) NS3/4A cleavage of IPS-1 2) NS3/4A cleavage of TRIF 3) NS5A interference with MyD88 and 4) HCV core induced SOCS-3 expression. This blockade results in accumulation of virus products and/or changes in cell physiology that activate NFκB and inflammatory pathways.

CHAPTER 6: TOWARDS THERAPY

These studies demonstrate some of the ways that HCV subverts host cell physiology and signaling pathways to initiate and maintain infection early in the virus lifecycle. In addition to the knowledge gained about the biology of HCV infection, these observations suggest potential areas for therapeutic development.

I have shown that assembly of HCV virions within the liver is linked to VLDL production and that this association facilitates binding/entry through an interaction between apoE on the virion and the LDL-R on hepatocytes. Thus HCV takes advantage of a host receptor–ligand interaction to support infection. With this understanding one could envision different approaches for disrupting this interaction. One option would be to block apoE-LDL-R interaction directly with molecules that inhibit LDL-R expression or function, however such an approach would lead to side effects of increased serum cholesterol and risk for cardiovascular disease. Another approach would be to block VLDL production, such as with an MTP inhibitor. Indeed we showed that this blocked release of infectious HCV. Such a strategy may be useful as part of a short course of combined therapy, however in clinical trials of MTP inhibitors for use as cholesterol lowering agents, patients developed hepatic steatosis within a few months of initiating therapy. A related idea is dietary modification to alter VLDL production, such as consuming more omega-3 fatty acids which have been shown to reduce VLDL production. It would be interesting to conduct a retrospective study of HCV patients already taking these supplements to see if this idea has merit. A final approach least likely to interfere with host metabolism would be to try to uncouple HCV from the

VLDL synthesis machinery within the hepatocyte, perhaps by identifying and targeting regions within core or NS5A that facilitate lipoprotein association.

I have also shown that HCV NS3/4A mediates a very efficient blockade of the innate immune response by cleaving IPS-1. In many cells this may occur even before there are significant levels of HCV RNA present to stimulate RIG-I. However HCV RNA in infected cells remains a potent potential activator of innate immunity as demonstrated by the induction of ISGs when IPS-1 signaling is restored with NS3/4A protease inhibitor treatment. One implication of this observation is that NS3/4A protease inhibitors can have dual efficacy as innate immune agonists in addition to their direct effect on disrupting polyprotein processing. These compounds are already in clinical trials and may soon be approved as combination therapy with interferon and ribavirin. Another way to take advantage of the PAMPs present during HCV infection would be to try to find agonists of RIG-I signaling that would bridge activated RIG-I molecules to downstream signaling components independently of IPS-1. This is an area of ongoing interest in the Gale lab.

Finally, I have shown that hepatocytes can mount a RIG-I independent response to HCV infection which involves NF κ B activation leading to ISG and inflammatory cytokine production. It is unclear whether this response serves a protective antiviral role in HCV infection or if it is a mediator of inappropriate chronic inflammation leading to liver injury. It is likely a combination of both. Studies of the role of NLR family members in HCV infection and their potential crosstalk with RLR and TLR signaling pathways may help clarify this response and suggests ways to enhance the antiviral response while dampening the chronic inflammatory response.

APPENDIX A: 269 Genes regulated by HCV infection.

Genes at least 2 fold up (grey) or down (white) in at least 1 time point condition as detected by microarray

Sequence Description	7-4hr	7-12hr	7-24hr	7-36hr	7-72hr	7.5-4hr	7.5-12hr	7.5-24hr	7.5-36hr	7.5-72hr
26 serine protease	0.76	2.90	1.35	1.85	4.70	1.04	0.73	1.27	7.39	0.45
acheron	0.94	0.99	0.93	1.00	1.12	1.23	1.00	1.02	0.98	3.37
activating transcription factor 3	0.78	1.07	0.91	1.10	3.79	0.99	1.05	1.06	1.11	7.16
ADP-ribosylation factor 3	1.04	1.04	1.05	1.06	1.44	0.87	0.89	1.03	1.00	0.48
adult retina protein	1.58	0.91	0.85	0.99	0.83	1.03	1.05	0.93	0.90	2.28
albumin	1.44	1.03	1.03	1.23	1.50	2.56	1.34	1.39	1.31	0.36
alpha-fetoprotein	1.03	0.41	1.40	0.37	1.39	1.37	1.24	1.00	1.37	0.55
amphiregulin (schwannoma-derived growth factor)	0.93	1.17	1.05	1.06	1.72	0.95	1.06	1.07	1.26	7.61
angiomin like 2	0.81	1.01	1.08	0.99	1.22	0.94	1.03	0.97	1.05	2.14
angiotensin II receptor-like 1	1.09	0.98	1.21	1.51	2.47	0.83	0.85	1.15	2.49	0.52
ankyrin repeat domain 1 (cardiac muscle)	0.89	1.10	1.11	1.06	1.41	0.93	1.08	1.07	1.43	6.66
ankyrin repeat domain 11	1.19	0.76	1.16	1.20	2.95	1.11	1.01	0.98	0.78	2.23
arsenic (+3 oxidation state) methyltransferase	0.58	0.96	1.22	1.04	0.90	1.10	0.92	1.55	2.22	1.26
arylsulfatase F	1.17	1.45	1.33	1.47	1.48	0.41	1.13	0.97	1.17	0.66
asparagine synthetase	1.01	1.02	1.01	0.99	1.12	0.95	1.00	1.03	1.17	2.58
atonal homolog 1 (Drosophila)	1.21	3.29	0.61	1.13	0.65	0.12	0.43	0.48	0.82	0.42
ATPase, Ca ⁺⁺ transporting, plasma membrane 3	0.66	2.23	0.71	0.66	1.98	0.44	0.63	0.94	1.19	0.60
B double prime 1, subunit of RNA polymerase III transcription initiation factor IIIB	1.17	0.97	1.01	1.07	1.51	0.87	0.91	0.86	0.86	2.07
BarH-like homeobox 1	1.18	0.90	0.94	1.17	0.90	1.16	1.00	1.02	1.02	0.29
BCL2 binding component 3	0.36	1.00	1.00	1.00	1.63	1.00	1.00	1.00	1.00	0.36
BCL2 binding component 3	0.84	1.03	1.02	0.92	1.72	0.86	1.14	1.01	1.17	3.41
Bcl2 modifying factor BCL2/adenovirus E1B 19kDa interacting protein 3-like	1.32	0.96	0.92	0.87	1.05	1.19	0.96	0.94	1.18	2.04
	0.97	1.05	1.07	0.87	0.92	0.99	1.03	0.97	1.02	2.36

Sequence Description	7-4hr	7-12hr	7-24hr	7-36hr	7-72hr	7.5-4hr	7.5-12hr	7.5-24hr	7.5-36hr	7.5-72hr
bone gamma-carboxyglutamate (gla) protein (osteocalcin)	0.81	0.80	0.98	0.95	1.27	0.89	0.94	1.02	1.01	0.48
bone morphogenetic protein 2	0.81	0.99	1.03	1.07	1.15	0.93	1.02	0.86	0.95	2.37
brain expressed, X-linked 1	1.03	1.24	1.05	0.52	1.93	0.98	1.04	0.99	1.06	2.66
cadherin-like 26	1.32	1.67	3.28	2.18	4.29	2.03	1.96	2.03	3.61	1.00
calcium binding protein 5	0.76	1.91	0.76	0.77	2.67	0.72	0.93	1.27	2.78	0.39
calcium/calmodulin-dependent protein kinase (CaM kinase) II beta	1.34	0.95	0.59	1.14	1.55	1.02	0.52	1.12	4.64	0.50
calpain 6	0.84	1.29	1.58	1.04	1.02	0.28	0.99	0.91	0.91	1.03
CaM-KII inhibitory protein	1.40	1.14	1.26	1.24	1.38	0.49	1.33	1.40	1.41	0.70
cAMP responsive element binding protein 5	0.87	0.98	0.96	0.92	0.86	0.89	1.08	1.01	1.04	2.49
cancer/testis antigen 3	0.89	1.00	0.50	0.85	0.94	1.10	0.96	6.92	1.29	0.84
CD160 antigen	0.33	0.56	1.14	0.91	0.71	0.93	1.44	1.91	3.25	0.98
centaurin, beta 5	0.95	1.18	1.00	1.02	0.84	0.76	1.06	1.10	1.01	0.45
chemokine (C-X-C motif) ligand 2	1.03	1.03	0.83	0.79	1.41	1.08	1.22	1.01	1.09	4.24
chemokine (C-X-C motif) ligand 3	0.93	1.20	1.58	0.90	5.02	1.07	1.09	1.03	1.17	2.83
chromogranin A (parathyroid secretory protein 1)	1.31	0.68	1.07	1.27	1.24	1.24	1.04	1.05	1.01	0.32
chromosome 10 open reading frame 83	1.80	0.39	1.00	1.00	1.00	1.18	1.00	0.94	8.14	1.41
chromosome 11 open reading frame 11	0.83	1.00	1.23	0.91	1.22	1.27	1.07	0.94	1.04	2.51
chromosome 13 open reading frame 18	0.83	0.76	0.96	1.80	1.25	1.16	0.94	1.30	2.21	1.15
chromosome 21 open reading frame 100	1.00	1.24	1.00	1.00	1.00	1.00	1.00	0.81	4.87	1.00
chromosome 7 open reading frame 33	0.56	1.00	0.57	4.92	0.82	0.65	0.59	2.15	6.89	0.78
chromosome 7 open reading frame 6	0.33	0.62	1.49	0.96	0.38	0.69	0.94	0.96	1.69	0.05
cofactor required for Sp1 transcriptional activation, subunit 9, 33kDa	1.06	1.04	0.94	1.00	0.45	1.05	1.01	1.01	1.02	1.43
complement component (3b/4b) receptor 1, including Knops blood group system	10.01	0.31	0.31	0.58	0.01	0.96	1.24	1.08	0.80	11.75
cone-rod homeobox	1.08	0.41	0.63	1.53	0.79	1.20	0.72	1.53	2.74	0.90
core promoter element binding protein	0.95	1.00	0.96	1.03	1.56	0.96	1.05	1.02	1.11	2.58

Sequence Description	7-4hr	7-12hr	7-24hr	7-36hr	7-72hr	7.5-4hr	7.5-12hr	7.5-24hr	7.5-36hr	7.5-72hr
corticotropin releasing hormone binding protein	0.45	1.35	0.67	1.00	1.26	1.00	0.73	2.23	2.53	1.26
cyclin G2	1.32	1.06	0.87	0.87	0.94	1.15	1.02	0.96	1.04	2.09
cyclin M1	1.11	1.17	0.91	1.04	0.94	1.10	0.97	1.01	0.84	0.39
cystathionase (cystathionine gamma-lyase)	0.93	1.01	1.02	1.01	1.06	1.02	1.06	0.98	1.04	2.11
cysteine-rich secretory protein 3	2.21	1.25	1.21	7.67	0.01	1.00	1.00	1.00	1.00	1.00
cysteine-rich, angiogenic inducer, 61	0.92	1.07	0.89	0.97	1.34	0.86	0.88	1.02	1.13	2.10
dermcidin	0.89	1.30	1.02	1.23	0.98	0.95	0.89	1.06	2.23	0.82
discs, large homolog 3 (neuroendocrine-dlg, Drosophila)	0.60	2.05	1.76	1.00	2.60	0.97	0.82	1.50	8.16	1.00
distal-less homeo box 5	1.80	1.00	0.46	0.95	0.45	1.00	1.00	2.49	9.76	0.77
DKFZP572C163 protein	0.97	0.18	1.22	0.69	2.90	1.13	1.33	1.23	4.26	0.69
DNA-damage-inducible transcript 4	0.89	1.07	1.10	0.88	1.06	0.94	1.00	1.00	1.28	2.50
DnaJ (Hsp40) homolog, subfamily C, member 3	1.03	1.11	0.99	1.08	1.21	0.83	0.93	1.01	0.97	2.00
dual specificity phosphatase 1	0.81	1.06	0.89	0.84	1.89	0.92	1.19	1.02	1.05	3.38
dual specificity phosphatase 8	0.72	1.04	0.98	1.17	1.18	0.81	0.95	1.07	1.07	2.47
dynein, cytoplasmic, light intermediate polypeptide 2	0.97	1.14	0.96	1.07	1.09	0.89	1.02	0.96	0.94	2.24
dynein, cytoplasmic, light intermediate polypeptide 2	0.97	1.19	0.91	1.01	0.98	0.91	0.99	0.97	0.89	2.39
E74-like factor 4 (ets domain transcription factor)	1.19	0.96	0.63	1.32	1.32	1.22	1.29	1.53	2.75	0.96
early growth response 1	0.70	0.82	0.62	0.70	0.66	0.94	2.56	0.95	1.03	2.03
echinoderm microtubule associated protein like 4	0.98	1.05	1.05	0.92	1.12	1.01	1.07	1.02	0.95	2.14
elastin (supravalvular aortic stenosis, Williams-Beuren syndrome)	1.17	1.22	2.10	0.75	0.00	1.41	1.08	1.01	0.89	1.23
endothelin 1	0.80	1.31	1.07	0.99	1.24	0.83	1.10	1.04	1.31	2.24
EphA3	0.98	0.77	0.62	0.74	0.03	0.91	0.74	2.41	3.62	0.70
epoxide hydrolase 1, microsomal (xenobiotic)	1.10	1.05	1.01	1.01	1.57	0.75	1.00	1.07	0.84	0.34
epsin 3	0.76	0.94	1.04	1.97	0.49	0.72	1.16	3.09	2.99	1.33
Fer3-like (Drosophila)	0.84	1.10	0.79	1.77	1.42	0.42	1.17	0.94	1.02	0.74
ferritin, heavy polypeptide 1	1.00	1.00	1.00	2.82	1.57	2.70	1.01	1.45	1.43	0.31

Sequence Description	7-4hr	7-12hr	7-24hr	7-36hr	7-72hr	7.5-4hr	7.5-12hr	7.5-24hr	7.5-36hr	7.5-72hr
FGFR1 oncogene partner 2	1.02	1.08	1.23	0.87	0.45	1.07	1.09	1.02	1.02	1.39
fibroblast growth factor 21	0.58	0.53	0.91	1.12	1.41	0.87	0.93	1.38	2.59	1.47
filamin C, gamma (actin binding protein 280)	1.02	0.91	1.06	1.07	1.34	0.88	0.92	1.11	0.97	2.61
FLJ10378 protein	1.15	1.36	0.81	0.91	0.04	1.19	1.03	0.97	0.96	1.37
FLJ16046 protein	1.17	0.57	1.33	0.41	0.10	2.36	0.98	1.08	1.02	26.69
forkhead box O3A	0.93	0.95	1.10	1.13	1.06	0.95	1.05	1.03	1.07	2.64
fucosyltransferase 1 (galactoside 2-alpha-L-fucosyltransferase)	1.17	0.89	0.75	0.79	1.74	0.87	1.07	1.03	1.01	2.82
glioma-associated oncogene homolog (zinc finger protein)	1.40	1.60	1.63	0.82	1.22	1.14	1.07	0.93	1.04	3.07
glutamate receptor, ionotropic, kainate 4	0.73	2.01	8.28	0.74	0.01	1.23	0.92	0.93	1.21	1.19
GREB1 protein	0.98	0.93	3.08	0.83	0.65	1.03	1.06	0.98	0.85	1.28
growth arrest and DNA-damage-inducible, gamma	1.22	0.99	1.09	1.20	1.76	0.88	1.05	1.17	2.17	0.77
growth differentiation factor 1	1.03	1.00	0.83	1.35	4.03	0.77	1.15	1.15	1.21	0.60
growth differentiation factor 15	1.08	1.11	1.00	0.88	1.35	0.87	1.11	1.07	1.39	4.13
growth differentiation factor 9	0.61	0.66	0.51	2.42	0.57	1.03	0.63	1.14	8.10	0.58
GRP1 (general receptor for phosphoinositides 1)-associated scaffold protein	0.69	1.23	0.70	0.80	2.14	0.79	1.06	1.01	0.87	0.87
GrpE-like 2, mitochondrial (E. coli)	0.94	1.13	1.20	0.90	0.42	1.10	1.10	0.96	1.18	1.11
guanylate cyclase 2D, membrane (retina-specific)	0.72	0.73	0.74	0.88	1.02	0.96	1.00	1.52	2.17	1.27
H63 breast cancer expressed gene	0.20	0.43	1.92	1.34	0.02	1.54	0.73	0.77	0.97	1.87
homeo box B1	1.52	1.50	0.79	0.91	2.23	0.62	0.86	1.14	2.69	0.81
Homo sapiens cDNA FLJ11827 fis, clone HEMBA1006502.	1.00	1.11	1.16	3.66	0.33	0.68	0.69	5.98	5.70	1.07
Homo sapiens mRNA for small proline rich protein like protein, complete cds.	1.05	1.44	1.16	0.87	0.42	1.12	0.99	0.96	1.06	0.98
Homo sapiens POU domain, class 4, transcription factor 3 (POU4F3), mRNA	0.58	1.46	1.78	1.77	1.20	0.24	0.64	0.85	1.26	0.67

Sequence Description	7-4hr	7-12hr	7-24hr	7-36hr	7-72hr	7.5-4hr	7.5-12hr	7.5-24hr	7.5-36hr	7.5-72hr
Homo sapiens ribonuclease, RNase A family, 8 (RNASE8), mRNA	1.01	0.57	1.39	1.05	0.76	0.92	0.91	2.57	2.19	1.11
Homo sapiens similar to Olfactory receptor 10Z1 (LOC128368), mRNA; PREDICTED: Homo sapiens olfactory receptor, family 10, subfamily Z, member 1 (OR10Z1), mRNA	0.69	0.93	1.20	1.39	1.15	0.46	1.15	1.02	1.03	0.80
Homo sapiens testis-specific transcript, Y-linked 9 (TTY9) on chromosome Y	0.18	0.16	1.15	1.00	1.75	1.00	1.00	5.96	8.23	1.00
Homo sapiens TIGA1 (TIGA1), mRNA	1.03	1.18	1.00	0.99	0.94	1.01	1.06	1.00	1.11	2.19
homocysteine-inducible, endoplasmic reticulum stress-inducible, ubiquitin-like domain member 1	0.93	0.97	0.98	1.08	0.99	1.00	1.06	1.08	1.09	2.16
homolog of mouse LGP1	1.00	1.20	0.80	0.99	1.55	0.95	0.92	0.97	0.92	0.45
HpalI tiny fragments locus 9C	1.05	0.93	1.08	1.04	0.95	1.11	1.02	1.03	1.11	2.21
HSPC065 protein	1.01	0.97	0.99	1.08	1.14	1.05	1.03	1.08	0.98	0.44
hydroxy-delta-5-steroid dehydrogenase, 3 beta-and steroid delta-isomerase 1	0.88	0.71	1.50	1.32	1.03	0.86	1.29	1.87	3.19	0.84
hydroxysteroid (17-beta) dehydrogenase 3	0.68	0.63	0.91	1.18	0.70	1.14	0.73	1.72	2.35	1.24
hypothetical protein BC000919	0.86	2.25	0.97	1.03	0.72	1.15	1.03	0.95	1.00	0.85
hypothetical protein BC002926	0.89	1.13	1.17	1.08	1.58	0.70	0.85	1.08	1.11	0.39
hypothetical protein BC012317	0.97	1.10	0.91	0.97	7.45	1.40	0.99	0.98	1.06	5.66
hypothetical protein BC017397	0.98	1.60	0.25	0.38	0.01	2.64	0.76	0.98	0.71	1.02
hypothetical protein DKFZp434K1172	0.19	0.33	0.54	0.41	0.70	0.83	0.94	2.53	12.44	1.00
hypothetical protein FLJ10134	1.06	1.17	1.06	0.90	0.34	0.98	1.07	1.09	1.13	1.11
hypothetical protein FLJ10159	1.12	0.99	0.88	0.97	0.95	0.94	0.92	1.01	0.90	2.28
hypothetical protein FLJ10618	0.81	1.09	1.01	1.00	0.91	0.86	1.05	0.95	0.97	2.33
hypothetical protein FLJ11004	2.43	1.12	1.19	1.24	0.62	0.90	1.00	1.05	1.22	0.12

Sequence Description	7-4hr	7-12hr	7-24hr	7-36hr	7-72hr	7.5-4hr	7.5-12hr	7.5-24hr	7.5-36hr	7.5-72hr
hypothetical protein FLJ20152	1.13	1.09	0.98	0.77	0.60	0.82	0.99	0.94	1.02	2.05
hypothetical protein FLJ20203	0.96	1.04	1.03	0.97	1.07	1.02	1.10	1.01	1.05	2.01
hypothetical protein FLJ21069	1.13	1.03	0.84	1.01	0.65	1.22	1.09	1.06	0.85	2.26
hypothetical protein FLJ23749	0.68	0.85	1.96	1.41	0.01	0.85	0.96	0.80	1.02	1.31
hypothetical protein FLJ25955	0.31	0.25	0.66	0.89	1.01	0.93	1.29	2.08	5.75	1.04
hypothetical protein FLJ32803	0.85	1.14	0.93	1.02	1.24	0.83	0.84	0.16	1.09	0.95
hypothetical protein FLJ32844	0.96	1.32	1.41	3.25	0.15	1.27	0.79	0.76	1.43	21.5 1
hypothetical protein FLJ34790	1.00	0.53	1.58	1.08	1.34	1.12	0.58	3.19	5.21	0.73
hypothetical protein FLJ35036	1.01	0.97	0.92	0.88	0.77	1.06	1.16	0.95	1.07	2.19
hypothetical protein FLJ35821	1.00	0.26	0.66	0.88	0.93	1.00	1.31	2.83	4.47	1.00
hypothetical protein FLJ38377	2.38	1.77	1.04	0.87	0.02	2.34	0.85	1.40	0.63	0.68
hypothetical protein FLJ39370	1.24	0.84	0.93	0.87	0.60	1.48	0.91	0.90	1.05	2.30
hypothetical protein LOC257106	1.12	0.56	0.84	1.09	2.12	0.57	0.61	1.72	3.27	0.89
hypothetical protein LOC283849	0.70	0.80	0.62	1.28	1.09	0.95	1.15	1.08	1.00	0.42
hypothetical protein LOC339903	1.00	9.47	1.50	1.10	1.51	0.99	1.13	1.03	1.04	1.47
hypothetical protein MGC20460	0.66	0.63	0.96	1.46	0.90	1.02	1.01	1.50	4.61	1.86
hypothetical protein MGC22776	1.33	0.68	0.70	0.86	0.45	0.62	1.00	4.96	5.87	1.35
hypothetical protein MGC29898	1.01	1.28	3.14	0.55	0.01	1.19	0.93	1.04	0.68	2.35
hypothetical protein MGC35023	0.66	0.60	0.97	0.85	1.10	0.83	0.68	1.82	2.68	0.69
Hypothetical protein similar to topoisomerase (DNA) III beta (H. sapiens) (LOC129020), mRNA	1.02	1.06	1.46	0.93	2.58	0.59	0.83	1.37	7.03	1.00
immune costimulatory protein B7-H4	0.24	0.50	1.06	0.74	0.44	0.79	0.86	1.93	3.40	1.06
insulin-like growth factor 2 receptor	1.04	1.12	1.12	1.07	1.08	0.96	1.10	1.03	0.86	2.35

Sequence Description	7-4hr	7-12hr	7-24hr	7-36hr	7-72hr	7.5-4hr	7.5-12hr	7.5-24hr	7.5-36hr	7.5-72hr
interferon regulatory factor 2 binding protein 2	0.79	0.98	1.04	0.89	1.01	0.95	1.10	0.92	1.04	2.13
interferon, alpha 10	1.33	0.74	0.53	0.82	0.64	1.59	1.30	0.91	1.39	3.44
interleukin 17B	0.84	3.26	1.23	1.17	1.03	0.90	0.97	1.13	1.23	1.02
interleukin 28B (interferon, lambda 3)	0.94	0.88	1.49	1.42	0.85	0.58	0.54	1.91	3.61	1.73
jub, ajuba homolog (Xenopus laevis)	0.86	0.99	1.00	1.13	1.29	0.95	0.92	0.98	1.06	2.15
jumonji domain containing 2A	1.06	0.97	1.10	1.05	1.13	0.82	1.04	0.95	0.98	2.06
KIAA0355	0.59	1.21	1.13	1.43	1.41	0.48	0.78	0.89	1.05	0.97
KIAA0963	0.88	0.99	1.13	0.93	3.03	0.74	1.09	1.12	1.12	0.65
KIAA1110 protein	0.44	1.39	0.93	0.88	1.38	1.43	1.32	1.49	2.59	1.10
KIAA1984	1.13	0.93	1.43	1.07	0.87	1.13	0.82	2.81	1.08	0.98
latent transforming growth factor beta binding protein 1	1.01	1.05	1.15	0.77	0.85	1.16	0.93	0.87	1.08	2.67
lectin, galactoside-binding, soluble, 1 (galectin 1)	0.92	0.86	0.74	1.03	2.40	1.08	1.00	1.06	0.92	0.68
LIM homeobox transcription factor 1, beta	0.82	1.07	0.78	1.18	0.78	1.20	1.10	1.10	1.82	0.48
Lutheran blood group (Auberger b antigen included)	1.38	0.70	1.33	1.30	1.46	0.41	2.63	1.39	1.42	0.63
MAD2 mitotic arrest deficient-like 1 (yeast)	0.91	1.14	1.11	0.93	0.94	1.01	1.07	1.01	1.10	2.24
major histocompatibility complex, class II, DQ beta 1	0.77	0.70	0.75	0.97	1.02	0.88	1.08	1.27	2.22	1.30
makorin, ring finger protein, 3	1.07	1.05	1.05	0.94	0.44	1.11	1.01	0.99	1.00	1.13
membrane protein, palmitoylated 2 (MAGUK p55 subfamily member 2)	0.35	0.75	0.67	1.33	1.29	0.50	0.87	1.57	3.40	0.75
metallothionein-like 5, testis-specific (tesmin)	1.00	1.00	1.00	1.00	1.00	1.26	1.05	1.05	0.92	2.01
methionine-tRNA synthetase	1.05	1.14	0.95	0.92	1.32	1.14	1.03	1.03	1.17	2.57
methylene tetrahydrofolate dehydrogenase (NAD+ dependent), methenyltetrahydrofolate cyclohydrolase	0.95	1.09	0.98	1.15	1.03	0.96	1.08	1.06	1.11	2.79
mitogen-activated protein kinase kinase kinase 10	1.50	0.94	0.83	1.33	1.43	0.42	2.86	1.43	0.73	0.65
motile sperm domain containing 1	1.01	1.10	1.06	0.94	0.89	1.05	1.05	0.99	0.98	2.38

Sequence Description	7-4hr	7-12hr	7-24hr	7-36hr	7-72hr	7.5-4hr	7.5-12hr	7.5-24hr	7.5-36hr	7.5-72hr
myeloid/lymphoid or mixed-lineage leukemia (trithorax homolog, Drosophila); translocated to, 3	1.40	0.43	2.87	1.00	1.63	0.40	1.36	1.37	1.35	0.48
Nanog homeobox	0.94	0.55	0.32	0.83	0.37	1.01	0.88	0.94	0.90	1.08
neutrophil cytosolic factor 2 (65kDa, chronic granulomatous disease, autosomal 2)	0.95	1.07	1.01	0.91	1.62	1.15	1.14	0.95	1.25	3.27
nidogen (enactin)	1.04	0.97	1.16	0.98	1.19	0.87	0.95	0.91	0.84	0.46
nitric oxide synthase trafficking	1.10	1.11	0.97	1.10	1.19	0.91	0.90	1.05	0.96	2.53
NK2 transcription factor related, locus 8 (Drosophila)	2.31	0.26	0.75	1.13	0.01	0.98	1.15	0.97	1.02	0.91
nuclear factor of kappa light polypeptide gene enhancer in B-cells inhibitor, epsilon	0.85	1.13	0.85	1.09	1.37	0.98	0.98	1.07	1.00	2.36
nucleosome assembly protein 1-like 5	0.27	6.88	0.67	1.00	1.00	1.37	1.00	1.09	0.91	1.21
Orphan sodium- and chloride-dependent neurotransmitter transporter NTT4 (Fragment). [Source:SWISSPROT;Accession:Q9H1V8]	1.06	0.94	0.98	1.05	0.96	1.05	1.02	0.99	1.01	0.49
ovarian zinc finger protein	0.74	0.95	1.15	1.09	1.22	0.75	0.72	2.44	2.18	0.80
p53-regulated apoptosis-inducing protein 1	0.75	0.85	1.38	0.86	0.01	1.33	1.12	1.13	1.39	1.00
period homolog 2 (Drosophila)	0.81	1.02	1.09	0.97	1.04	0.90	1.03	0.97	1.06	2.07
phenylethanolamine N-methyltransferase	1.09	0.93	1.13	0.86	1.48	0.96	1.59	2.08	4.52	0.69
phosphodiesterase 6H, cGMP-specific, cone, gamma	0.87	0.41	0.72	1.20	1.23	1.06	1.05	0.17	1.11	1.34
phosphoenolpyruvate carboxykinase 2 (mitochondrial)	0.96	1.10	0.99	0.96	1.07	0.98	1.04	0.98	1.00	2.00
phospholipase C, beta 2	0.38	4.14	0.91	2.55	0.24	0.81	0.45	1.19	4.16	1.10
phospholipase C, beta 3 (phosphatidylinositol-specific)	0.50	0.67	0.94	0.95	0.99	1.00	0.93	1.05	2.72	0.78
phospholipid scramblase 1	1.00	1.06	1.04	1.01	0.46	1.06	0.99	0.97	0.99	1.04
PI-3-kinase-related kinase SMG-1	1.02	0.92	0.93	1.07	0.81	0.66	0.95	0.81	0.78	2.73

Sequence Description	7-4hr	7-12hr	7-24hr	7-36hr	7-72hr	7.5-4hr	7.5-12hr	7.5-24hr	7.5-36hr	7.5-72hr
platelet-derived growth factor receptor, beta polypeptide	1.22	1.04	0.51	6.64	0.01	1.30	1.02	0.92	0.99	2.77
pleckstrin and Sec7 domain containing 2 pleckstrin homology-like domain, family A, member 1	0.50	0.57	1.16	0.91	0.97	0.96	1.11	1.53	2.34	4.33
polymerase (DNA directed) iota	0.90	1.14	1.16	1.10	1.27	0.92	1.19	1.06	1.08	2.93
polymerase (DNA directed) kappa	0.81	0.86	1.01	0.87	0.76	1.17	0.99	0.98	0.86	2.26
potassium channel tetramerisation domain containing 13	1.00	0.98	0.93	1.13	1.22	1.01	0.94	0.95	0.85	2.73
potassium voltage-gated channel, shaker-related subfamily, member 5	0.32	0.73	0.79	1.03	0.76	0.71	0.92	2.89	0.89	0.79
procollagen-proline, 2-oxoglutarate 4-dioxygenase (proline 4-hydroxylase), alpha polypeptide III	1.21	1.84	1.70	0.73	0.01	1.48	0.97	0.95	1.05	1.24
proenkephalin	0.93	0.82	1.15	0.81	1.62	1.02	1.11	1.05	2.04	1.46
pro-melanin-concentrating hormone-like 1	0.81	1.33	1.58	0.94	0.02	1.30	1.34	0.87	0.91	25.08
protein kinase, AMP-activated, beta 2 non-catalytic subunit	0.53	0.70	1.50	0.41	0.40	0.79	0.99	1.08	3.41	1.05
protein kinase, lysine deficient 2	0.98	1.33	1.33	1.06	1.39	0.92	1.31	0.97	0.99	2.30
protein phosphatase 1, regulatory (inhibitor) subunit 3B	0.63	9.96	0.73	2.16	1.24	1.02	0.93	2.10	0.95	0.64
protein phosphatase 1, regulatory (inhibitor) subunit 3C	0.74	0.71	2.92	0.70	1.63	2.51	2.42	1.38	1.33	0.40
protein phosphatase 1, regulatory (inhibitor) subunit 9A	1.01	1.09	1.02	1.04	0.31	1.30	0.94	0.99	1.00	1.00
protein tyrosine phosphatase type IVA, member 1	0.95	1.09	1.11	0.97	1.19	0.84	1.06	0.95	0.90	2.36
putative lymphocyte G0/G1 switch gene	0.86	1.05	1.14	0.97	1.15	0.95	1.11	1.02	1.20	2.22
putative NFkB activating protein	1.00	1.98	0.95	1.31	1.90	1.06	0.82	0.99	1.05	2.10
putative NFkB activating protein	1.00	0.34	1.00	2.79	1.66	2.73	2.50	1.49	3.13	0.35
putative NFkB activating protein	0.78	0.96	1.10	1.02	2.58	1.05	1.00	1.10	0.95	0.63

Sequence Description	7-4hr	7-12hr	7-24hr	7-36hr	7-72hr	7.5-4hr	7.5-12hr	7.5-24hr	7.5-36hr	7.5-72hr
PX domain containing serine/threonine kinase	0.96	1.06	1.18	1.05	0.79	1.63	0.93	0.91	0.94	2.97
RAB25, member RAS oncogene family	0.26	0.39	1.04	1.75	1.31	0.36	0.76	1.32	5.90	0.96
retinitis pigmentosa GTPase regulator interacting protein 1	1.82	0.36	1.27	1.01	0.84	1.01	1.03	1.52	2.53	1.03
Rho guanine nucleotide exchange factor (GEF) 4	1.41	0.83	0.69	0.93	0.01	1.03	1.07	0.94	1.17	0.93
ribosomal protein S6 kinase, 70kDa, polypeptide 2	1.02	0.85	0.86	1.05	2.05	0.90	0.70	1.07	0.87	0.86
ribosomal protein, large, P1	1.38	1.03	1.06	1.39	1.73	1.00	1.00	3.16	3.41	0.31
ring finger protein 19	1.06	1.12	0.98	1.02	1.13	0.79	1.05	1.01	0.81	2.84
SEC14-like 3 (S. cerevisiae)	0.66	0.90	0.69	1.43	1.78	0.86	1.53	1.78	2.85	1.00
serine/threonine kinase 31	7.28	1.14	3.37	0.38	0.01	2.48	1.09	1.08	0.96	12.26
sestrin 2	0.97	1.08	0.93	1.05	1.48	1.05	0.97	1.09	1.18	3.34
SH3 domain protein D19	0.89	1.11	0.97	0.98	1.00	1.00	1.12	1.02	1.03	2.08
similar to hypothetical protein FLJ13659	1.28	1.07	56.16	0.44	0.14	1.60	1.06	1.06	0.81	5.81
similar to lymphocyte antigen 6 complex, locus G5B; G5b protein; open reading frame 31	1.37	0.77	1.01	1.05	1.15	0.80	0.92	1.54	2.62	2.03
similar to Taxol resistant associated protein 3 (TRAG-3)	0.87	0.69	1.17	0.87	2.09	1.17	0.87	0.78	0.84	0.47
SMAD, mothers against DPP homolog 5 (Drosophila)	1.08	1.13	1.09	0.95	0.75	1.02	1.09	1.02	1.00	2.15
Snf7 homologue associated with Alix 3	1.04	1.00	0.95	0.78	1.03	1.06	0.99	0.98	0.94	2.61
solute carrier family 22 (organic cation transporter), member 15	0.97	0.98	0.97	0.87	0.80	0.96	1.05	0.95	1.03	2.46
solute carrier family 26 (sulfate transporter), member 2	0.75	0.77	0.77	0.80	0.77	1.14	0.82	2.02	4.11	2.54
solute carrier family 7 (cationic amino acid transporter, y+ system), member 8	0.90	0.83	1.53	0.99	0.91	1.35	1.13	0.83	2.37	11.15
solute carrier family 9 (sodium/hydrogen exchanger), isoform 9	0.47	0.53	1.03	1.12	1.14	1.14	3.06	1.42	3.28	1.18
solute carrier organic anion transporter family,	2.04	1.65	2.37	0.24	0.01	1.06	1.07	0.98	1.12	2.38

Sequence Description	7-4hr	7-12hr	7-24hr	7-36hr	7-72hr	7.5-4hr	7.5-12hr	7.5-24hr	7.5-36hr	7.5-72hr
member 3A1										
syntaxin 3A	1.04	1.09	1.10	0.92	1.07	0.95	1.09	1.04	1.12	2.01
syntaxin binding protein 2	1.05	1.17	0.90	1.08	1.48	0.86	1.03	1.06	0.98	0.39
target of myb1-like 2 (chicken)	2.09	1.00	0.85	1.67	2.48	0.67	0.75	1.13	6.64	0.27
taste receptor, type 2, member 14	0.70	1.59	1.13	1.93	1.05	0.92	0.81	1.00	2.22	0.72
TBC1 domain family, member 5	0.26	0.76	1.87	0.93	0.02	0.97	0.96	0.81	1.34	2.13
thrombospondin, type I, domain containing 1	0.97	0.77	1.03	0.90	1.27	1.27	1.11	0.98	1.04	2.20
thyrotropin-releasing hormone receptor	0.64	0.79	0.83	1.05	0.50	1.17	1.04	0.95	2.02	1.63
tissue factor pathway inhibitor 2	0.84	0.75	1.24	1.11	3.54	1.12	1.00	1.06	1.02	2.27
transcription elongation factor B polypeptide 3B (elongin A2)	1.75	1.00	1.30	1.38	1.00	0.74	0.83	3.02	9.61	0.09
tribbles homolog 3 (Drosophila)	0.92	1.10	1.05	1.01	1.33	0.88	1.02	1.01	1.16	3.28
trinucleotide repeat containing 9	0.95	1.18	0.96	0.97	1.21	0.76	0.94	0.99	0.96	0.45
tumor protein p53 binding protein, 2	0.84	1.05	1.08	1.07	1.04	0.98	1.09	0.97	0.90	2.09
tumor protein p73	1.30	1.63	0.75	0.84	0.68	0.91	1.32	1.42	2.25	1.62
UDP-N-acetylglucosamine:a-1,3-D-mannoside beta-1,4-N-acetylglucosaminyltransferase IV	0.17	1.79	0.53	2.17	1.08	0.84	0.95	1.20	3.42	1.13
unc-5 homolog B (C. elegans)	1.16	1.17	1.87	1.25	1.16	1.01	1.08	1.25	1.10	3.65
uncoupling protein 2 (mitochondrial, proton carrier)	0.95	1.11	0.97	1.07	1.37	0.89	0.91	1.08	1.05	0.49
Unknown	0.54	0.67	0.73	0.91	1.11	0.93	0.91	1.18	2.82	1.14
Unknown	1.64	0.61	1.34	1.39	1.00	1.00	1.15	2.00	3.30	0.61
Unknown	1.05	0.91	1.03	1.17	0.42	1.16	0.97	1.12	2.06	0.87
Unknown	1.42	0.59	1.04	0.33	0.09	0.76	0.93	2.73	3.85	0.63
Unknown	1.00	0.23	1.44	0.76	7.33	1.13	1.72	1.00	9.13	0.65
Unknown	0.56	1.13	1.56	1.81	1.57	0.86	0.78	1.17	2.53	0.92
Unknown	1.94	1.17	1.33	1.31	0.12	0.85	0.95	0.79	3.78	0.69
Unknown	1.19	1.27	1.33	1.56	1.06	0.77	0.96	0.99	2.22	0.98
Unknown	1.00	1.07	0.93	1.04	0.67	1.03	1.75	3.33	0.90	0.79
Unknown	2.52	0.64	1.28	1.20	1.60	1.01	1.34	0.80	1.01	0.19
Unknown	1.18	1.03	1.00	0.95	1.59	2.53	1.02	1.45	1.45	0.35
Unknown	0.41	3.96	0.71	1.05	0.24	0.14	1.35	0.89	0.96	0.67

Sequence Description	7-4hr	7-12hr	7-24hr	7-36hr	7-72hr	7.5-4hr	7.5-12hr	7.5-24hr	7.5-36hr	7.5-72hr
Unknown	0.46	0.94	0.89	0.66	1.43	0.86	0.82	1.49	0.70	0.57
Unknown	0.55	6.71	2.54	0.76	2.82	0.50	1.14	1.39	1.05	0.56
Unknown	0.87	1.11	0.97	1.08	1.29	0.95	1.06	0.95	0.86	2.16
Unknown	1.02	0.80	0.92	1.53	0.86	0.79	0.84	1.17	0.97	2.36
Unknown	1.16	1.14	0.96	0.89	0.32	1.08	1.00	0.98	1.00	1.00
Unknown	1.31	1.52	1.38	1.19	0.01	1.05	1.02	0.96	1.06	1.06
Unknown	1.05	1.39	0.65	1.05	0.02	1.12	1.06	1.01	1.07	3.30
Unknown	1.07	1.56	0.43	0.18	0.02	2.62	0.89	1.22	0.95	5.34
Unknown	1.15	1.20	0.89	0.86	0.34	1.32	1.03	1.01	0.95	1.06
vav 3 oncogene	1.13	1.11	1.13	0.86	0.31	1.40	1.14	0.96	0.94	0.95
vesicle-associated membrane protein 2 (synaptobrevin 2)	1.00	0.96	0.99	1.23	0.88	1.07	1.05	1.03	1.05	0.44
v-jun sarcoma virus 17 oncogene homolog (avian)	0.95	0.96	0.84	1.08	1.28	0.89	1.02	0.87	0.83	3.58
v-Ki-ras2 Kirsten rat sarcoma 2 viral oncogene homolog	0.97	1.36	1.07	1.14	0.90	0.77	1.20	1.03	1.10	2.40
v-rel reticuloendotheliosis viral oncogene homolog B, nuclear factor of kappa light polypeptide gene enhancer in B-cells 3 (avian)	0.90	1.12	0.99	0.97	1.52	0.94	1.01	1.05	1.13	2.21
zinc finger motif enhancer binding protein 2	0.97	1.20	1.19	1.03	1.45	0.96	1.23	1.02	1.13	2.15
zinc finger protein 131 (clone pHZ-10)	0.98	0.97	0.99	1.06	1.09	1.02	0.98	1.00	0.84	2.01
zinc finger protein 165	1.41	1.31	0.85	1.11	1.64	1.16	0.90	0.98	1.05	2.40
zinc finger protein 19 (KOX 12)	1.04	0.95	1.15	1.04	0.88	1.01	0.95	1.03	1.17	0.49
zinc finger protein 31 (KOX 29)	1.01	0.93	0.91	0.85	0.94	1.47	1.19	1.08	1.36	2.29
zinc finger protein 319	0.95	1.07	1.06	1.07	1.11	1.03	1.14	0.98	0.94	2.03
zinc finger protein 41	0.50	0.63	0.96	1.60	1.36	0.84	0.89	2.97	0.93	1.10

REFERENCES

- (1) Abe T, Kaname Y, Hamamoto I, Tsuda Y, Wen X, Taguwa S et al. Hepatitis C Virus Nonstructural Protein 5A Modulates the Toll-Like Receptor-MyD88-Dependent Signaling Pathway in Macrophage Cell Lines. *The Journal of Virology* 2007; 81(17):8953-8966.
- (2) Adams CM, Reitz J, De Brabander JK, Feramisco JD, Li L, Brown MS et al. Cholesterol and 25-Hydroxycholesterol Inhibit Activation of SREBPs by Different Mechanisms, Both Involving SCAP and Insigs. *J Biol Chem* 2004; 279(50):52772-52780.
- (3) Agnello V, Abel G, Elfahal M, Knight GB, Zhang QX. Hepatitis C virus and other Flaviviridae viruses enter cells via low density lipoprotein receptor. *Proceedings of the National Academy of Sciences* 1999; 96(22):12766-12771.
- (4) Akira S, Uematsu S, Takeuchi O. Pathogen recognition and innate immunity. *Cell* 2006; 124(4):783-801.
- (5) Alexopoulou L, Holt AC, Medzhitov R, Flavell RA. Recognition of double-stranded RNA and activation of NF-kappaB by Toll-like receptor 3. *Nature* 2001; 413(6857):732-738.
- (6) Allen IC, Scull MA, Moore CB, Holl EK, McElvania-TeKippe E, Taxman DJ et al. The NLRP3 Inflammasome Mediates In Vivo Innate Immunity to Influenza A Virus through Recognition of Viral RNA. *Immunity* 2009; 30(4):556-565.

- (7) Alter HJ, Purcell RH, Holland PV, Popper H. Transmissible agent in non-A, non-B hepatitis. *Lancet* 1978; 1(8062):459-463.
- (8) Alter HJ, Klein HG. The hazards of blood transfusion in historical perspective. *Blood* 2008; 112(7):2617-2626.
- (9) Andre P, Komurian-Pradel F, Deforges S, Perret M, Berland JL, Sodoyer M et al. Characterization of Low- and Very-Low-Density Hepatitis C Virus RNA-Containing Particles. *The Journal of Virology* 2002; 76(14):6919-6928.
- (10) Andreo U, Maillard P, Kalinina O, Walic M, Meurs E, Martinot M et al. Lipoprotein lipase mediates hepatitis C virus (HCV) cell entry and inhibits HCV infection. *Cellular Microbiology* 2007; 9(10):2445-2456.
- (11) Barba G, Harper F, Harada T, Kohara M, Goulinet S, Matsuura Y et al. Hepatitis C virus core protein shows a cytoplasmic localization and associates to cellular lipid storage droplets. *Proc Natl Acad Sci U S A* 1997; 74(4):1200-1205.
- (12) Bartosch B, Dubuisson J, Cosset FL. Infectious Hepatitis C Virus Pseudoparticles Containing Functional E1-E2 Envelope Protein Complexes. *J Exp Med* 2003; 197(5):633-642.
- (13) Bartosch B, Vitelli A, Granier C, Goujon C, Dubuisson J, Pascale S et al. Cell Entry of Hepatitis C Virus Requires a Set of Co-receptors That Include the CD81 Tetraspanin and the SR-B1 Scavenger Receptor. *J Biol Chem* 2003; 278(43):41624-41630.

- (14) Bays HE, Tighe AP, Sadovsky R, Davidson MH. Prescription omega-3 fatty acids and their lipid effects: physiologic mechanisms of action and clinical implications. *Expert Review of Cardiovascular Therapy* 2008; 6(3):391-409.
- (15) Benko S, Philpott DJ, Girardin SE. The microbial and danger signals that activate Nod-like receptors. *Cytokine* 2008; 43(3):368-373.
- (16) Bode JG, Ludwig S, Ehrhardt C, Albrecht U, Erhardt A, Schaper F et al. IFN-alpha antagonistic activity of HCV core protein involves induction of suppressor of cytokine signaling-3. *FASEB J* 2003; 17(3):488-490.
- (17) Bradley D, McCaustland K, Krawczynski K, Spelbring J, Humphrey C, Cook E. Hepatitis C virus: buoyant density of the factor VIII-derived isolate in sucrose. *Journal of Medical Virology* 1991; 34(3):206-208.
- (18) Breiman A, Grandvaux N, Lin R, Ottone C, Akira S, Yoneyama M et al. Inhibition of RIG-I-Dependent Signaling to the Interferon Pathway during Hepatitis C Virus Expression and Restoration of Signaling by IKK ϵ . *The Journal of Virology* 2005; 79(7):3969-3978.
- (19) Catanese MT, Graziani R, von Hahn T, Moreau M, Huby T, Paonessa G et al. High-Avidity Monoclonal Antibodies against the Human Scavenger Class B Type I Receptor Efficiently Block Hepatitis C Virus Infection in the Presence of High-Density Lipoprotein. *The Journal of Virology* 2007; 81(15):8063-8071.

- (20) Chang KS, Jiang J, Cai Z, Luo G. Human Apolipoprotein E Is Required for Infectivity and Production of Hepatitis C Virus in Cell Culture. *The Journal of Virology* 2007; 81(24):13783-13793.
- (21) Chappell DA, Medh JD. Receptor-mediated mechanisms of lipoprotein remnant catabolism. *Progress in Lipid Research* 1998; 37(6):393-422.
- (22) Chen Z, Benureau Y, Rijnbrand R, Yi J, Wang T, Warter L et al. GB Virus B Disrupts RIG-I Signaling by NS3/4A-Mediated Cleavage of the Adaptor Protein MAVS. *J Virol* 2007; 81(2):964-976.
- (23) Choo QL, Kuo G, Weiner AJ, Overby LR, Bradley DW, Houghton M. Isolation of a cDNA clone derived from a blood-borne non-A, non-B viral hepatitis genome. *Science* 1989; 244:359-362.
- (24) Cormier EG, Tsamis F, Kajumo F, Durso RJ, Gardner JP, Dragic T. CD81 is an entry coreceptor for hepatitis C virus. *Proceedings Of The National Academy Of Sciences Of The United States Of America* 2004; 101(19):7270-7274.
- (25) Diebold SS, Kaisho T, Hemmi H, Akira S, Reis e Sousa. Innate antiviral responses by means of TLR7-mediated recognition of single-stranded RNA. *Science* 2004; 303(5663):1529-1531.
- (26) Drummer HE, Maerz A, Pountourios P. Cell surface expression of functional hepatitis C virus E1 and E2 glycoproteins. *FEBS Lett* 2003; 546(2-3):385-390.

- (27) Egger D, Wolk B, Gosert R, Bianchi L, Blum HE, Moradpour D et al. Expression of hepatitis C virus proteins induces distinct membrane alterations including a candidate viral replication complex. *J Virol* 2002; 76(12):5974-5984.
- (28) Evans MJ, von Hahn T, Tscherne DM, Syder AJ, Panis M, Wolk B et al. Claudin-1 is a hepatitis C virus co-receptor required for a late step in entry. *Nature* 2007; 446(7137):801-805.
- (29) Feinstone SM, Kapikian A, Purcell RH, Alter HJ, Holland PV. Transfusion-associated hepatitis not due to viral hepatitis type A or B. *N Engl J Med* 1975; 292(15):767-770.
- (30) Flint M, Maidens C, Loomis-Price LD, Shotton C, Dubuisson J, Monk P et al. Characterization of Hepatitis C Virus E2 Glycoprotein Interaction with a Putative Cellular Receptor, CD81. *The Journal of Virology* 1999; 73(8):6235-6244.
- (31) Foy E, li K, Sumpter R, Jr., Loo YM, Johnson CL, Wang C et al. Control of antiviral defenses through hepatitis C virus disruption of retinoic acid-inducible gene-I signaling. *Proc Natl Acad Sci U S A* 2005; 102(8):2986-2991.
- (32) Foy E, li K, Wang C, Sumpter R, Ikeda M, Lemon SM et al. Regulation of interferon regulatory factor-3 by the hepatitis C virus serine protease. *Science* 2003; 300:1145-1148.

- (33) Franchi L, Eigenbrod T, Munoz-Planillo R, Nunez G. The inflammasome: a caspase-1-activation platform that regulates immune responses and disease pathogenesis. *Nat Immunol* 2009; 10(3):241-247.
- (34) Gale M, Jr., Blakely CM, Hopkins DA, Melville MW, Wambach M, Romano PR et al. Regulation of interferon-induced protein kinase PKR: modulation of P58^{IPK} inhibitory function by a novel protein, P52^{rIPK}. *Mol Cell Biol* 1998; 18:859-871.
- (35) Gale M, Jr., Blakely CM, Kwieciszewski B, Tan S-L, Dossett M, Korth MJ et al. Control of PKR protein kinase by hepatitis C virus nonstructural 5A protein: molecular mechanisms of kinase regulation. *Mol Cell Biol* 1998; 18:5208-5218.
- (36) Gastaminza P, Cheng G, Wieland S, Zhong J, Liao W, Chisari FV. Cellular Determinants of Hepatitis C Virus Assembly, Maturation, Degradation, and Secretion. *The Journal of Virology* 2008; 82(5):2120-2129.
- (37) Germe R, Crance J-M, Garin D, Guimet J, Lortat-Jacob H, Ruigrok RWH et al. Cellular Glycosaminoglycans and Low Density Lipoprotein Receptor Are Involved in Hepatitis C Virus Adsorption. *Journal of Medical Virology* 2002; 68(2):206-215.
- (38) Goodman ZD, Ishak K. Histopathology of hepatitis C virus infection. *Semin Liver Dis* 1995; 15(1):70-81.
- (39) Grove J, Nielsen S, Zhong J, Bassendine MF, Drummer HE, Balfe P et al. Identification of a Residue in Hepatitis C Virus E2 Glycoprotein That

- Determines Scavenger Receptor BI and CD81 Receptor Dependency and Sensitivity to Neutralizing Antibodies. *The Journal of Virology* 2008; 82(24):12020-12029.
- (40) Guzman G. Overview of Liver Pathology. *Disease-a-Month* 2008; 54(7):419-431.
- (41) Heil F, Ahmad-Nejad P, Hemmi H, Hochrein H, Ampenberger F, Gellert T et al. The Toll-like receptor 7 (TLR7)-specific stimulus loxoribine uncovers a strong relationship within the TLR7, 8 and 9 subfamily. *Eur J Immunol* 2003; 33(11):2987-2997.
- (42) Heil F, Hemmi H, Hochrein H, Ampenberger F, Kirschning C, Akira S et al. Species-specific recognition of single-stranded RNA via toll-like receptor 7 and 8. *Science* 2004; 303(5663):1526-1529.
- (43) Hezode C, Forestier N, Dusheiko G, Ferenci P, Pol S, Goeser T et al. Telaprevir and Peginterferon with or without Ribavirin for Chronic HCV Infection. *N Engl J Med* 2009; 360(18):1839-1850.
- (44) Higginbottom A, Quinn ER, Kuo CC, Flint M, Wilson LH, Bianchi E et al. Identification of Amino Acid Residues in CD81 Critical for Interaction with Hepatitis C Virus Envelope Glycoprotein E2. *The Journal of Virology* 2000; 74(8):3642-3649.

- (45) Hollinger F, Gitnick G, Aarch R, Szmuness W, Mosley J, Stevens C et al. Non-A, non-B hepatitis transmission in chimpanzees: a project of the transfusion-transmitted viruses study group. *Intervirology* 1978; 10(1):60-68.
- (46) Hoofnagle JH, Seeff LB. Peginterferon and Ribavirin for Chronic Hepatitis C. *N Engl J Med* 2006; 355(23):2444-2451.
- (47) Hope RG, Murphy DJ, McLauchlan J. The Domains Required to Direct Core Proteins of Hepatitis C Virus and GB Virus-B to Lipid Droplets Share Common Features with Plant Oleosin Proteins. *J Biol Chem* 2002; 277(6):4261-4270.
- (48) Hornung V, Ellegast J, Kim S, Brzozka K, Jung A, Kato H et al. 5'-Triphosphate RNA Is the Ligand for RIG-I. *Science* 2006.
- (49) Horvath CM. The Jak-STAT pathway stimulated by interferon alpha or interferon beta. *Sci STKE* 2004; 2004(260):tr10.
- (50) Hourieux C, Patient R, Morin A, Blanchard E, Moreau A, Trassard S et al. The genotype 3-specific hepatitis C virus core protein residue phenylalanine 164 increases steatosis in an in vitro cellular model. *Gut* 2007; 56(9):1302-1308.
- (51) Hsu M, Zhang J, Flint M, Logvinoff C, Cheng-Mayer C, Rice CM et al. Hepatitis C virus glycoproteins mediate pH-dependent cell entry of pseudotyped retroviral particles. *Proceedings Of The National Academy Of Sciences Of The United States Of America* 2003; 100(12):7271-7276.

- (52) Huang H, Sun F, Owen DM, Li W, Chen Y, Gale M, Jr. et al. Hepatitis C virus production by human hepatocytes dependent on assembly and secretion of very low-density lipoproteins. *Proceedings of the National Academy of Sciences* 2007; 104(14):5848-5853.
- (53) Hussain MM, Rava P, Pan X, Dai K, Dougan SK, Iqbal J et al. Microsomal triglyceride transfer protein in plasma and cellular lipid metabolism. *Current Opinion in Lipidology* 2008; 19(3):277-284.
- (54) Hussain MM, Rava P, Pan X, Dai K, Dougan SK, Iqbal J et al. Microsomal triglyceride transfer protein in plasma and cellular lipid metabolism. *Current Opinion in Lipidology* 2008; 19(3):277-284.
- (55) Ichinohe T, Lee HK, Ogura Y, Flavell R, Iwasaki A. Inflammasome recognition of influenza virus is essential for adaptive immune responses. *J Exp Med* 2009; 206(1):79-87.
- (56) Itoh K, Watanabe A, Funami K, Seya T, Matsumoto M. The clathrin-mediated endocytic pathway participates in dsRNA-induced IFN-beta production. *J Immunol* 2008; 181(8):5522-5529.
- (57) Johnson CL, Gale M, Jr. CARD games between virus and host get a new player. *Trends Immunol* 2005.
- (58) Johnson CL, Owen DM, Gale M, Jr. Functional and therapeutic analysis of hepatitis C virus NS3/4A protease control of antiviral immune defense. *J Biol Chem* 2007.

- (59) Johnston JB, Barrett JW, Nazarian SH, Goodwin M, Ricuttio D, Wang G et al. A Poxvirus-Encoded Pysin Domain Protein Interacts with ASC-1 to Inhibit Host Inflammatory and Apoptotic Responses to Infection. *Immunity* 2005; 23(6):587-598.
- (60) Kang DC, Gopalkrishnan RV, Wu Q, Jankowsky E, Pyle AM, Fisher PB. mda-5: An interferon-inducible putative RNA helicase with double-stranded RNA-dependent ATPase activity and melanoma growth-suppressive properties. *Proc Natl Acad Sci U S A* 2002; 99(2):637-642.
- (61) Kanneganti TD, Body-Malapel M, Amer A, Park JH, Whitfield J, Franchi L et al. Critical Role for Cryopyrin/Nalp3 in Activation of Caspase-1 in Response to Viral Infection and Double-stranded RNA. *J Biol Chem* 2006; 281(48):36560-36568.
- (62) Kapadia SB, Barth H, Baumert T, McKeating JA, Chisari FV. Initiation of Hepatitis C Virus Infection Is Dependent on Cholesterol and Cooperativity between CD81 and Scavenger Receptor B Type I. *The Journal of Virology* 2007; 81(1):374-383.
- (63) Kato H, Takeuchi O, Mikamo-Satoh E, Hirai R, Kawai T, Matsushita K et al. Length-dependent recognition of double-stranded ribonucleic acids by retinoic acid-inducible gene-I and melanoma differentiation-associated gene 5. *J Exp Med* 2008; 205(7):1601-1610.

- (64) Kato H, Takeuchi O, Mikamo-Satoh E, Hirai R, Kawai T, Matsushita K et al. Length-dependent recognition of double-stranded ribonucleic acids by retinoic acid-inducible gene-I and melanoma differentiation-associated gene 5. *J Exp Med* 2008; 205(7):1601-1610.
- (65) Kato H, Takeuchi O, Sato S, Yoneyama M, Yamamoto M, Matsui K et al. Differential roles of MDA5 and RIG-I helicases in the recognition of RNA viruses. *Nature* 2006; 441(7089):101-105.
- (66) Kawai T, Takahashi K, Sato S, Coban C, Kumar H, Kato H et al. IPS-1, an adaptor triggering RIG-I- and Mda5-mediated type I interferon induction. *Nat Immunol* 2005; 6(10):981-988.
- (67) Kolykhalov AA, Agapov EV, Blight KJ, Mihalik K, Feinstone SM, Rice CM. Transmission of hepatitis C by intrahepatic inoculation with transcribed RNA. *Science* 1997; 277:570-574.
- (68) Krieger M, Smith L, Anderson RG, Goldstein JL, Kao Y, Pownall H et al. Reconstituted low density lipoprotein: a vehicle for the delivery of hydrophobic fluorescent probes to cells. *Journal of Supramolecular Structure* 1979; 10(4):467-478.
- (69) Krieger N, Lohmann V, Bartenschlager R. Enhancement of Hepatitis C Virus RNA Replication by Cell Culture-Adaptive Mutations. *The Journal of Virology* 2001; 75(10):4614-4624.

- (70) Lau JYN, Tam RC, Liang TJ, Hong Z. Mechanism of action of ribavirin in the combination treatment of chronic HCV infection. *Hepatology* 2002; 35(5):1002-1009.
- (71) Lauer GM, Walker BD. Hepatitis C Virus Infection. *N Engl J Med* 2001; 345(1):41-52.
- (72) Lavillette D, Tarr AW, Voisset C, Donot P, Bartosch B, Bain C et al. Characterization of host-range and cell entry properties of the major genotypes and subtypes of hepatitis C virus. *Hepatology* 2005; 41(2):265-274.
- (73) Lerat H, Honda M, Beard MR, Loesch K, Sun J, Yang Y et al. Steatosis and liver cancer in transgenic mice expressing the structural and nonstructural proteins of hepatitis C virus. *Gastroenterology* 2002; 122(2):352-365.
- (74) Levy S, Todd SC, Maecker HT. CD81 (TAPA-1): A molecule involved in signal transduction and cell adhesion in the immune system. *Annual Review of Immunology* 1998; 16(1):89-109.
- (75) Li K, Foy E, Ferreon JC, Nakamura M, Ferreon AC, Ikeda M et al. Immune evasion by hepatitis C virus NS3/4A protease-mediated cleavage of the Toll-like receptor 3 adaptor protein TRIF. *Proc Natl Acad Sci U S A* 2005; 102(8):2992-2997.
- (76) Li WX. Canonical and non-canonical JAK-STAT signaling. *Trends Cell Biol* 2008; 18(11):545-551.

- (77) Lindenbach BD, Evans MJ, Syder AJ, Wolk B, Tellinghuisen TL, Liu CC et al. Complete replication of hepatitis C virus in cell culture. *Science* 2005; 309(5734):623-626.
- (78) Lohmann V, Korner F, Kock J-O, Theilmann L, Bartenschlager R. Replication of subgenomic hepatitis C virus RNAs in a hepatoma cell line. *Science* 1999; 285:110-113.
- (79) Loo YM, Owen DM, li K, Erickson AK, Johnson CL, Fish PM et al. Viral and therapeutic control of IFN-beta promoter stimulator 1 during hepatitis C virus infection. *Proc Natl Acad Sci U S A* 2006; 103(15):6001-6006.
- (80) Maheshwari A, Ray S, Thuluvath PJ. Acute hepatitis C. *The Lancet* 2008; 372(9635):321-332.
- (81) Maillard P, Huby T, Andreo U, Moreau M, Chapman J, Budkowska A. The interaction of natural hepatitis C virus with human scavenger receptor SR-BI/Cla1 is mediated by ApoB-containing lipoproteins. *FASEB J* 2006;05-4728fje.
- (82) Major ME, Feinstone SM. The molecular virology of hepatitis C. *Hepatology* 1997; 25(6):1572-1538.
- (83) Marques JT, Devosse T, Wang D, Zamanian-Daryoush M, Serbinowski P, Hartmann R et al. A structural basis for discriminating between self and nonself double-stranded RNAs in mammalian cells. *Nat Biotechnol* 2006; 24(5):559-565.

- (84) Martin C, Nielsen SU, Ibrahim S, Bassendine MF, Toms GL. Binding of liver derived, low density hepatitis C virus to human hepatoma cells. *Journal of Medical Virology* 2008; 80(5):816-823.
- (85) Matsumoto M, Funami K, Tanabe M, Oshiumi H, Shingai M, Seto Y et al. Subcellular localization of Toll-like receptor 3 in human dendritic cells. *J Immunol* 2003; 171(6):3154-3162.
- (86) Matsumoto M, Kikkawa S, Kohase M, Miyake K, Seya T. Establishment of a monoclonal antibody against human Toll-like receptor 3 that blocks double-stranded RNA-mediated signaling. *Biochem Biophys Res Commun* 2002; 293(5):1364-1369.
- (87) McHutchison JG, Everson GT, Gordon SC, Jacobson IM, Sulkowski M, Kauffman R et al. Telaprevir with Peginterferon and Ribavirin for Chronic HCV Genotype 1 Infection. *N Engl J Med* 2009; 360(18):1827-1838.
- (88) Mengshol JA, Golden-Mason L, Rosen HR. Mechanisms of Disease: HCV-induced liver injury. *Nat Clin Pract Gastroenterol Hepatol* 2007; 4(11):622-634.
- (89) Mercer DF, Schiller DE, Elliott JF, Douglas DN, Hao C, Rinfret A et al. Hepatitis C virus replication in mice with chimeric human livers. *Nat Med* 2001; 7(8):927-933.
- (90) Meyer K, Basu A, Ray R. Functional Features of Hepatitis C Virus Glycoproteins for Pseudotype Virus Entry into Mammalian Cells. *Virology* 2000; 276(1):214-226.

- (91) Meylan E, Curran J, Hofmann K, Moradpour D, Binder M, Bartenschlager R et al. Cardif is an adaptor protein in the RIG-I antiviral pathway and is targeted by hepatitis C virus. *Nature* 2005.
- (92) Mihm S, Fayyazi A, Hartmann H, Ramadori G. Analysis of Histopathological Manifestations of Chronic Hepatitis C Virus Infection With Respect to Virus Genotype. *Hepatology* 1997; 26(3):735-739.
- (93) Miyamoto H, Okamoto H, Sato K, Tanaka T, Mishiro S. Extraordinarily low density of hepatitis C virus estimated by sucrose density gradient centrifugation and the polymerase chain reaction. *J Gen Virol* 1992; 73(3):715-718.
- (94) Miyanari Y, Atsuzawa K, Usuda N, Watashi K, Hishiki T, Zayas M et al. The lipid droplet is an important organelle for hepatitis C virus production. *Nat Cell Biol* 2007; 9(9):1089-1097.
- (95) Molina S, Castet V, Fournier-Wirth C, Pichard-Garcia L, Avner R, Harats D et al. The low-density lipoprotein receptor plays a role in the infection of primary human hepatocytes by hepatitis C virus. *Journal of Hepatology* 2007; 46(3):411-419.
- (96) Monazahian M, Böhme I, Bonk S, Koch A, Scholz C, Grethe S et al. Low density lipoprotein receptor as a candidate receptor for hepatitis C virus. *Journal of Medical Virology* 1999; 57(3):223-229.

- (97) Moore CB, Bergstralh DT, Duncan JA, Lei Y, Morrison TE, Zimmermann AG et al. NLRX1 is a regulator of mitochondrial antiviral immunity. *Nature* 2008; 451(7178):573-577.
- (98) Moradpour D, Evans MJ, Gosert R, Yuan Z, Blum HE, Goff SP et al. Insertion of green fluorescent protein into nonstructural protein 5A allows direct visualization of functional hepatitis C virus replication complexes. *J Virol* 2004; 78(14):7400-7409.
- (99) Morikawa K, Zhao Z, Date T, Miyamoto M, Murayama A, Akazawa D et al. The roles of CD81 and glycosaminoglycans in the adsorption and uptake of infectious HCV particles. *Journal of Medical Virology* 2007; 79(6):714-723.
- (100) Moriya K, Yotsuyanagi H, Shintani Y, Fujie H, Ishibashi K, Matsuura Y et al. Hepatitis C virus core protein induces hepatic steatosis in transgenic mice. *J Gen Virol* 1997; 78:1527-1531.
- (101) Murali A, Li X, Ranjith-Kumar CT, Bhardwaj K, Holzenburg A, Li P et al. Structure and function of LGP2, a DEX(D/H) helicase that regulates the innate immunity response. *J Biol Chem* 2008; 283(23):15825-15833.
- (102) Muruve DA, Petrilli V, Zaiss AK, White LR, Clark SA, Ross PJ et al. The inflammasome recognizes cytosolic microbial and host DNA and triggers an innate immune response. *Nature* 2008; 452(7183):103-107.

- (103) Nahmias Y, Goldwasser J, Casali M, van Poll D, Wakita T, Chung RT et al. Apolipoprotein B-dependent hepatitis C virus secretion is inhibited by the grapefruit flavonoid naringenin. *Hepatology* 2008; 45(5):1437-1445.
- (104) Nathoo N, Lautzenheiser F, Barnett G. The first direct human blood transfusion: The forgotten legacy of George W. Crile. *Operative Neurosurgery* 2009; 64:20-26.
- (105) Nielsen SU, Bassendine MF, Burt AD, Martin C, Pumeechockchai W, Toms GL. Association between Hepatitis C Virus and Very-Low-Density Lipoprotein (VLDL)/LDL Analyzed in Iodixanol Density Gradients. *The Journal of Virology* 2006; 80(5):2418-2428.
- (106) Perlemuter G, Sabile A, Letteron P, Vona G, Topilco A, Chretien, Y. Hepatitis C virus core protein inhibits microsomal triglyceride transfer protein activity and very low density lipoprotein secretion: a model of viral-related steatosis. *FASEB J* 2002; 16(2):185-194.
- (107) Petracca R, Falugi F, Galli G, Norais N, Rosa D, Campagnoli S et al. Structure-Function Analysis of Hepatitis C Virus Envelope-CD81 Binding. *The Journal of Virology* 2000; 74(10):4824-4830.
- (108) Pileri P, Uematsu Y, Campagnoli S, Galli G, Falugi F, Petracca R et al. Binding of Hepatitis C Virus to CD81. *Science* 1998; 282(5390):938-941.

- (109) Ploss A, Evans MJ, Gaysinskaya VA, Panis M, You H, de Jong YP et al. Human occludin is a hepatitis C virus entry factor required for infection of mouse cells. *Nature* 2009.
- (110) Preiss S, Thompson A, Chen X, Rodgers S, Markova V, Desmond P et al. Characterization of the innate immune signalling pathways in hepatocyte cell lines. *Journal Of Viral Hepatitis* 2008; 15(12):888-900.
- (111) Prince AM, Huima-Byron T, Parker TS, Levine DM. Visualization of hepatitis C virions and putative defective interfering particles isolated from low-density lipoproteins. *Journal Of Viral Hepatitis* 1996; 3(1):11-17.
- (112) Roccasecca R, Ansuini H, Vitelli A, Meola A, Scarselli E, Acali S et al. Binding of the Hepatitis C Virus E2 Glycoprotein to CD81 Is Strain Specific and Is Modulated by a Complex Interplay between Hypervariable Regions 1 and 2. *The Journal of Virology* 2003; 77(3):1856-1867.
- (113) Rosa D, Campagnoli S, Moretto C, Guenzi E, Cousens L, Chin M et al. A quantitative test to estimate neutralizing antibodies to the hepatitis C virus: cytofluorimetric assessment of envelope glycoprotein 2 binding to target cells. *Proc Natl Acad Sci U S A* 1996; 93(5):1759-1763.
- (114) Saito H, Dhanasekaran P, Nguyen D, Baldwin F, Weisgraber KH, Wehrli S et al. Characterization of the Heparin Binding Sites in Human Apolipoprotein E. *J Biol Chem* 2003; 278(17):14782-14787.

- (115) Saito T, Gale M, Jr. Differential recognition of double-stranded RNA by RIG-I-like receptors in antiviral immunity. *J Exp Med* 2008; 205(7):1523-1527.
- (116) Saito T, Hirai R, Loo YM, Owen D, Johnson CL, Sinha SC et al. Regulation of innate antiviral defenses through a shared repressor domain in RIG-I and LGP2. *Proc Natl Acad Sci U S A* 2006.
- (117) Saito T, Owen DM, Jiang F, Marcotrigiano J, Gale M, Jr. Innate immunity induced by composition-dependent RIG-I recognition of hepatitis C virus RNA. *Nature* 2008; 454(7203):523-527.
- (118) Scarselli E, Ansuini H, Cerino R, Roccasecca RM, Acali S, Filocamo G et al. The human scavenger receptor class B type I is a novel candidate receptor for the hepatitis C virus. *EMBO* 2002; 21(19):5017-5025.
- (119) Sen GC. Viruses and interferons. *Annu Rev Microbiol* 2001; 55:255-281.
- (120) Seth RB, Sun L, Ea CK, Chen ZJ. Identification and characterization of MAVS, a mitochondrial antiviral signaling protein that activates NF-kappaB and IRF 3. *Cell* 2005; 122(5):669-682.
- (121) Shepard CW, Finelli L, Alter MJ. Global epidemiology of hepatitis C virus infection. *Lancet Infect Dis* 2005; 5(9):558-567.
- (122) Simmonds P. Genetic diversity and evolution of hepatitis C virus - 15 years on. *J Gen Virol* 2004; 85(11):3173-3188.

- (123) Simons JN, Pilot-Matias T, Leary T. Identification of two flavivirus-like genomes in the GB hepatitis agent. *Proc Natl Acad Sci U S A* 1995; 92:3401-3405.
- (124) Sumpter R, Loo Y-M, Foy E, Li K, Yoneyama M, Fujita T et al. Regulating intracellular anti-viral defense and permissiveness to hepatitis C virus RNA replication through a cellular RNA helicase, RIG-I. *J Virol* 2005; 79(5):2689-2699.
- (125) Takahashi K, Yoneyama M, Nishihori T, Hirai R, Kumeta H, Narita R et al. Nonself RNA-Sensing Mechanism of RIG-I Helicase and Activation of Antiviral Immune Responses. *Molecular Cell* 2008; 29(4):428-440.
- (126) Tattoli I, Carneiro LA, Jehanno M, Magalhaes J, Shu Y, Philpott DJ et al. NLRX1 is a mitochondrial NOD-like receptor that amplifies NF- κ B and JNK pathways by inducing reactive oxygen species production. *EMBO Rep* 2008; 9(3):293-300.
- (127) Thomas PG, Dash P, Aldridge J, Ellebedy AH, Reynolds C, Funk AJ et al. The Intracellular Sensor NLRP3 Mediates Key Innate and Healing Responses to Influenza A Virus via the Regulation of Caspase-1. *Immunity* 2009; 30(4):566-575.
- (128) Thomssen R, Bonk S, Propfe C, Heermann KH, Kachel HG, Uy A. Association of hepatitis C virus in human sera with β -lipoprotein. *Medical Microbiology and Immunology* 1992; 181(5):293-300.

- (129) Timpe JM, Stamataki Z, Jennings A, Hu K, Farquhar MJ, Harris HJ et al. Hepatitis C virus cell-cell transmission in hepatoma cells in the presence of neutralizing antibodies. *Hepatology* 2008; 47(1):17-24.
- (130) Truong TQ, Falstraull L, Tremblay C, Brissette L. Low density lipoprotein-receptor plays a major role in the binding of very low density lipoproteins and their remnants on HepG2 cells. *The International Journal of Biochemistry & Cell Biology* 1999; 31(6):695-705.
- (131) Vandelli C, Renzo F, Romano L, Tisminetzky S, De Palma M, Stroffolini T et al. Lack of Evidence of Sexual Transmission of Hepatitis C among Monogamous Couples: Results of a 10-Year Prospective Follow-Up Study. *Am J Gastroenterol* 2004; 99(5):855-859.
- (132) Venkataraman T, Valdes M, Elsby R, Kakuta S, Caceres G, Saijo S et al. Loss of DExD/H box RNA helicase LGP2 manifests disparate antiviral responses. *J Immunol* 2007; 178(10):6444-6455.
- (133) Voisset C, Callens N, Blanchard E, Op De Beeck A, Dubuisson J, Vu-Dac N. High Density Lipoproteins Facilitate Hepatitis C Virus Entry through the Scavenger Receptor Class B Type I. *J Biol Chem* 2005; 280(9):7793-7799.
- (134) Wakita T, Pietschmann T, Kato T, Date T, Miyamoto M, Zhao Z et al. Production of infectious hepatitis C virus in tissue culture from a cloned viral genome. *Nat Med* 2005; 11(7):791-796.

- (135) Walsh MJ, Jonsson JR, Richardson MM, Lipka GM, Purdie DM, Clouston AD et al. Non-response to antiviral therapy is associated with obesity and increased hepatic expression of suppressor of cytokine signalling 3 (SOCS-3) in patients with chronic hepatitis C, viral genotype 1. *Gut* 2006; 55(4):529-535.
- (136) Wang C, Gale M, Jr., Keller BC, Huang H, Brown MS, Goldstein JL et al. Identification of FBL2 as a geranylgeranylated cellular protein required for hepatitis C virus RNA replication. *Mol Cell* 2005; 18(4):425-434.
- (137) Wetterau JR, Gregg RE, Harrity TW, Arbeeny C, Cap M, Connolly F et al. An MTP Inhibitor That Normalizes Atherogenic Lipoprotein Levels in WHHL Rabbits. *Science* 1998; 282(5389):751-754.
- (138) Wunschmann S, Medh JD, Klinzmann D, Schmidt WN, Stapleton JT. Characterization of Hepatitis C Virus (HCV) and HCV E2 Interactions with CD81 and the Low-Density Lipoprotein Receptor. *The Journal of Virology* 2000; 74(21):10055-10062.
- (139) Xu LG, Wang YY, Han KJ, Li LY, Zhai Z, Shu HB. VISA Is an Adapter Protein Required for Virus-Triggered IFN-beta Signaling. *Mol Cell* 2005; 19(6):727-740.
- (140) Yao H, Ye J. Long Chain Acyl-CoA Synthetase 3-mediated Phosphatidylcholine Synthesis Is Required for Assembly of Very Low Density Lipoproteins in Human Hepatoma Huh7 Cells. *J Biol Chem* 2008; 283(2):849-854.

- (141) Ye J, Wang C, Sumpter R, Jr., Brown MS, Goldstein JL, Gale M, Jr. Disruption of hepatitis C virus RNA replication through inhibition of host protein geranylgeranylation. *Proc Natl Acad Sci U S A* 2003; 100(26):15865-15870.
- (142) Yoneyama M, Kikuchi M, Matsumoto K, Imaizumi T, Miyagishi M, Taira K et al. Shared and unique functions of the DExD/H-box helicases RIG-I, MDA5, and LGP2 in antiviral innate immunity. *J Immunol* 2005; 175(5):2851-2858.
- (143) Yoneyama M, Kikuchi M, Natsukawa T, Shinobu N, Imaizumi T, Miyagishi M et al. The RNA helicase RIG-I has an essential function in double-stranded RNA-induced innate antiviral responses. *Nat Immunol* 2004; 5(7):730-737.
- (144) Zhang J, Randall G, Higginbottom A, Monk P, Rice CM, McKeating JA. CD81 Is Required for Hepatitis C Virus Glycoprotein-Mediated Viral Infection. *The Journal of Virology* 2004; 78(3):1448-1455.
- (145) Zhong J, Gastaminza P, Cheng G, Kapadia S, Kato T, Burton DR et al. Robust hepatitis C virus infection in vitro. *Proc Natl Acad Sci U S A* 2005; 102(26):9294-9299.